EDMs from theory to experiments
Nagoya, Japan, 2-4 March 2023
In-person presentation

High sensitivity storage ring proton EDM experiment

Yannis K. Semertzidis, IBS-CAPP & KAIST, South Korea

- In the next decade(s) we expect significant progress in electron (eEDM), neutron (nEDM), muon (μEDM), proton (pEDM),… EDM sensitivities.

- Statistics for 10^{-29} *e*-cm for pEDM, for best hadronic EDM experiment

- Systematics: using symmetries, spin-based alignment/background reduction

Storage Ring Proton EDM at Snowmass

- EDM physics is must do, exciting and timely, CP-violation, ~10^3 TeV New-Physics reach, axion physics, DM/DE.

- Hybrid, symmetric ring lattice and spin-based alignment. Minimized systematic error sources. Statistics and systematics of pEDM to better than 10^{-29}*e*-cm.

- Snowmass encouraged BNL and the srEDM collaboration to come up with a technically strong proposal for a storage ring proton EDM. BNL is currently funding the cost estimate of the storage ring EDM experiment.

- The srEDM has a talk at the P5 meeting at Fermilab/Argonne.

Timeline

- Snowmass/white paper, CDR, proposal/TDR, prototype/string-test, ring construction (3-5 years), storage (2-3 years) to first publication
- Cost estimation currently at BNL
- Possible interesting results within a decade.

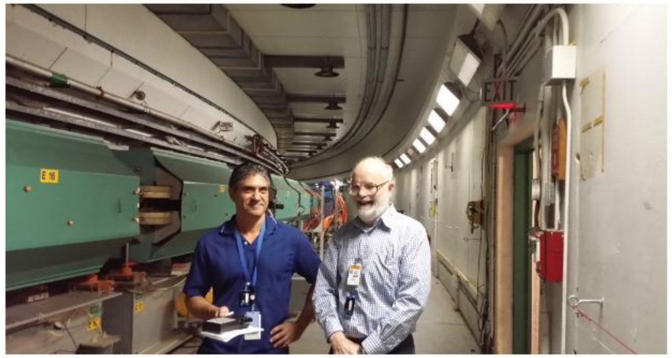

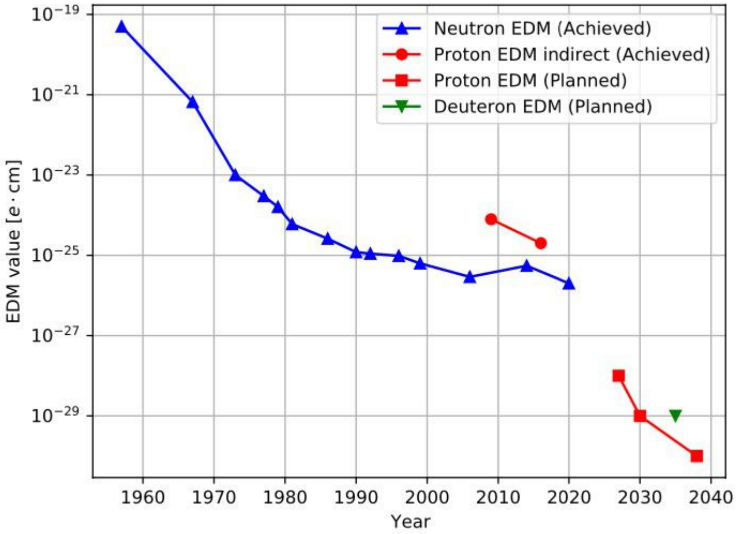

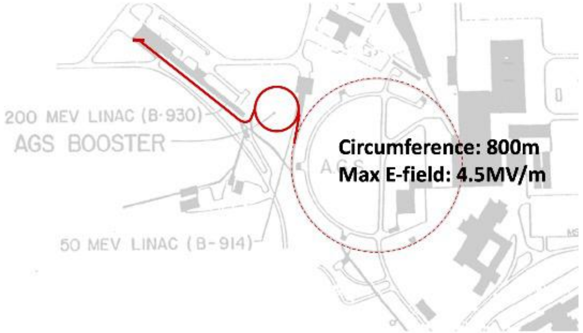

Circumference: 800m
Max E-field: 4.5MV/m

A Permanent EDM Violates both T & P Symmetries:

$$\vec{\mu} = g\left(\frac{q}{2m}\right)\vec{s}, \quad \mathcal{H} = -\vec{\mu}\cdot\vec{B} - \vec{d}\cdot\vec{E}$$

$$\vec{d} = \eta\left(\frac{q}{2mc}\right)\vec{s}$$

The EDM is *caused* by the spin

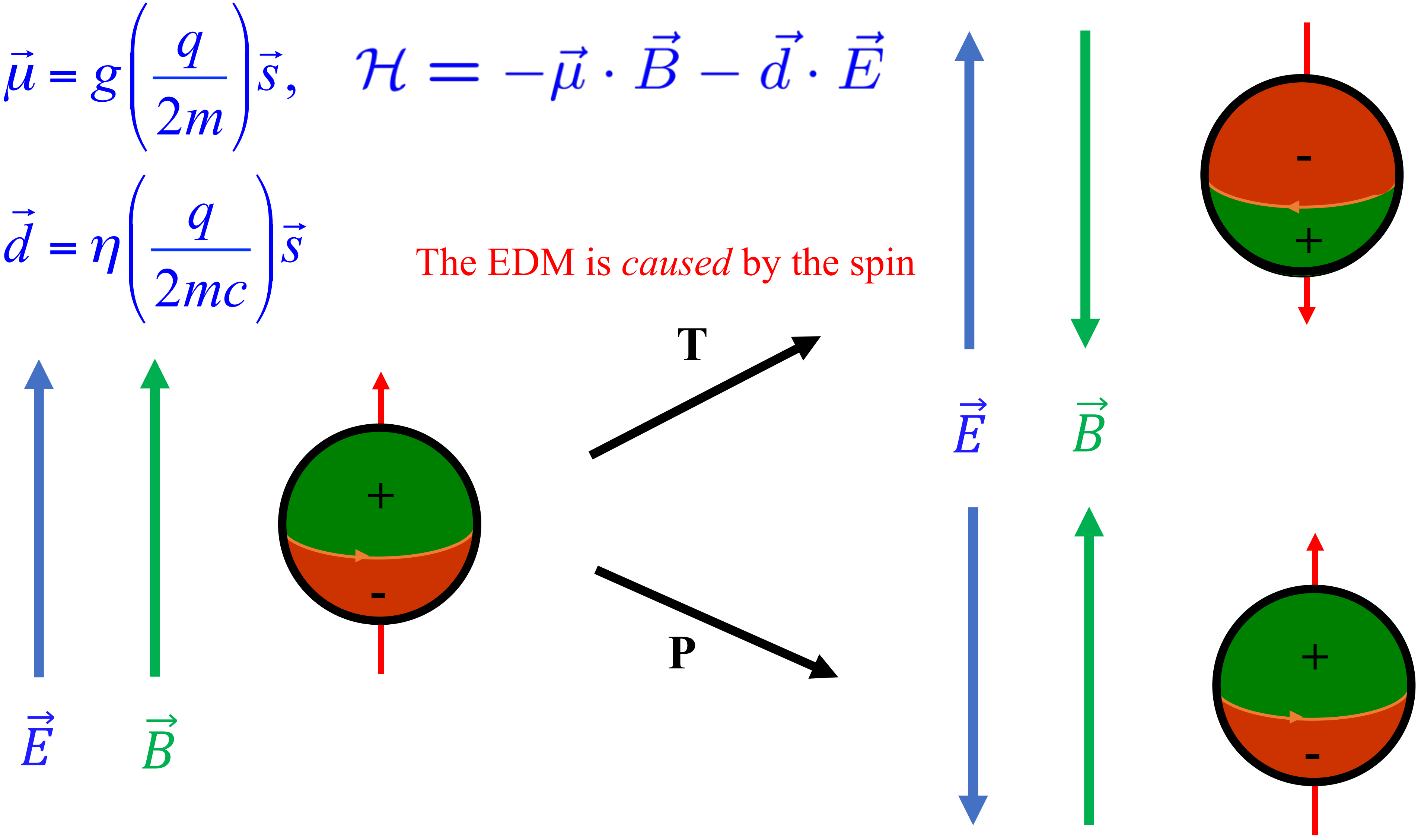

Reminder: batteries are allowed in the SM!

Snowmass paper on EDMs, why many EDMs:

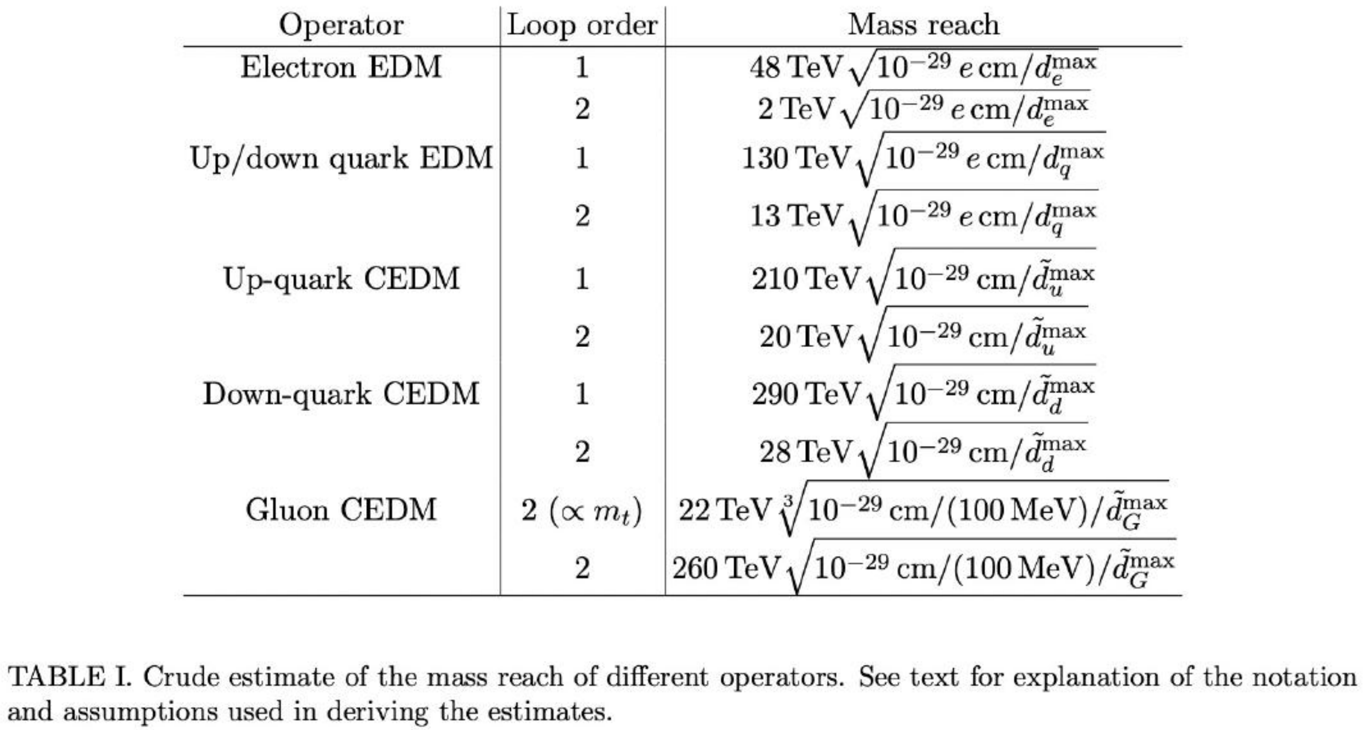

Operator	Loop order	Mass reach
Electron EDM	1	$48\,\mathrm{TeV}\sqrt{10^{-29}\,e\,\mathrm{cm}/d_e^{\max}}$
	2	$2\,\mathrm{TeV}\sqrt{10^{-29}\,e\,\mathrm{cm}/d_e^{\max}}$
Up/down quark EDM	1	$130\,\mathrm{TeV}\sqrt{10^{-29}\,e\,\mathrm{cm}/d_q^{\max}}$
	2	$13\,\mathrm{TeV}\sqrt{10^{-29}\,e\,\mathrm{cm}/d_q^{\max}}$
Up-quark CEDM	1	$210\,\mathrm{TeV}\sqrt{10^{-29}\,\mathrm{cm}/\tilde{d}_u^{\max}}$
	2	$20\,\mathrm{TeV}\sqrt{10^{-29}\,\mathrm{cm}/\tilde{d}_u^{\max}}$
Down-quark CEDM	1	$290\,\mathrm{TeV}\sqrt{10^{-29}\,\mathrm{cm}/\tilde{d}_d^{\max}}$
	2	$28\,\mathrm{TeV}\sqrt{10^{-29}\,\mathrm{cm}/\tilde{d}_d^{\max}}$
Gluon CEDM	2 ($\propto m_t$)	$22\,\mathrm{TeV}\sqrt[3]{10^{-29}\,\mathrm{cm}/(100\,\mathrm{MeV})/\tilde{d}_G^{\max}}$
	2	$260\,\mathrm{TeV}\sqrt{10^{-29}\,\mathrm{cm}/(100\,\mathrm{MeV})/\tilde{d}_G^{\max}}$

TABLE I. Crude estimate of the mass reach of different operators. See text for explanation of the notation and assumptions used in deriving the estimates.

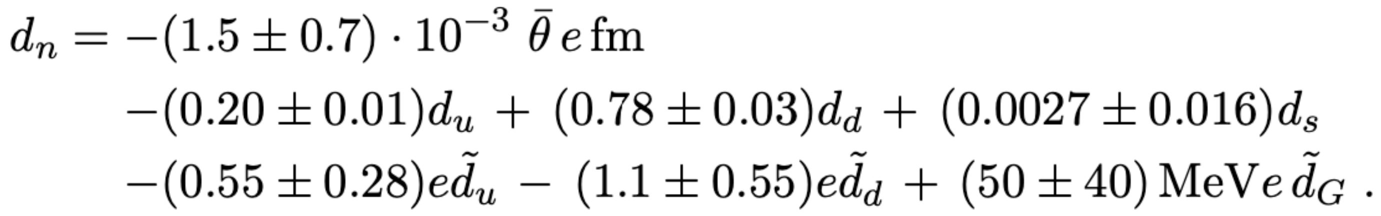

$$\begin{aligned} d_n = & -(1.5\pm0.7)\cdot10^{-3}\;\bar{\theta}\,e\,\mathrm{fm} \\ & -(0.20\pm0.01)d_u + (0.78\pm0.03)d_d + (0.0027\pm0.016)d_s \\ & -(0.55\pm0.28)e\tilde{d}_u - (1.1\pm0.55)e\tilde{d}_d + (50\pm40)\,\mathrm{MeV}\,e\,\tilde{d}_G\;. \end{aligned}$$

arXiv:2203.08103v1 [hep-ph] 15 Mar 2022

Electric dipole moments and the search for new physics

Ricardo Alarcon,[1] Jim Alexander,[2] Vassilis Anastassopoulos,[3] Takatoshi Aoki,[4] Rick Baartman,[5] Stefan Baeßler,[6,7] Larry Bartoszek,[8] Douglas H. Beck,[9] Franco Bedeschi,[10] Robert Berger,[11] Martin Berz,[12] Tanmoy Bhattacharya,[13,a] Michael Blaskiewicz,[14] Thomas Blum,[15,b] Themis Bowcock,[16] Kevin Brown,[14] Dmitry Budker,[17,18] Sergey Burdin,[16] Brendan C. Casey,[19] Gianluigi Casse,[20] Giovanni Cantatore,[21] Lan Cheng,[22] Timothy Chupp,[20] Vince Cianciolo,[23] Vincenzo Cirigliano,[13,24,c] Steven M. Clayton,[25] Chris Crawford,[26] B. P. Das,[27] Hooman Davoudiasl,[14] Jordy de Vries,[28,29,d] David DeMille,[30,31,e] Dmitri Denisov,[14] Milind V. Diwan,[14] John M. Doyle,[32] Jonathan Engel,[33] George Fanourakis,[34] Renee Fatemi,[35] Bradley W. Filippone,[36] Nadia Fomin,[37] Wolfram Fischer,[14] Antonios Gardikiotis,[38,3] R. F. Garcia Ruiz,[39] Claudio Gatti,[40] James Gooding,[16] Peter Graham,[41] Frederick Gray,[42] W. Clark Griffith,[43] Selcuk Haciomeroglu,[44] Gerald Gwinner,[45] Steven Hoekstra,[46,47] Georg H. Hoffstaetter,[2] Haixin Huang,[14] Nicholas R. Hutzler,[48,f] Marco Incagli,[10] Takeyasu M. Ito,[25,g] Taku Izubuchi,[49] Andrew M. Jayich,[50] Hoyong Jeong,[51] David Kaplan,[52] Marin Karuza,[53] David Kawall,[54] On Kim,[44] Ivan Koop,[55] Valeri Lebedev,[19] Jonathan Lee,[56] Soohyung Lee,[44] Kent K. H. Leung,[57] Chen-Yu Liu,[58,9,h] Joshua Long,[58,9] Alberto Lusiani,[59,10] William J. Marciano,[14] Marios Maroudas,[3] Andrei Matlashov,[44] Nobuyuki Matsumoto,[60] Richard Mawhorter,[61] Francois Meot,[14] Emanuele Mereghetti,[13] James P. Miller,[62] William M. Morse,[63,i] James Mott,[62,19] Zhanibek Omarov,[44,64] Chris O'Shaughnessy,[25] Cenap Ozben,[65] SeongTae Park,[44] Robert W. Pattie Jr.,[66] Alexander N. Petrov,[67,68] Giovanni Maria Piacentino,[69] Bradley R. Plaster,[26] Boris Podobedov,[14] Matthew Poelker,[70] Dinko Pocanic,[71] V. S. Prasannaa,[27] Joe Price,[16] Michael J. Ramsey-Musolf,[72,73] Deepak Raparia,[14] Surjeet Rajendran,[52] Matthew Reece,[74,j] Austin Reid,[58] Sergio Rescia,[14] Adam Ritz,[75] B. Lee Roberts,[62] Marianna S. Safronova,[76] Yasuhiro Sakemi,[77] Andrea Shindler,[78] Yannis K. Semertzidis,[44,64,k] Alexander Silenko,[79] Jaideep T. Singh,[80] Leonid V. Skripnikov,[67,68] Amarjit Soni,[14] Edward Stephenson,[58] Riad Suleiman,[81] Ayaki Sunaga,[82] Michael Syphers,[83] Sergey Syritsyn,[84] M. R. Tarbutt,[85] Pia Thoerngren,[86] Rob G. E. Timmermans,[87] Volodya Tishchenko,[14] Anatoly V. Titov,[67,68] Nikolaos Tsoupas,[14] Spyros Tzamarias,[88] Alessandro Variola,[40] Graziano Venanzoni,[10] Eva Vilella,[16] Joost Vossebeld,[16] Peter Winter,[89,l] Eunil Won,[51] Anatoli Zelenski,[14] Yan Zhou,[90] and Konstantin Zioutas[3]

[1] *Arizona State University, Tempe, AZ 85287, USA*
[2] *Cornell University, Ithaca, New York, USA*
[3] *University of Patras, Dept. of Physics, Patras-Rio, Greece*
[4] *The University of Tokyo, Meguro-ku, Tokyo, Japan*
[5] *TRIUMF, Vancouver, British Columbia, Canada*
[6] *University of Virginia, 382 McCormick Road, Charlottesville, VA 22903, USA*
[7] *Oak Ridge National Laboratory, 1 Bethel Valley Road, Oak Ridge, TN 37830, USA*
[8] *Bartoszek Engineering, Aurora, IL 60506, USA.*
[9] *University of Illinois at Urbana-Champaign, Urbana, IL 61801, USA*
[10] *National Institute for Nuclear Physics (INFN-Pisa), Pisa, Italy*
[11] *Philipps-Universitaet Marburg, Fachbereich Chemie,*
Hans-Meerwein-Str. 4, 35032 Marburg, Germany
[12] *Michigan State University, East Lansing, Michigan, USA*
[13] *T-2, Los Alamos National Laboratory, Los Alamos, NM 87545, USA*
[14] *Brookhaven National Laboratory, Upton, New York, USA*
[15] *Department of Physics, University of Connecticut, USA*
[16] *University of Liverpool, Liverpool, UK*
[17] *Helmholtz-Institute Mainz, Johannes Gutenberg University, Mainz, Germany*
[18] *University of California at Berkeley, Berkeley, California, USA*

EDM timelines, from Snowmass 2021 (2022).

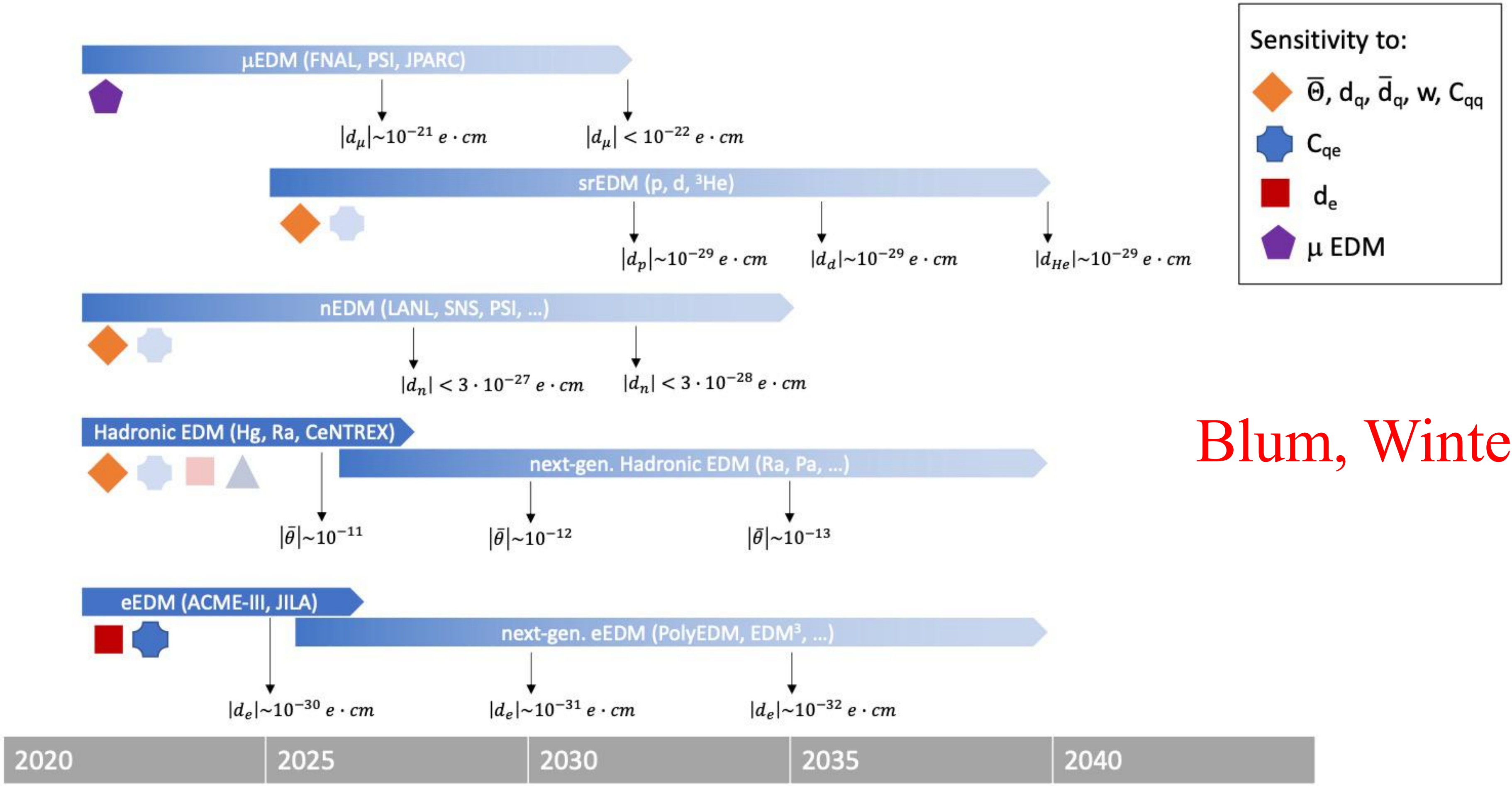

Blum, Winter *et al.*

Figure 3-1. *Timelines for the major current and planned EDM searches with their sensitivity to the important parameters of the effective field theory (see Fig. 3-2 for details). Solid (shaded) symbols indicate each experiment's primary (secondary) sensitivities. Measurement goals indicated by the black arrows are based on current plans of the various groups.*

Snowmass paper on EDMs

Neutron EDM

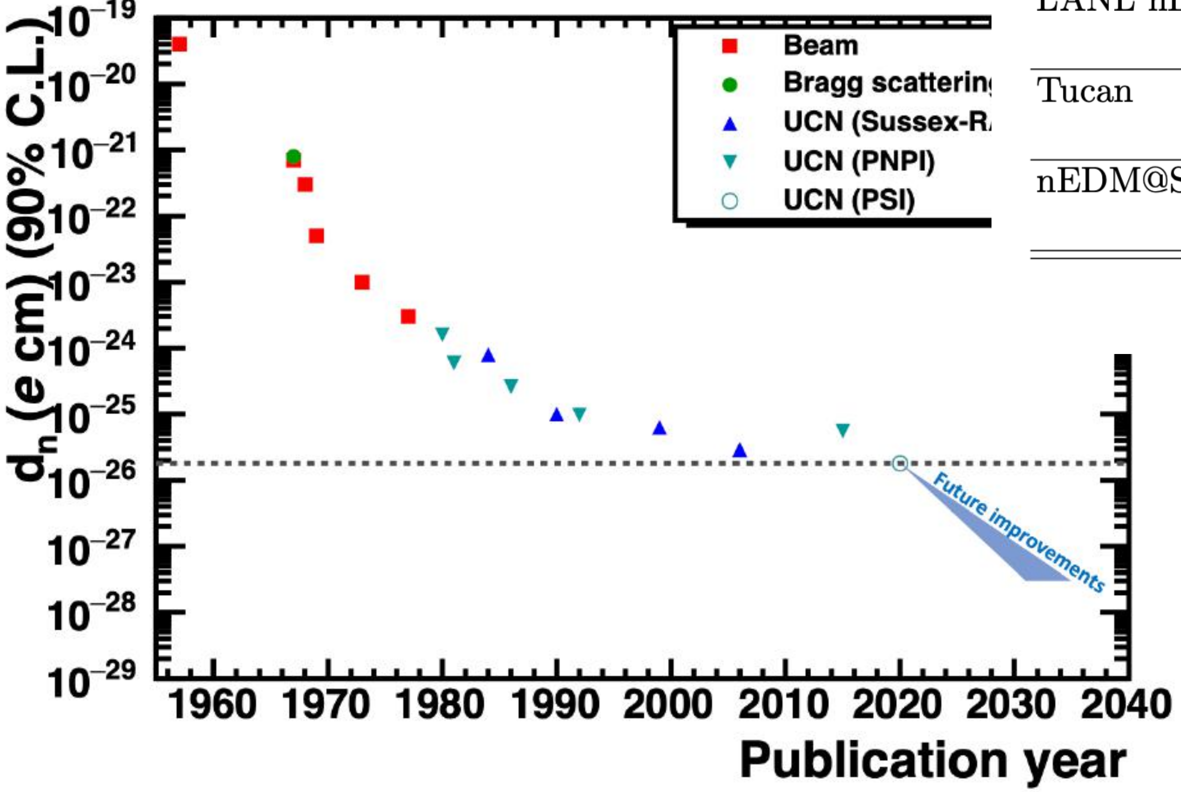

FIG. 3. Evolution of the nEDM results along with projected future results

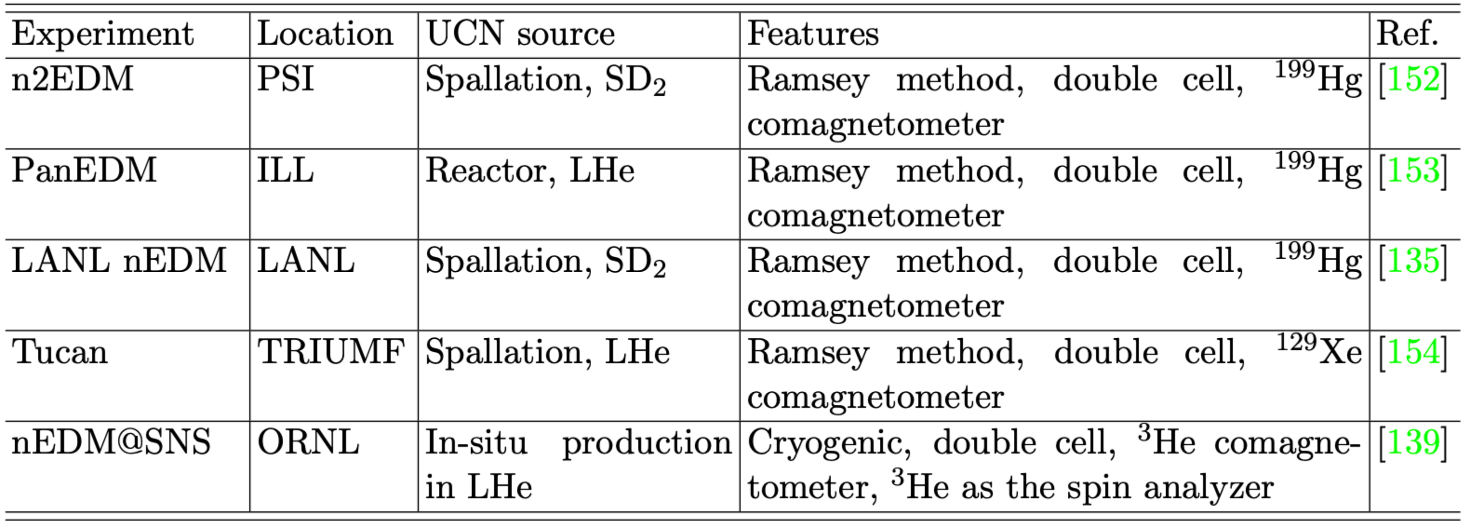

Experiment	Location	UCN source	Features	Ref.
n2EDM	PSI	Spallation, SD_2	Ramsey method, double cell, ^{199}Hg comagnetometer	[152]
PanEDM	ILL	Reactor, LHe	Ramsey method, double cell, ^{199}Hg comagnetometer	[153]
LANL nEDM	LANL	Spallation, SD_2	Ramsey method, double cell, ^{199}Hg comagnetometer	[135]
Tucan	TRIUMF	Spallation, LHe	Ramsey method, double cell, ^{129}Xe comagnetometer	[154]
nEDM@SNS	ORNL	In-situ production in LHe	Cryogenic, double cell, ^{3}He comagnetometer, ^{3}He as the spin analyzer	[139]

TABLE III. A list of the nEDM experiments that are being developed

Snowmass paper on EDMs

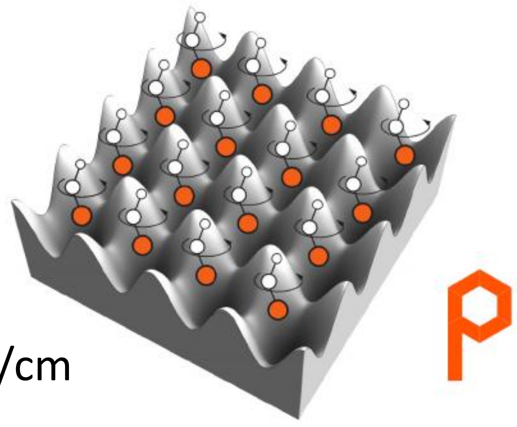

PolyEDM

Effective E-field with polar molecules: order GV/cm

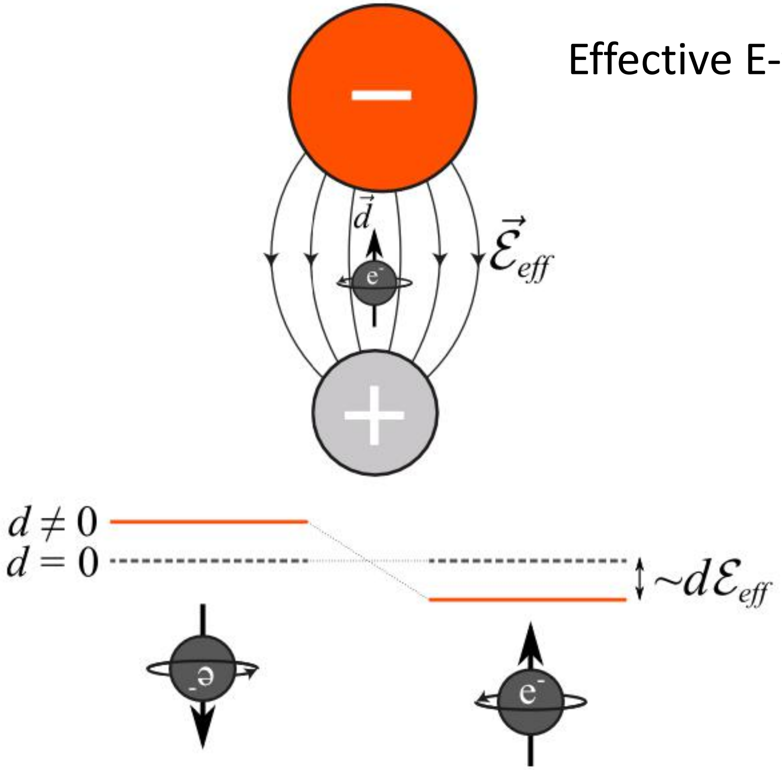

Figure: Laser-cooled polyatomic molecules, optically trapped, with full quantum control. Such a platform can be used to access new physics at the PeV scale.

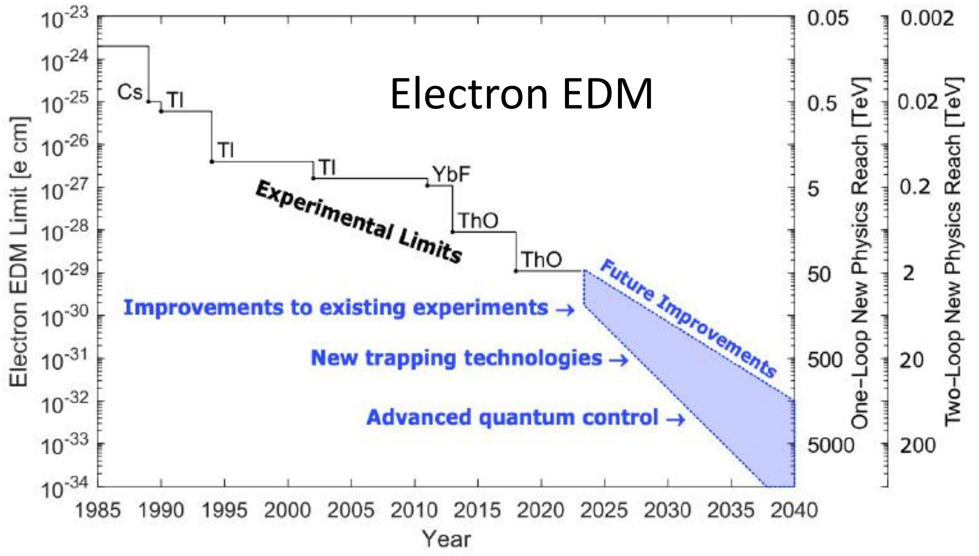

FIG. 5. Electron EDM limits versus time, along with new physics reach for one-loop and two-loop effects (see Eq. 2). All electron EDM experiments to date use AMO techniques. The solid line indicates the most sensitive experimental limit, including the species used. The shaded area indicates potential future improvements discussed in the text. Improvements in the next few years are driven largely by improvements to existing experiments and are quite likely, though as we go more into the future the projection becomes increasingly speculative and uncertain.

Snowmass paper on pEDM

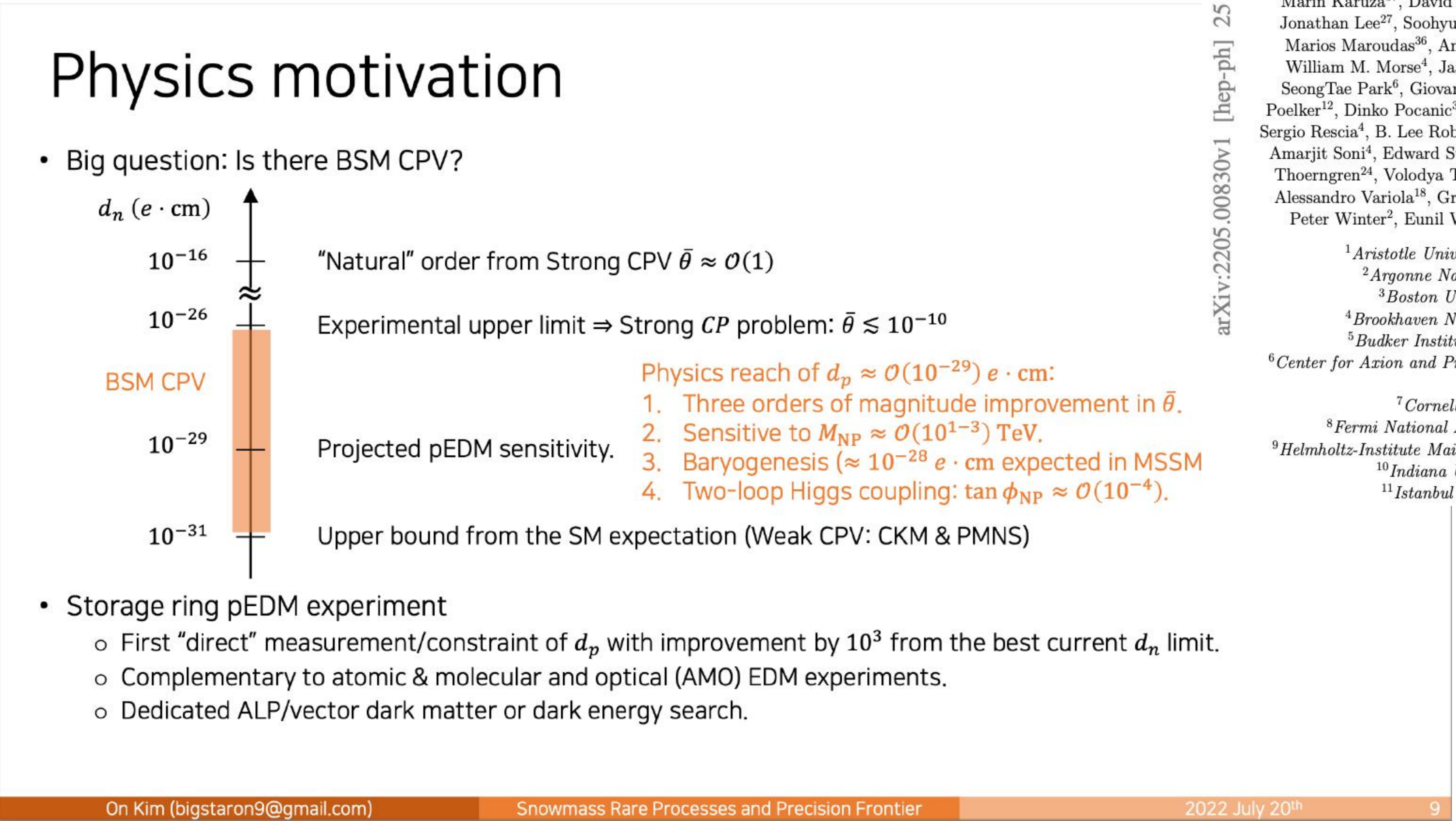

Physics motivation

- Big question: Is there BSM CPV?

$d_n\ (e \cdot \mathrm{cm})$

10^{-16} “Natural” order from Strong CPV $\bar{\theta} \approx \mathcal{O}(1)$

$\approx$

10^{-26} Experimental upper limit ⇒ Strong CP problem: $\bar{\theta} \lesssim 10^{-10}$

BSM CPV

Physics reach of $d_p \approx \mathcal{O}(10^{-29})\ e \cdot \mathrm{cm}$:

1. Three orders of magnitude improvement in $\bar{\theta}$.
2. Sensitive to $M_{\mathrm{NP}} \approx \mathcal{O}(10^{1-3})$ TeV.
3. Baryogenesis ($\approx 10^{-28}\ e \cdot \mathrm{cm}$ expected in MSSM
4. Two-loop Higgs coupling: $\tan \phi_{\mathrm{NP}} \approx \mathcal{O}(10^{-4})$.

10^{-29} Projected pEDM sensitivity.

10^{-31} Upper bound from the SM expectation (Weak CPV: CKM & PMNS)

- Storage ring pEDM experiment
  - First “direct” measurement/constraint of d_p with improvement by 10^3 from the best current d_n limit.
  - Complementary to atomic & molecular and optical (AMO) EDM experiments.
  - Dedicated ALP/vector dark matter or dark energy search.

The storage ring proton EDM experiment

Jim Alexander[7], Vassilis Anastassopoulos[36], Rick Baartman[28], Stefan Baeßler[39,22], Franco Bedeschi[19], Martin Berz[17], Michael Blaskiewicz[4], Themis Bowcock[33], Kevin Brown[4], Dmitry Budker[9,31], Sergey Burdin[33], Brendan C. Casey[8], Gianluigi Casse[34], Giovanni Cantatore[38], Timothy Chupp[34], Hooman Davoudiasl[4], Dmitri Denisov[4], Milind V. Diwan[4], George Fanourakis[20], Antonios Gardikiotis[30,36], Claudio Gatti[18], James Gooding[33], Renee Fatemi[32], Wolfram Fischer[4], Peter Graham[26], Frederick Gray[23], Selcuk Haciomeroglu[6], Georg H. Hoffstaetter[7], Haixin Huang[4], Marco Incagli[19], Hoyong Jeong[16], David Kaplan[13], Marin Karuza[37], David Kawall[29], On Kim[6], Ivan Koop[5], Valeri Lebedev[14,8], Jonathan Lee[27], Soohyung Lee[6], Alberto Lusiani[25,19], William J. Marciano[4], Marios Maroudas[36], Andrei Matlashov[6], Francois Meot[4], James P. Miller[3], William M. Morse[4], James Mott[3,8], Zhanibek Omarov[15,6], Cenap Ozben[11], SeongTae Park[6], Giovanni Maria Piacentino[35], Boris Podobedov[4], Matthew Poelker[12], Dinko Pocanic[39], Joe Price[33], Deepak Raparia[4], Surjeet Rajendran[13], Sergio Rescia[4], B. Lee Roberts[3], Yannis K. Semertzidis [*6,15], Alexander Silenko[14], Amarjit Soni[4], Edward Stephenson[10], Riad Suleiman[12], Michael Syphers[21], Pia Thoerngren[24], Volodya Tishchenko[4], Nicholaos Tsoupas[4], Spyros Tzamarias[1], Alessandro Variola[18], Graziano Venanzoni[19], Eva Vilella[33], Joost Vossebeld[33], Peter Winter[2], Eunil Won[16], Anatoli Zelenski[4], and Konstantin Zioutas[36]

[1] *Aristotle University of Thessaloniki, Thessaloniki, Greece*
[2] *Argonne National Laboratory, Lemont, Illinois, USA*
[3] *Boston University, Boston, Massachusetts, USA*
[4] *Brookhaven National Laboratory, Upton, New York, USA*
[5] *Budker Institute of Nuclear Physics, Novosibirsk, Russia*
[6] *Center for Axion and Precision Physics Research, Institute for Basic Science, Daejeon, Korea*
[7] *Cornell University, Ithaca, New York, USA*
[8] *Fermi National Accelerator Laboratory, Batavia, Illinois, USA*
[9] *Helmholtz-Institute Mainz, Johannes Gutenberg University, Mainz, Germany*
[10] *Indiana University, Bloomington, Indiana, USA*
[11] *Istanbul Technical University, Istanbul, Turkey*

arXiv:2205.00830v1 [hep-ph] 25 Apr 2022

ARIADNE and nucleon EDMs

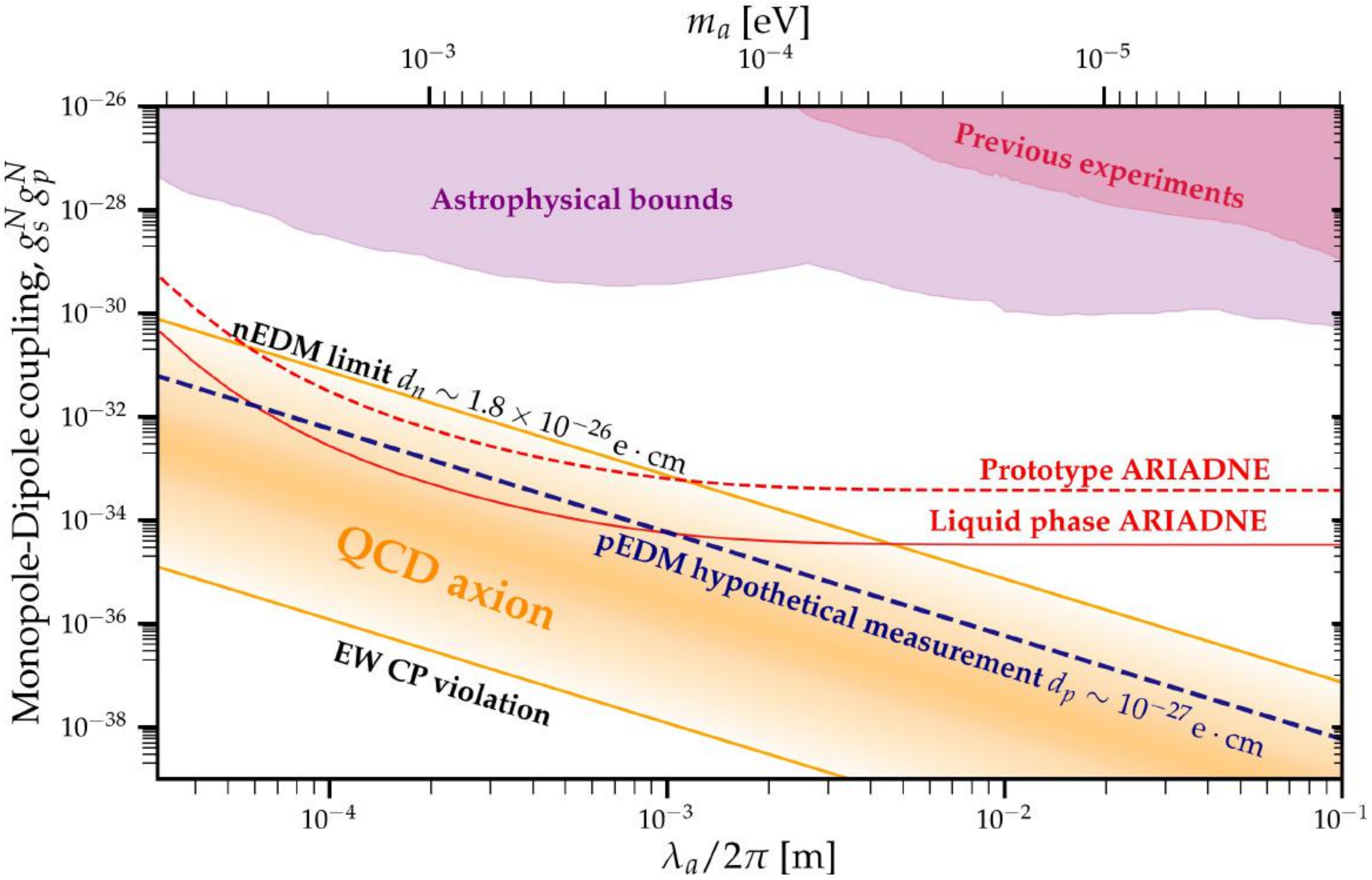

Y. K. Semertzidis and S. Youn. , 2104.14831

- Combine with ARIADNE and nucleon EDM provides decisive information
- Scenario:
  - ARIADNE: Null axion
  - pEDM measure: $d_p \sim 10^{-27} \mathrm{e} \cdot \mathrm{cm}$
  - Exclude QCD axion independent of axion DM:

$$0.2\ \mathrm{meV} \lesssim m_a \lesssim 3\mathrm{meV}$$

Snowmass paper on pEDM

ALP-EDM coupling

Signature Vertical rotation of polarization.
Setup Longitudinal initial polarization.
Sensitivity

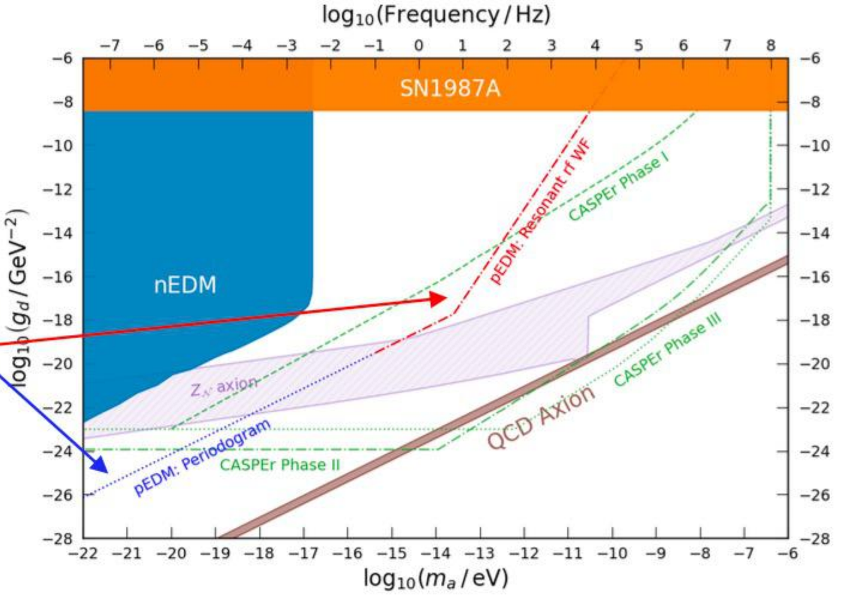

Storage ring pEDM

P. Graham and S. Rajendran, PRD 88, 035023 (2013)
S. Chang *et al.*, PRD 99, 083002 (2019)
On Kim and Y. Semertzidis, PRD 104, 096006 (2021)

arXiv:2205.00830v1 [hep-ph] 25 Apr 2022

The storage ring proton EDM experiment

Jim Alexander[7], Vassilis Anastassopoulos[36], Rick Baartman[28], Stefan Baeßler[39,22], Franco Bedeschi[19], Martin Berz[17], Michael Blaskiewicz[4], Themis Bowcock[33], Kevin Brown[4], Dmitry Budker[9,31], Sergey Burdin[33], Brendan C. Casey[8], Gianluigi Casse[34], Giovanni Cantatore[38], Timothy Chupp[34], Hooman Davoudiasl[4], Dmitri Denisov[4], Milind V. Diwan[4], George Fanourakis[20], Antonios Gardikiotis[30,36], Claudio Gatti[18], James Gooding[33], Renee Fatemi[32], Wolfram Fischer[4], Peter Graham[26], Frederick Gray[23], Selcuk Haciomeroglu[6], Georg H. Hoffstaetter[7], Haixin Huang[4], Marco Incagli[19], Hoyong Jeong[16], David Kaplan[13], Marin Karuza[37], David Kawall[29], On Kim[6], Ivan Koop[5], Valeri Lebedev[14,8], Jonathan Lee[27], Soohyung Lee[6], Alberto Lusiani[25,19], William J. Marciano[4], Marios Maroudas[36], Andrei Matlashov[6], Francois Meot[4], James P. Miller[3], William M. Morse[4], James Mott[3,8], Zhanibek Omarov[15,6], Cenap Ozben[11], SeongTae Park[6], Giovanni Maria Piacentino[35], Boris Podobedov[4], Matthew Poelker[12], Dinko Pocanic[39], Joe Price[33], Deepak Raparia[4], Surjeet Rajendran[13], Sergio Rescia[4], B. Lee Roberts[3], Yannis K. Semertzidis [*6,15], Alexander Silenko[14], Amarjit Soni[4], Edward Stephenson[10], Riad Suleiman[12], Michael Syphers[21], Pia Thoerngren[24], Volodya Tishchenko[4], Nicholaos Tsoupas[4], Spyros Tzamarias[1], Alessandro Variola[18], Graziano Venanzoni[19], Eva Vilella[33], Joost Vossebeld[33], Peter Winter[2], Eunil Won[16], Anatoli Zelenski[4], and Konstantin Zioutas[36]

[1] *Aristotle University of Thessaloniki, Thessaloniki, Greece*
[2] *Argonne National Laboratory, Lemont, Illinois, USA*
[3] *Boston University, Boston, Massachusetts, USA*
[4] *Brookhaven National Laboratory, Upton, New York, USA*
[5] *Budker Institute of Nuclear Physics, Novosibirsk, Russia*
[6] *Center for Axion and Precision Physics Research, Institute for Basic Science, Daejeon, Korea*
[7] *Cornell University, Ithaca, New York, USA*
[8] *Fermi National Accelerator Laboratory, Batavia, Illinois, USA*
[9] *Helmholtz-Institute Mainz, Johannes Gutenberg University, Mainz, Germany*
[10] *Indiana University, Bloomington, Indiana, USA*
[11] *Istanbul Technical University, Istanbul, Turkey*

Dipole-monopole interactions for the storage ring experiments

arXiv:2210.17547v1 [hep-ph] 31 Oct 2022

Axion field acting on muon (g-2) and proton EDM

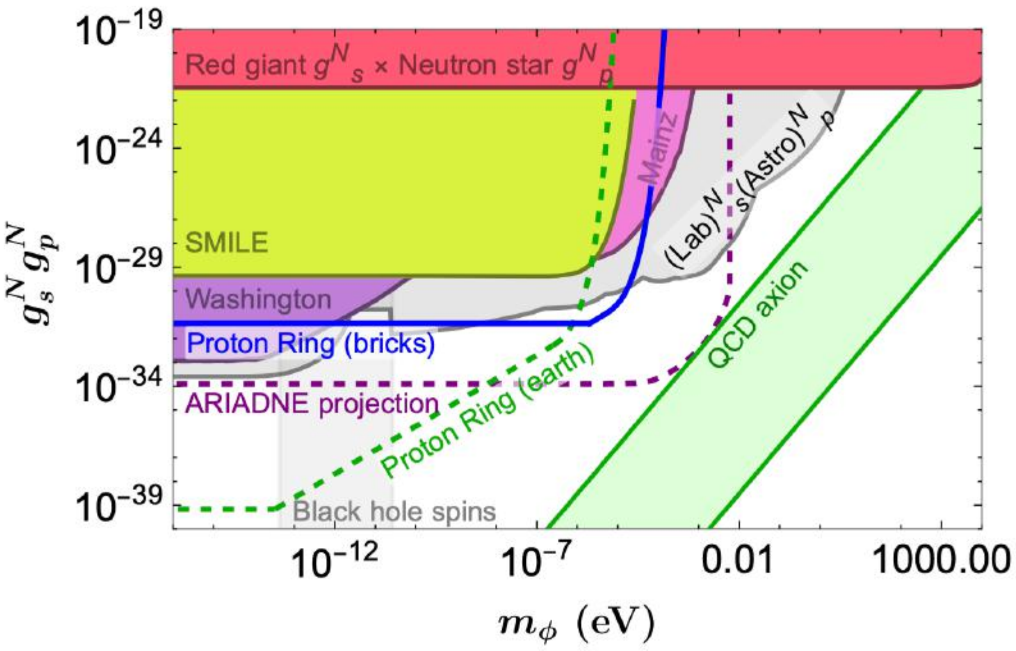

Figure 2. Expected sensitivity to axion forces in the proton storage ring experiment. The blue line corresponds to cubic lead bricks of 10cm size around the ring at a distance around 10cm from the beams generating spin precession out of the plane (EDM-like signature). We consider the conservative case of covering only $O(10\%)$ of the ring with bricks. This fraction is an important parameter, as the reach increases linearly with it. The green dashed line corresponds to the limits due to the axion field from the ground nucleons (spin precession on the ring plane). It is assumed that the ring is located around 150 cm above the ground. Combination of both configurations gives the strongest bounds to monopole-dipole forces on nucleons, beating astrophysics and existing laboratory bounds for any mass below $m_\phi = 10^{-5}$ eV. Bounds adapted from [30].

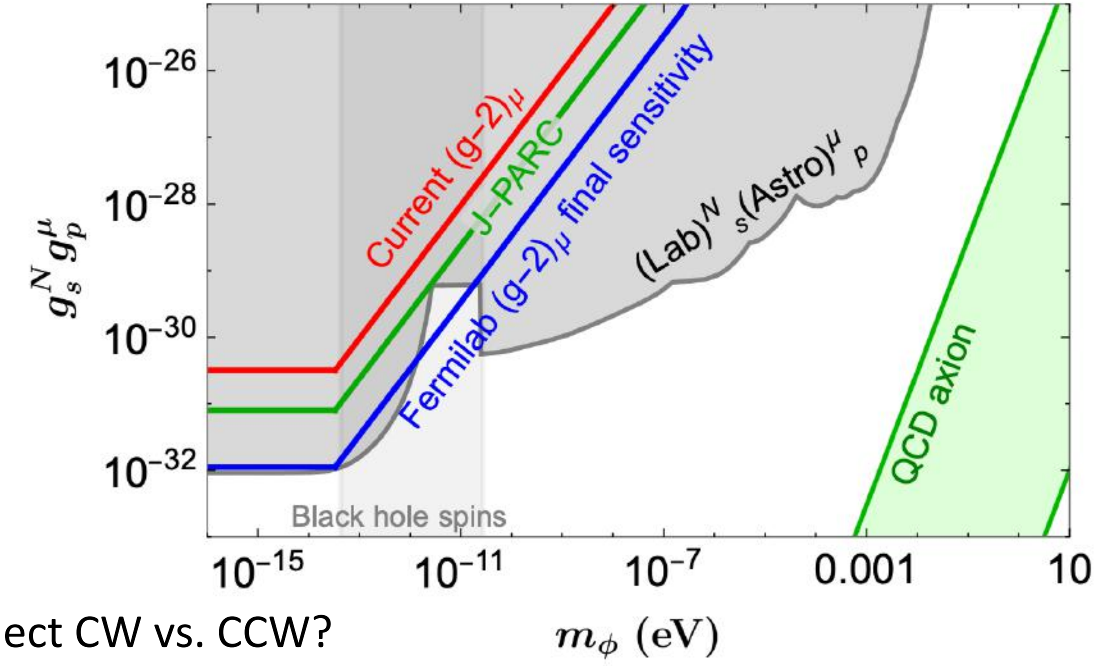

Inject CW vs. CCW?

Figure 1. Axion-mediated monopole-dipole forces on muons. The red line corresponds to the values required to explain the $(g-2)_\mu$ anomaly at Fermilab and BNL assuming a signal at the level $\delta\omega_a \approx 4$ rad/s. Bounds from astrophysics are shown in gray. The anomaly can be more easily explained in the region around $m_\phi \sim 10^{-12}$ eV, where the new force limits are the weakest. This is still in slight conflict with SN bounds. Note that the stronger bound on a new force with $m_\phi \sim 10^{-11}$ eV would also apply at $m_\phi \sim 10^{-12}$ eV if the force violated the EP maximally. Thus, for this relaxation of limits, we require the new force to obey the EP at the ~ 1 percent level, which is reasonable in many models (*e.g.* mediation via the higgs). The green line corresponds to the expected sensitivity at J-PARC, which will reach the 0.45 ppm level of precision. The final sensitivity of Fermilab $(g-2)_\mu$, at the 0.1ppm level which corresponds to $\delta w_a = O(0.1)$ rad/s, is in blue.

Storage ring pEDM at $10^{-29}e$-cm, best hadronic EDM exp.

- High physics reach at hundreds of TeV New-Physics mass scale, improve sensitivity to θ_{QCD} by three orders of magnitude. Best sensitivity to Higgs CPV

- If found, it can help explain the matter-antimatter asymmetry of the universe.

- Together with ARIADNE (monopole-dipole interactions) probe high frequency axion dark matter and axion physics in unique ways.

- Direct search for low/very low frequency axion dark matter

- High intensity polarized proton and deuteron beams available. The natural beam lifetime is very long, opportunity for high statistical accuracy.

Muon g-2 experiment

- Muon g-2 results announcement at Fermilab, April 2021 reached >3B people.

- Muon g-2 success. The collaboration developed several new tools for systematic error probing.

- High-precision numerical integrators for beam/spin dynamics simulations.

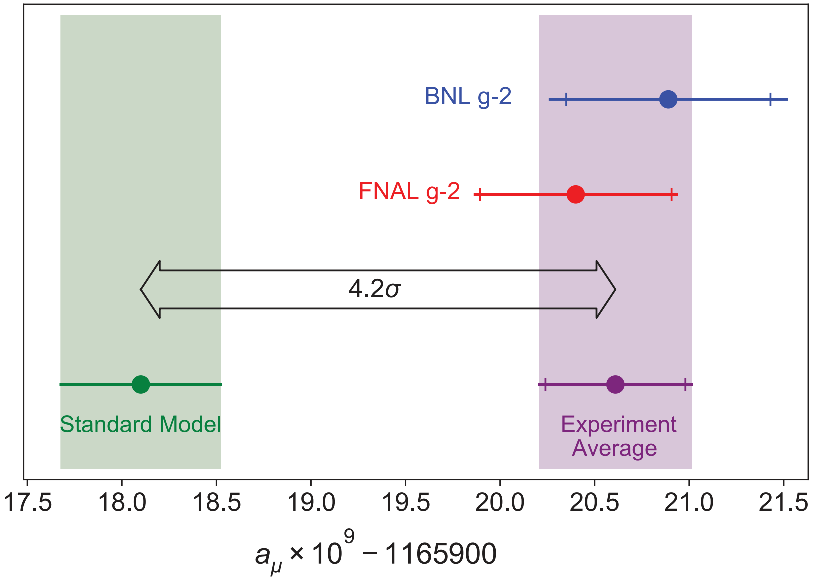

FIG. 4. From top to bottom: experimental values of a_μ from BNL E821, this measurement, and the combined average. The inner tick marks indicate the statistical contribution to the total uncertainties. The Muon $g-2$ Theory Initiative recommended value [13] for the standard model is also shown.

Overview of Muon $g-2$ Experiment at Fermilab (E989)

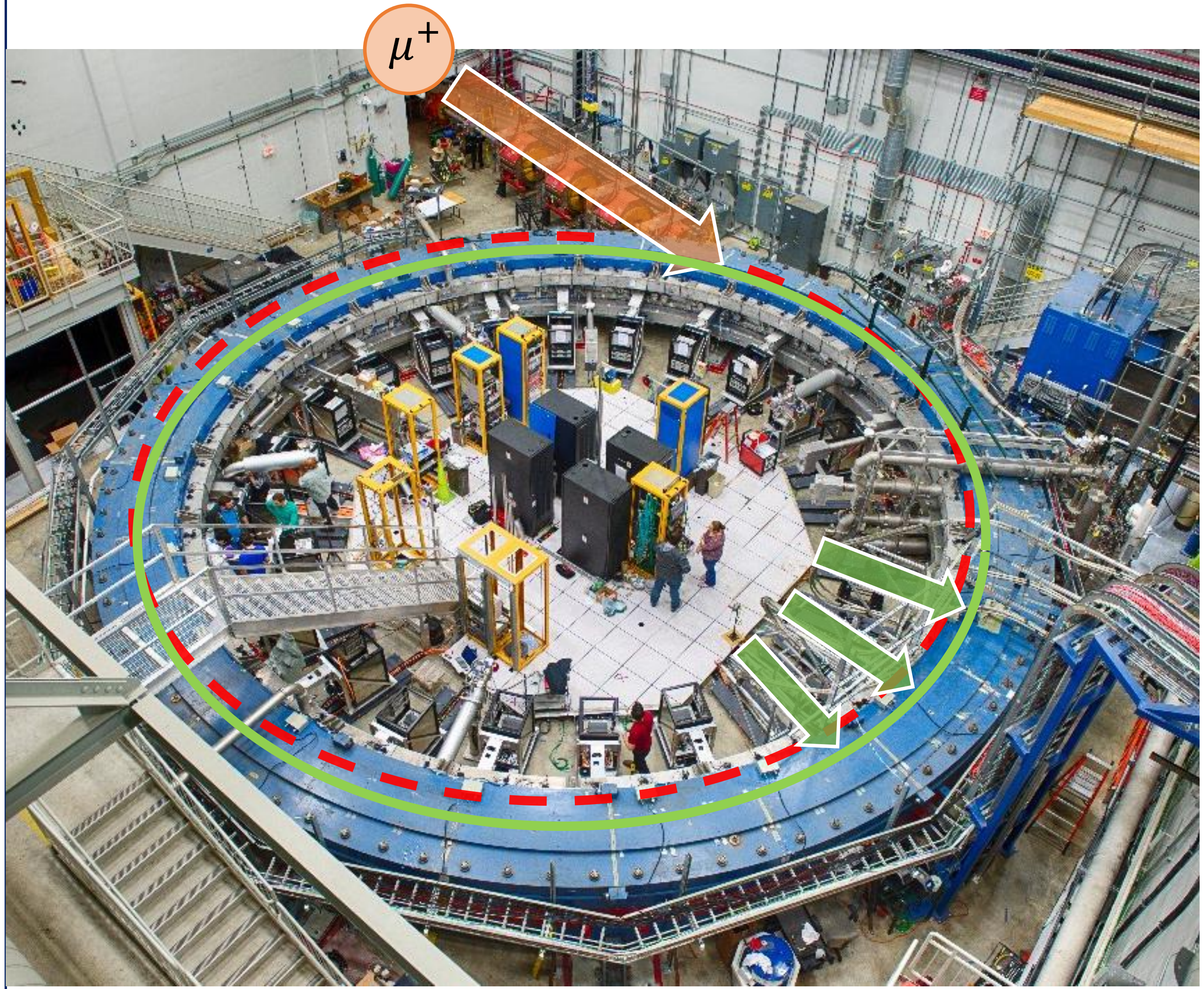

▶ Kick

- Muons are kicked onto the design orbit by the fast non-ferric **kicker magnet** system.

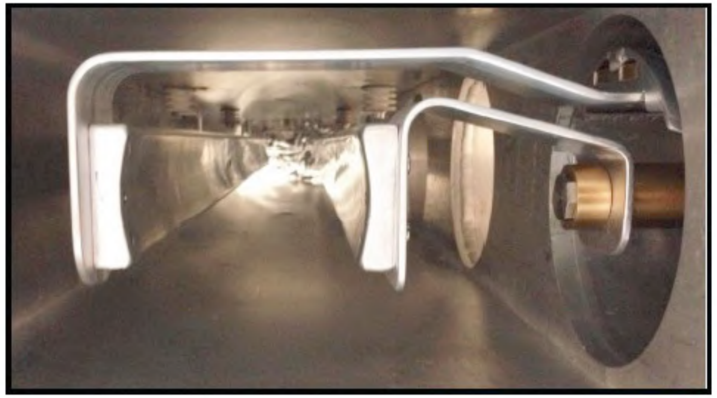

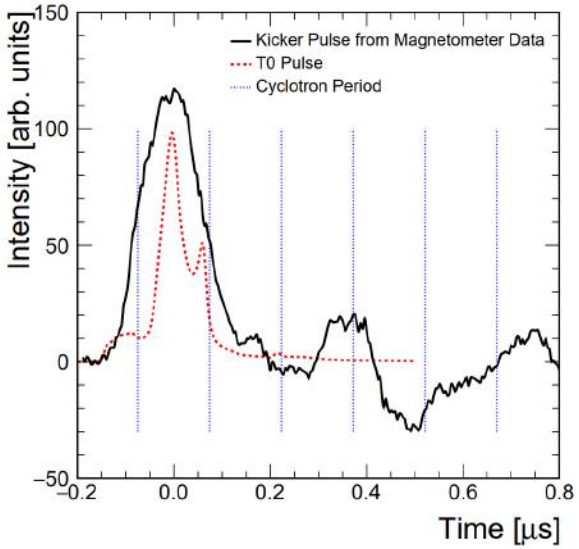

Coherent betatron oscillations influence the g-2 phase

- CBO frequency $f_{cbo} = f_c\left(1 - \sqrt{1-n}\right)$. Radial oscillations, through aliasing, became a problem
- A very high-frequency, cascaded through various effects down to g-2 frequency

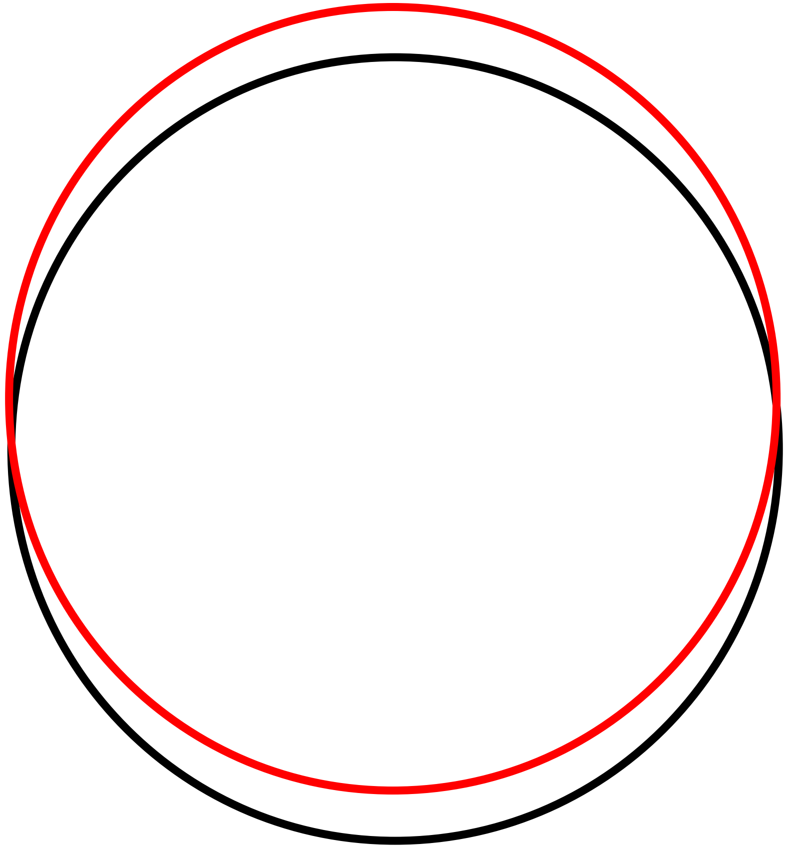

Straw trackers

▶ Straw trackers

- Measures trajectories of the decay positrons and extrapolates to find the muon distribution.

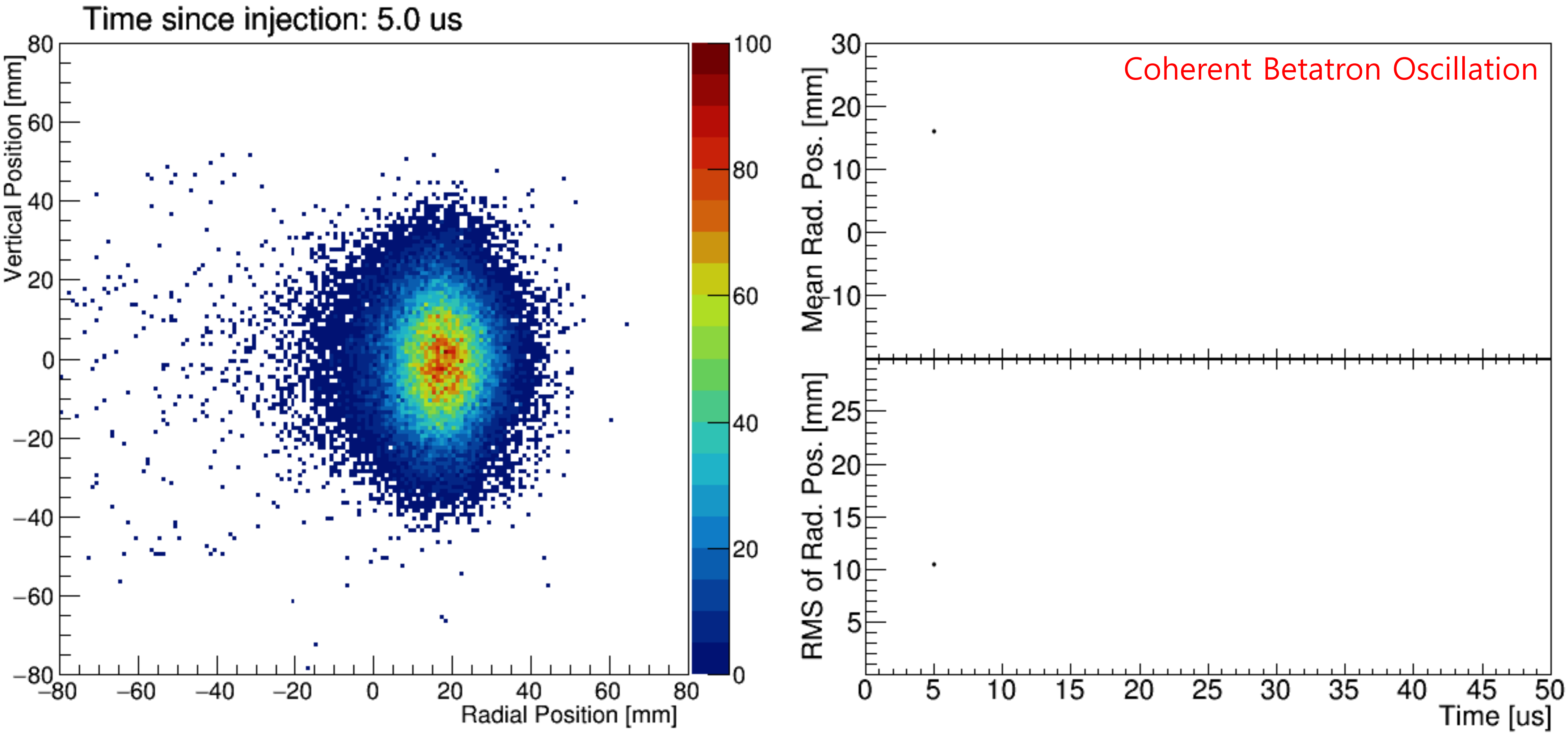

CBO in the 2001 Data Set

$$f(t) = N_0 e^{-\lambda t}[1 + A\cos(\omega_a t + \phi)]$$

Residuals from fitting the 5-parameter function

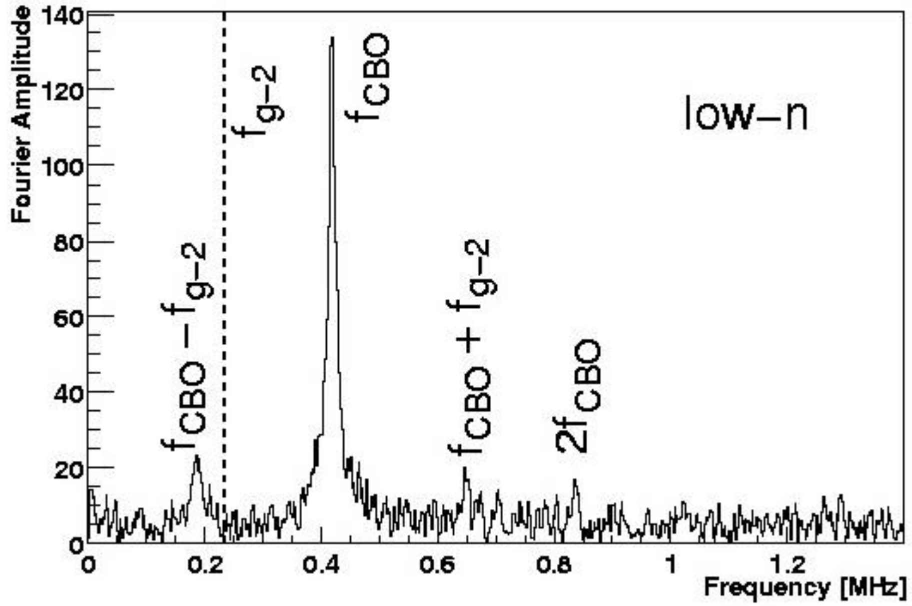

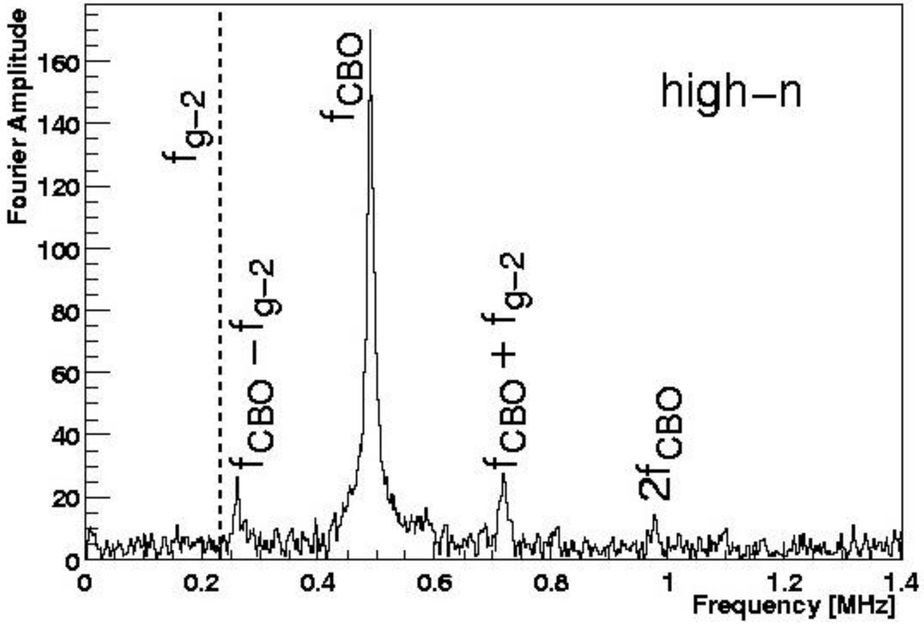

CBO in the Data Set

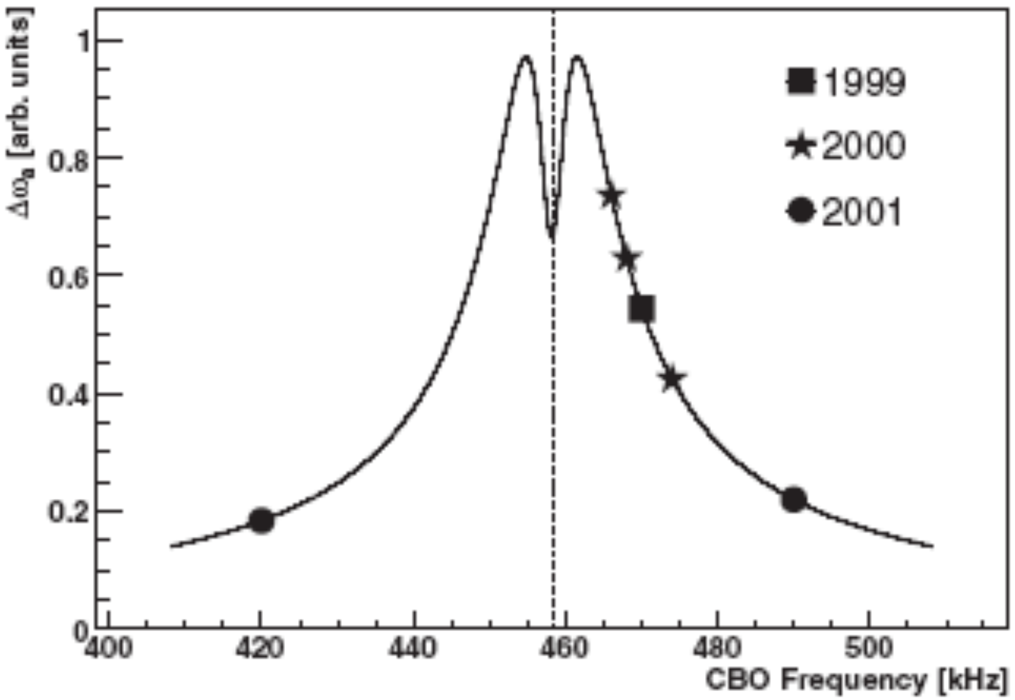

FIG. 36. The relative pull ($\Delta\omega$) versus the CBO modulation frequency *if not* addressed by the fitting function. A typical full vertical scale is several ppm; the actual scale depends on the specifics of the fit and the data set used. The R00 data were acquired under run conditions in which ω_a was very sensitive to CBO. This sensitivity was minimized in the R01 period where low- and high-n subperiods, each having CBO frequencies well below or above twice the $(g-2)$ frequency, were employed.

The effect depends on the CBO frequency

Yuri Orlov suggested to fix it by using a pair of plates (PE) as mini-kicker: We tried his method at Fermilab; it worked.

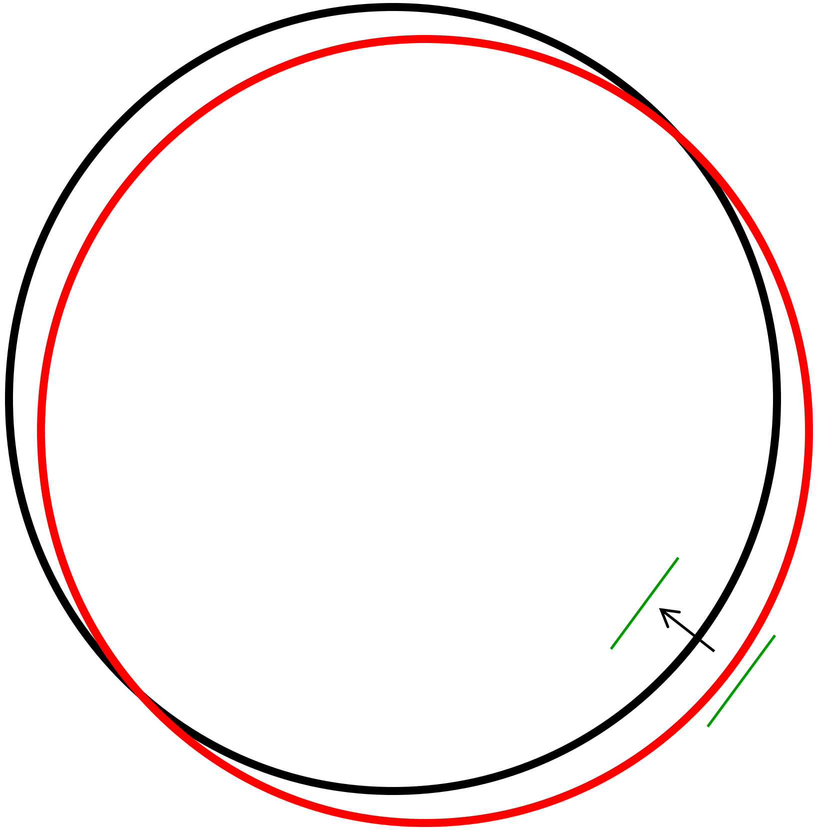

PE plates are 1m long
Apply rf E-field 470KHz

QUAD-RF SYSTEM

On Kim’s slide

RF rack

- Generates and amplifies RF signals.

Quad-RF feedthrough

- Couples to existing quad HV system.

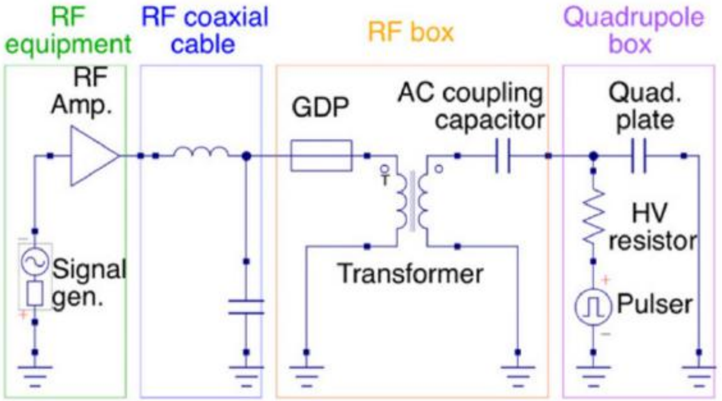

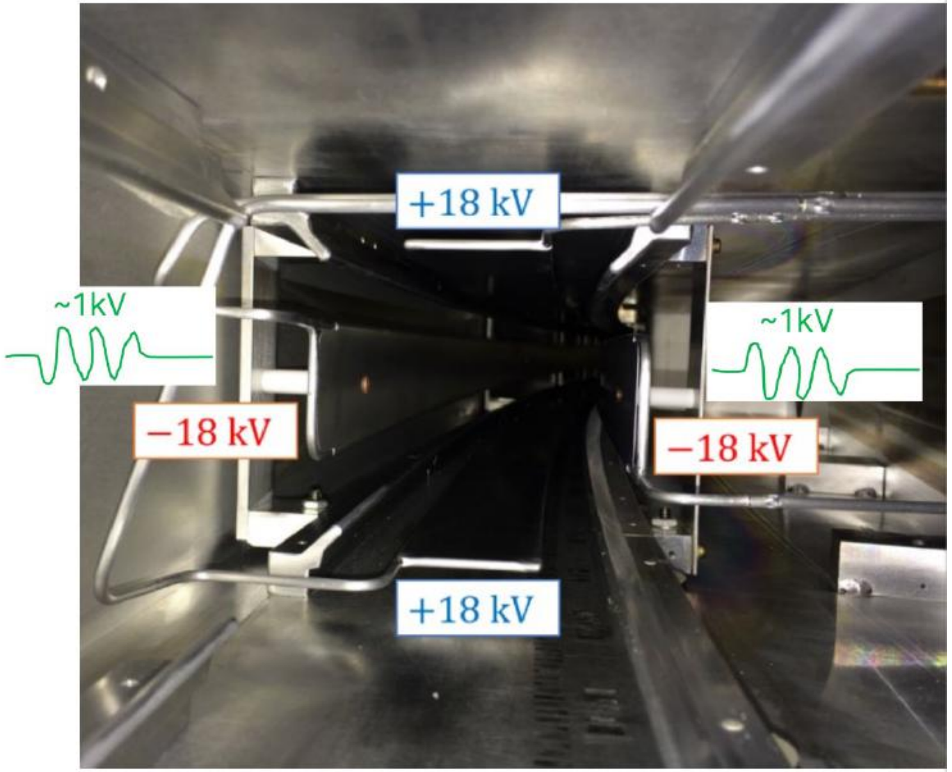

Quad HV + RF

- ~1 kV RF signals are superposed to Quad HV.
- Only applied during the early storage < 30 us.
- Typically applied to inner/outer plates to reduce the CBO amplitude, but can be applied to top/bottom plates as well to reduce muon losses more.

Simulation

Parameter	Run-1d	Run-2	(Projected) RF CBO reduction
τ_{CBO} [μs]	190 ± 11	259.8 ± 9.3	-
$A^{N}_{\mathrm{CBO}} \times 10^4$	32.4 ± 1.0	32.7 ± 0.4	1.8
$A^{A}_{\mathrm{CBO}} \times 10^4$	5.9 ± 1.4	3.4 ± 0.7	0.3
$A^{\phi}_{\mathrm{CBO}} \times 10^4$	1.1 ± 0.7	0.4 ± 0.7	0.1

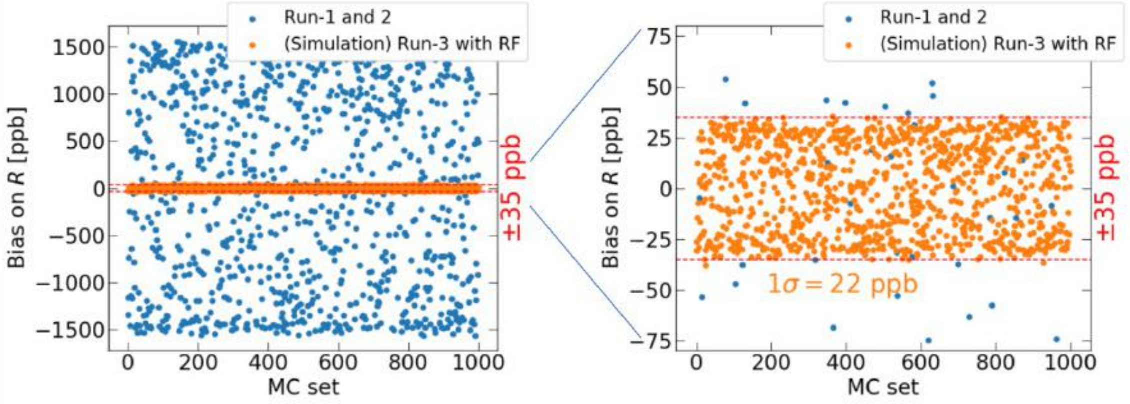

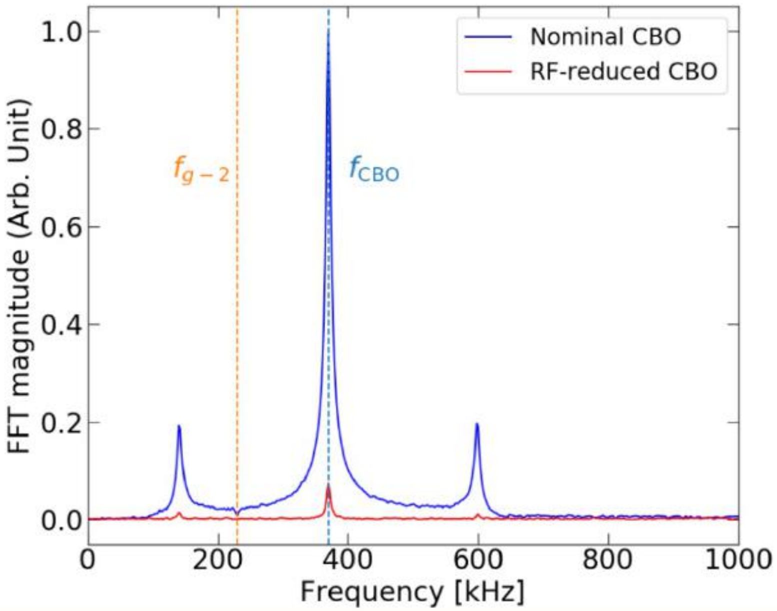

On Kim's slide

Estimated reduction of the CBO systematic uncertainty

- Details can be found in DocDB 24590.
- Dominant CBO fit parameters would be reduced by an order of magnitude (see Table left).
- Estimated reduction in the CBO systematic uncertainty: by a factor of 50.
- Final CBO uncertainty would've been < 1 ppb.

Data

- When focused only on the CBO reduction.
- CBO amplitude was reduced by an order of magnitude.
- Final CBO amplitude after 30 us: < 1 mm.

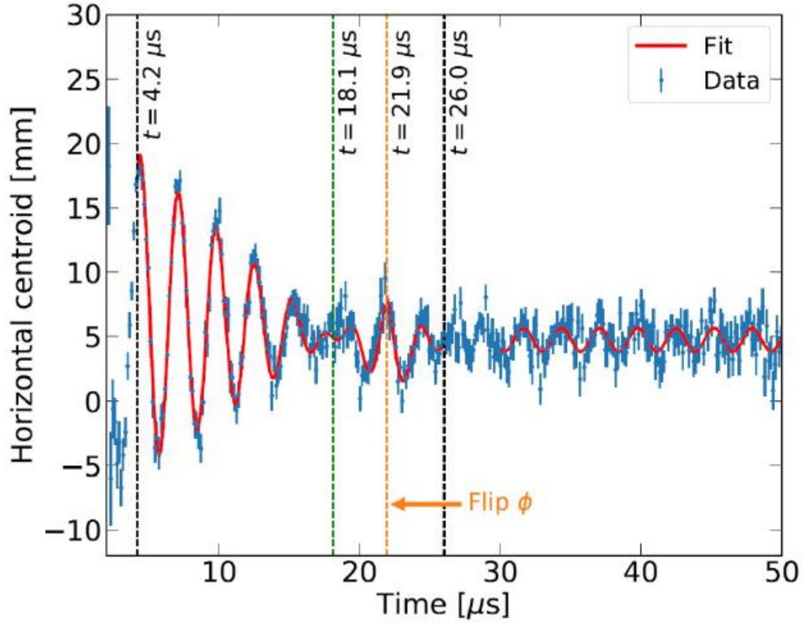

RF CBO amplitude reduction (data from muon g-2 experiment)

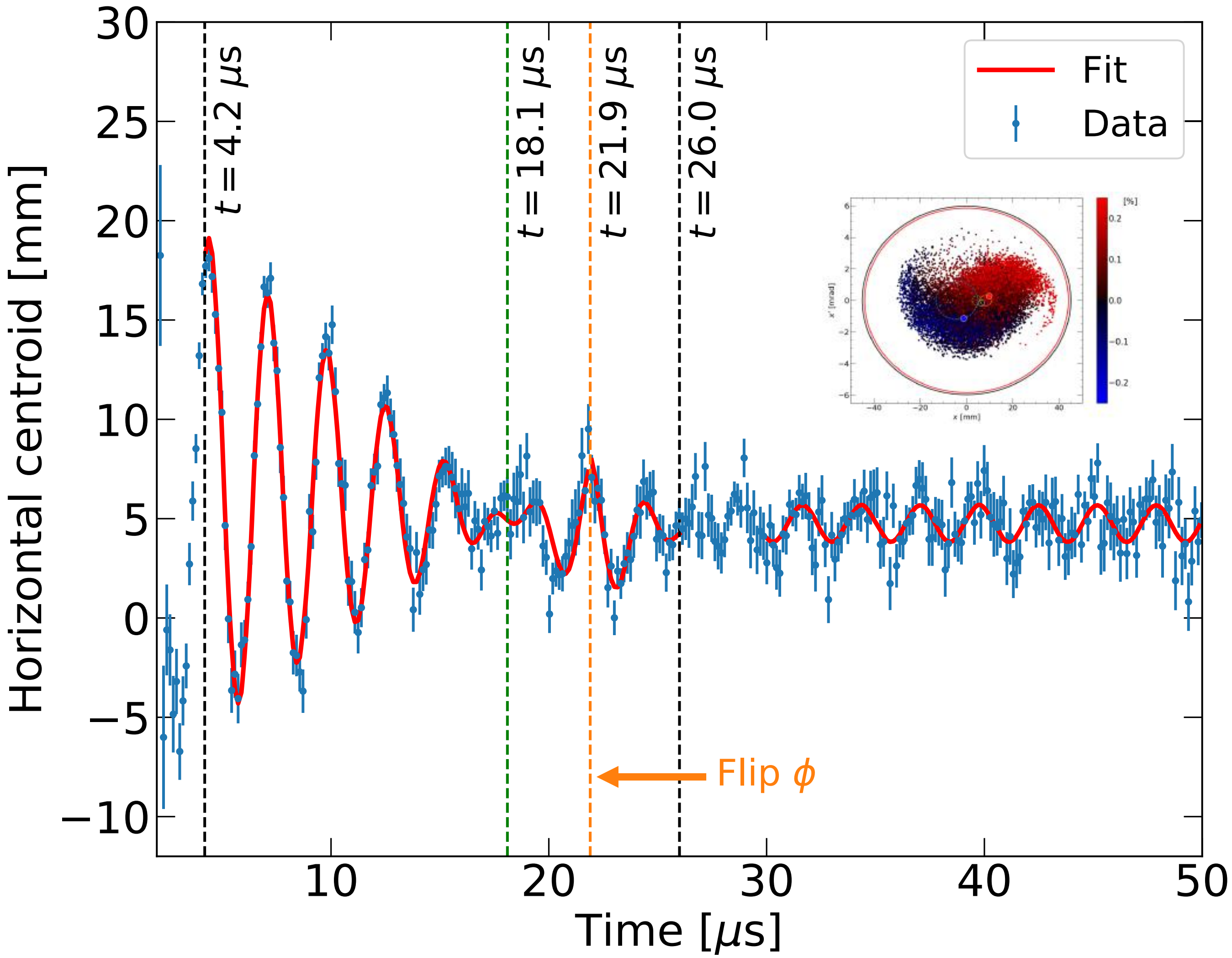

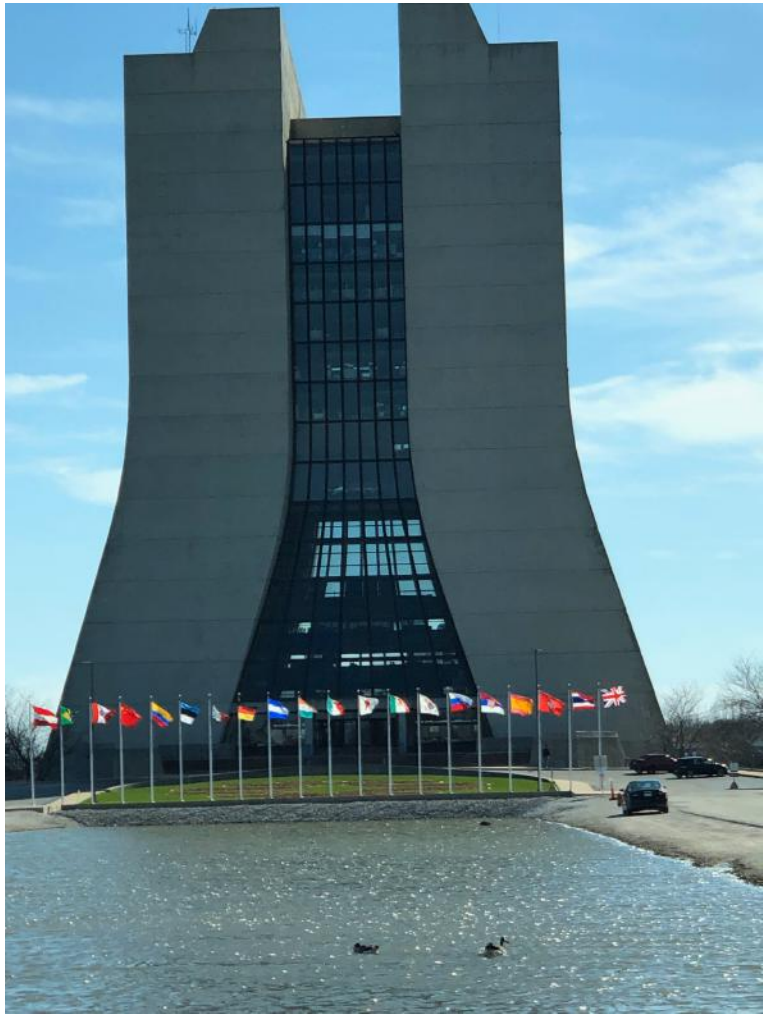

On Kim *et al*, New J. Phys. **22** (2020) 063002

Hadronic Electric Dipole Moments

Input to hadronic EDM

- Theta-QCD (part of the SM)
- CP-violation sources beyond the SM

Several alternative simple systems could provide invaluable complementary information (e.g. proton, neutron and ^{3}He, deuteron,…).

EDMs of different systems (Marciano)

θ_{QCD}:

$$d_n \simeq -d_p \simeq 3\times 10^{-16}\,\bar{\theta}\ \text{e}\cdot\text{cm}$$

$$d_D\left(\bar{\theta}\right)/d_N\left(\bar{\theta}\right) \approx 1/3$$

Super-Symmetry (SUSY) model predictions:

$$d_n \simeq 1.4\left(d_d - 0.25 d_u\right) + 0.83e\left(d_u^c + d_d^c\right) - 0.27e\left(d_u^c - d_d^c\right)$$

$$d_p \simeq 1.4\left(d_d - 0.25 d_u\right) + 0.83e\left(d_u^c + d_d^c\right) + 0.27e\left(d_u^c - d_d^c\right)$$

$$d_D \simeq \left(d_u + d_d\right) - 0.2e\left(d_u^c + d_d^c\right) - 6e\left(d_u^c - d_d^c\right)$$

$$d_N^{I=1} \simeq 0.87\left(d_u - d_d\right) + 0.27e\left(d_u^c - d_d^c\right) \qquad d_N^{I=1} = \left(d_p - d_n\right)/2$$

$$d_N^{I=0} \simeq 0.5\left(d_u + d_d\right) + 0.83e\left(d_u^c + d_d^c\right) \qquad d_N^{I=0} = \left(d_p + d_n\right)/2$$

Storage ring Electric Dipole Moments

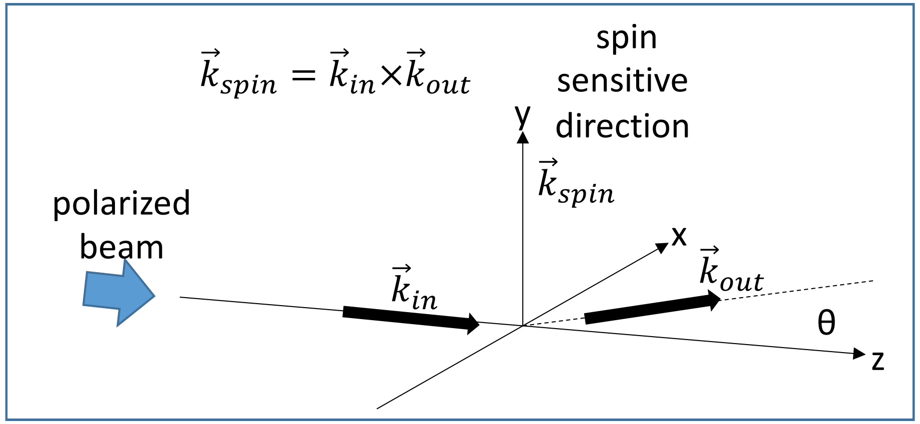

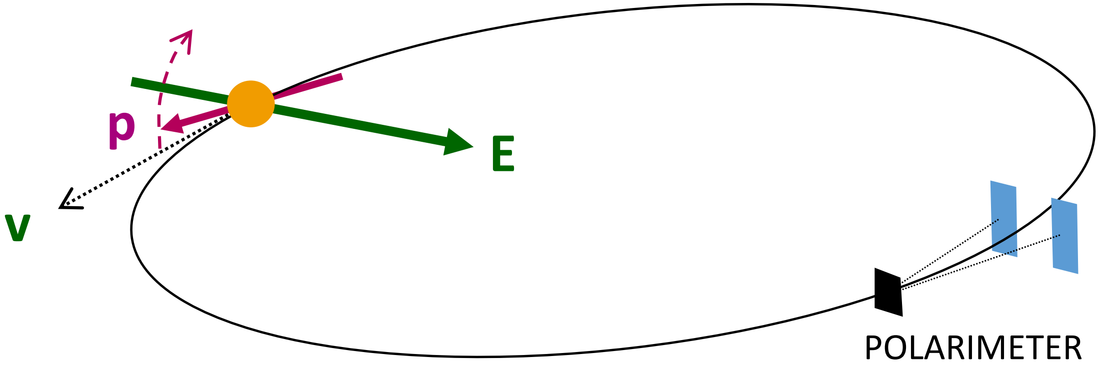

Phys. Rev. Lett. 93, 052001 (2004)

Frozen spin method:

- Spin aligned with the momentum vector
- Radial E-field precesses EDM/spin vertically
- Monitoring the spin using a polarimeter

Storage Ring EDM experiments, frozen spin method

Pure electric bending, w/ “magic” momentum

F.J.M. Farley *et al.*, “A new method of measuring electric dipole moments in storage rings,” Phys. Rev. Lett. 93, 052001 (2004)

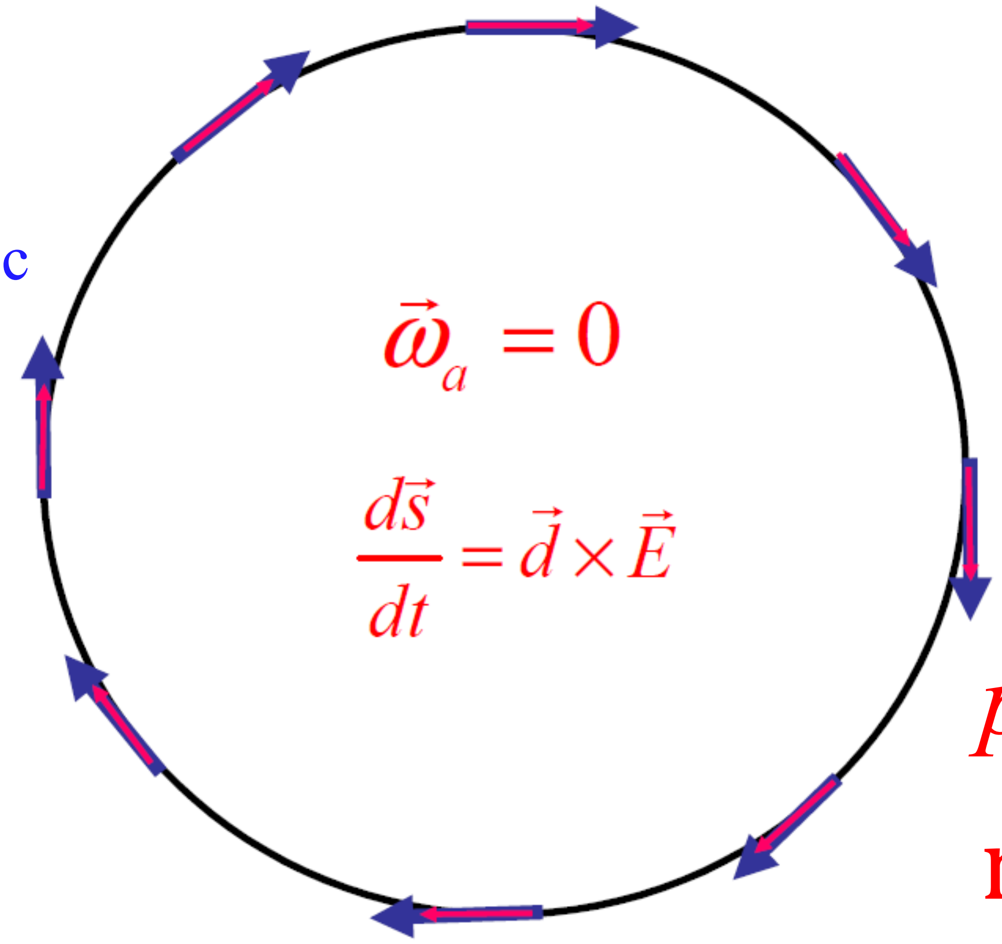

$$\vec{\omega}_a = 0$$

$$\frac{d\vec{s}}{dt} = \vec{d} \times \vec{E}$$

$p = \frac{mc}{\sqrt{a}}$, a: magnetic moment anomaly

Electric fields: Freezing the g-2 spin precession

$$\vec{\omega}_a = -\frac{q}{m}\left[a - \left(\frac{mc}{p}\right)^2\right]\frac{\vec{\beta}\times\vec{E}}{c} = 0$$

- The g-2 spin precession is zero at "magic" momentum (3.1GeV/c for muons,…), so the focusing system can be electric

$$p = \frac{mc}{\sqrt{a}}, with\ a = G = \frac{g-2}{2}, \gamma_m = \sqrt{1+1/a}$$

- The "magic" momentum concept with electric focusing was first used in the last muon g-2 experiment at CERN, at BNL & FNAL.

Proton Statistical Error (233MeV): 10^{-29} *e*-cm

Phys. Rev. D **104**, 096006 (2021)

$$\sigma_d = \frac{2.33\hbar}{E_R P A \sqrt{N_c f \tau_p T_{tot}}}$$

τ_p : 2×10^3s Polarization Lifetime (Spin Coherence Time)
A : 0.6 Left/right asymmetry observed by the polarimeter
P : 0.8 Beam polarization
N_c : 4×10^{10}p/cycle Total number of stored particles per cycle (10^3s)
T_{Tot}: 2×10^7s Total running time per year
f : 1% Useful event rate fraction (efficiency for EDM)
E_R : 4.5 MV/m Radial electric field strength

Systematic errors

^{3}He Co-magnetometer in nEDM experiment

If nEDM = 10^{-26} e·cm,

10 kV/cm → 0.1 μHz shift

$\cong$ B field of 2×10^{-15} T.

Co-magnetometer :

Uniformly samples the B Field faster than the relaxation time.

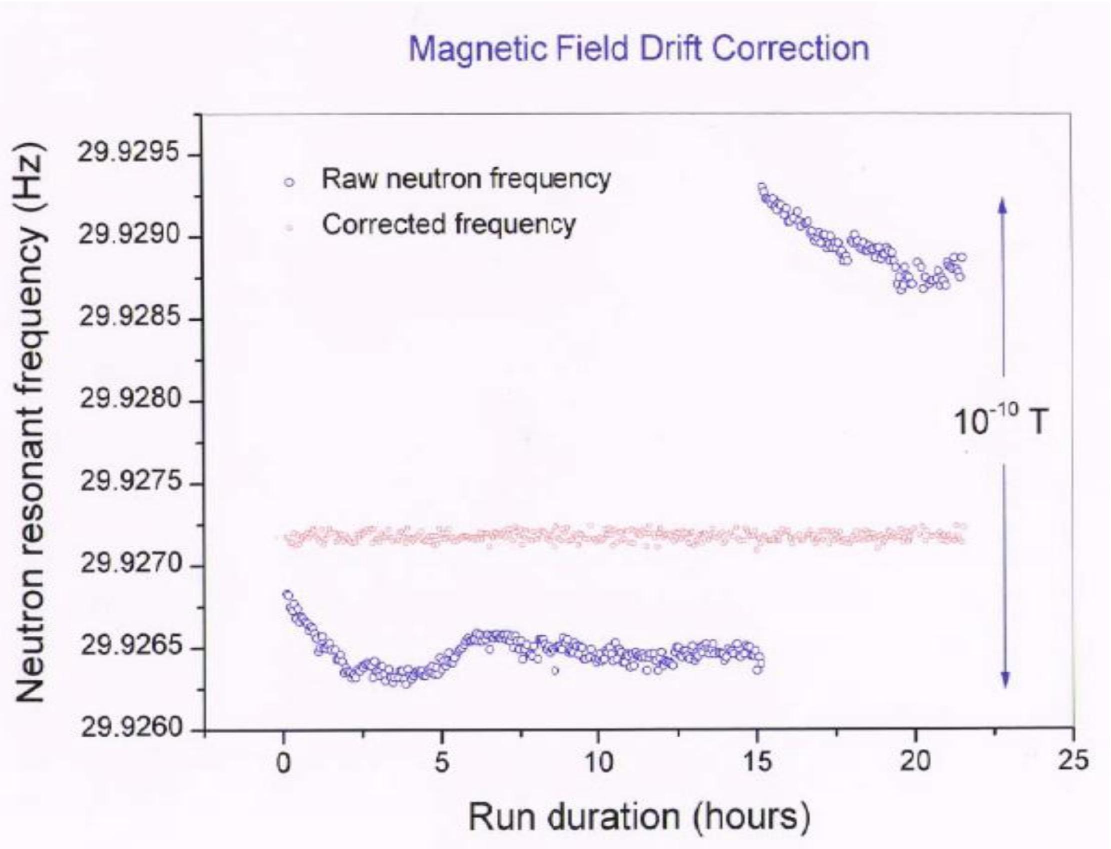

Data: ILL nEDM experiment with ^{199}Hg co-magnetometer

EDM of ^{199}Hg < 10^{-28} e-cm (measured); atomic EDM ~ Z^2 → ^{3}He EDM << 10^{-30} e-cm

Under gravity, the center of mass of He-3 is higher than UCN by $\Delta h \approx 0.13$ cm, sets ΔB = 30 pGauss (1 nA of leakage current). $\Delta B/B=10^{-3}$.

Storage Ring Electric Dipole Moments exp. options

Fields	**Example**	**EDM signal term**	**Comments**
Dipole magnetic field **(B)** **(Parasitic)**	Muon g-2	Tilt of the spin precession plane. **(Limited statistical sensitivity due to spin precession)**	Eventually limited by geometrical alignment. **Requires consecutive CW and CCW injection to eliminate systematic errors**
Combination of electric & and magnetic fields **(E, B)** **(Combined lattice)**	Deuteron, ^{3}He, proton, muon, etc.	Mainly: $\boxed{\frac{d\vec{s}}{dt} = \vec{d} \times \left(\vec{v} \times \vec{B}\right)}$	High statistical sensitivity. **Requires consecutive CW and CCW injection with main fields flipping sign to eliminate systematic errors**
Radial Electric field **(E)** & Electric focusing **(E)** **(All electric lattice)**	Proton, etc.	$\boxed{\frac{d\vec{s}}{dt} = \vec{d} \times \vec{E}}$	Large ring, CW & CCW storage. **Requires demonstration of adequate sensitivity to radial B-field syst. error**
Radial Electric field **(E)** & Magnetic focusing **(B)** **(Hybrid, symmetric lattice)**	Proton, etc.	$\boxed{\frac{d\vec{s}}{dt} = \vec{d} \times \vec{E}}$	Large ring, CW & CCW storage. **Only lattice to achieve direct cancellation of main systematic error sources (its own "co-magnetometer").** GOLD STANDARD!

Effect as a function of azimuthal harmonic *N*

COMPREHENSIVE SYMMETRIC-HYBRID RING DESIGN FOR A … PHYS. REV. D **105,** 032001 (2022)

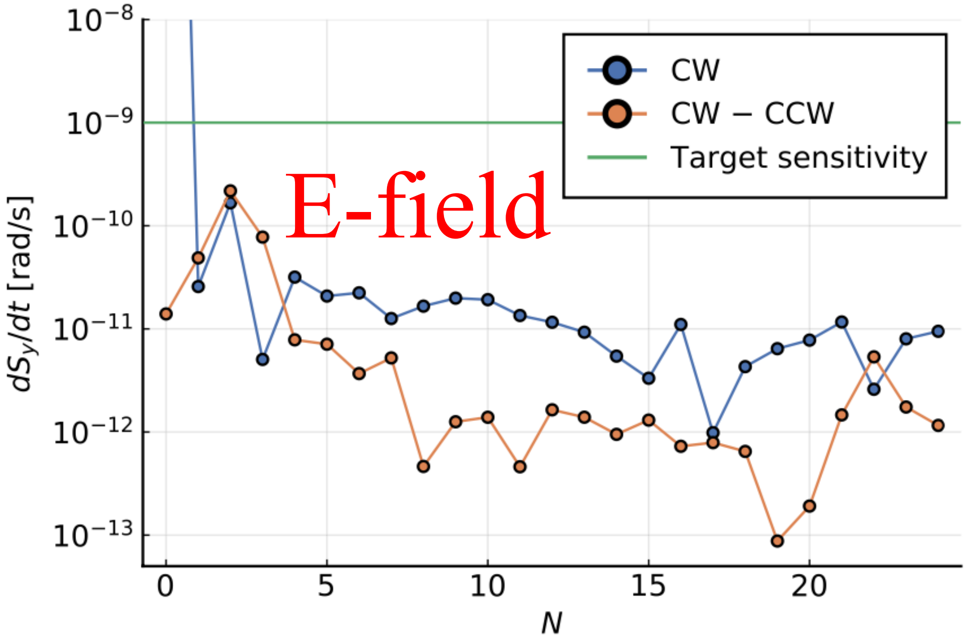

FIG. 7. *Longitudinal polarization case* $S_s = 1$, sensitive to EDM. Vertical spin precession rate vs $E_y = 10$ V/m field N harmonic around the ring azimuth. For $N = 0$, the precession rate for the CW (or CCW) beam is around 5 rad/s. The difference of the precession rates for CR beams (orange) is below the target sensitivity for all N. Irregularities of the low values are due to the inability to determine the exact precession rate from the simulation results. Hence, the points only show a statistical upper limit of the possible vertical precession rate; actual rates could be lower. More about this is in Appendix B.

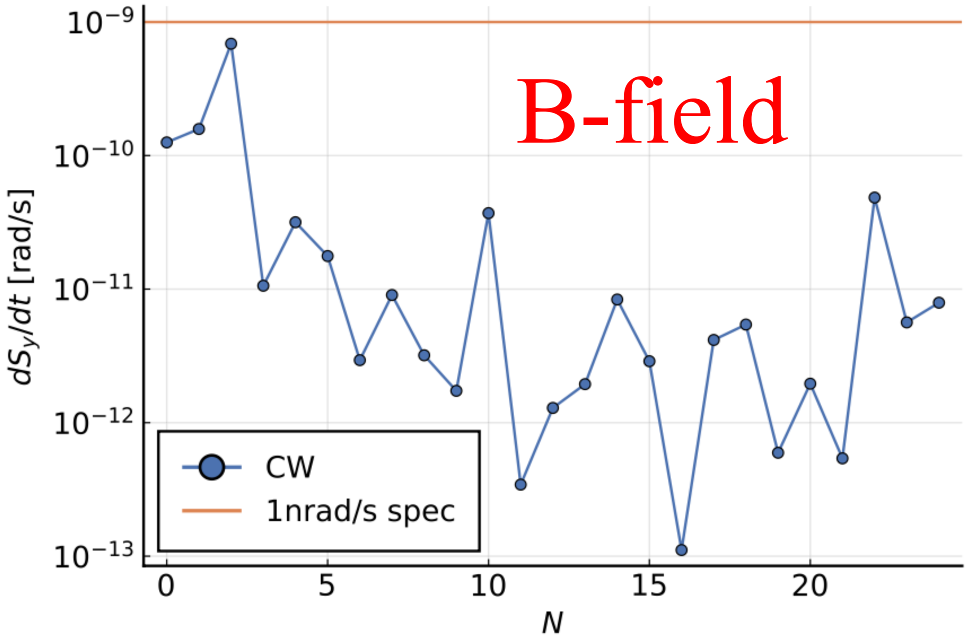

FIG. 8. *Longitudinal polarization case* $S_s = 1$, *CW beam only.* Vertical spin precession rate vs $B_x = 1$ nT field N harmonic around the ring azimuth. The magnetic field amplitude is chosen to be similar to beam separation requirements in Sec. IV A, and more than $B_x = 1$ nT splits the CR beams too much. Irregularities of the low values are due to the inability to determine the exact precession rate from the simulation results. Hence, the points only show a statistical upper limit of the possible vertical precession rate; actual rates could be lower. More about this is in Appendix B.

Ring planarity:
The average vertical speed in deflectors needs to be zero!

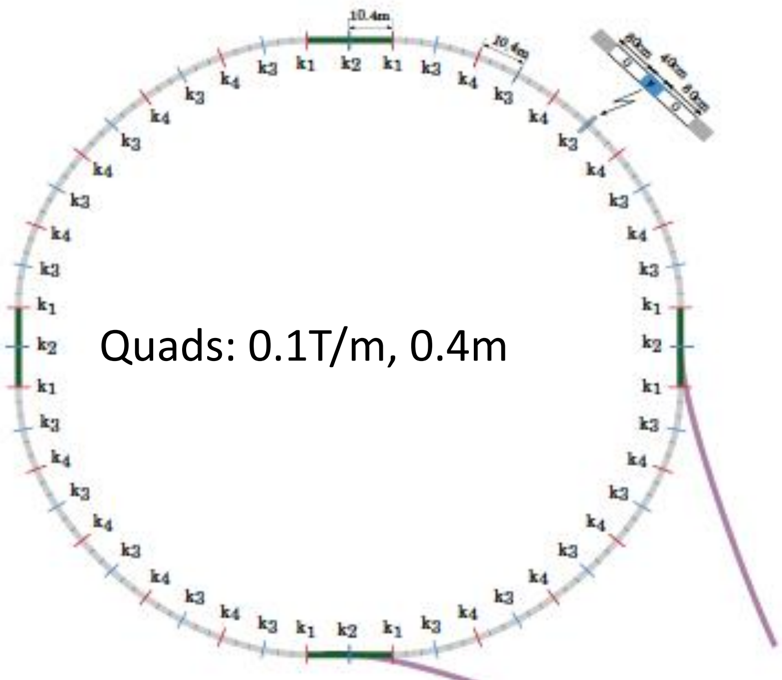

Quads: 0.1T/m, 0.4m

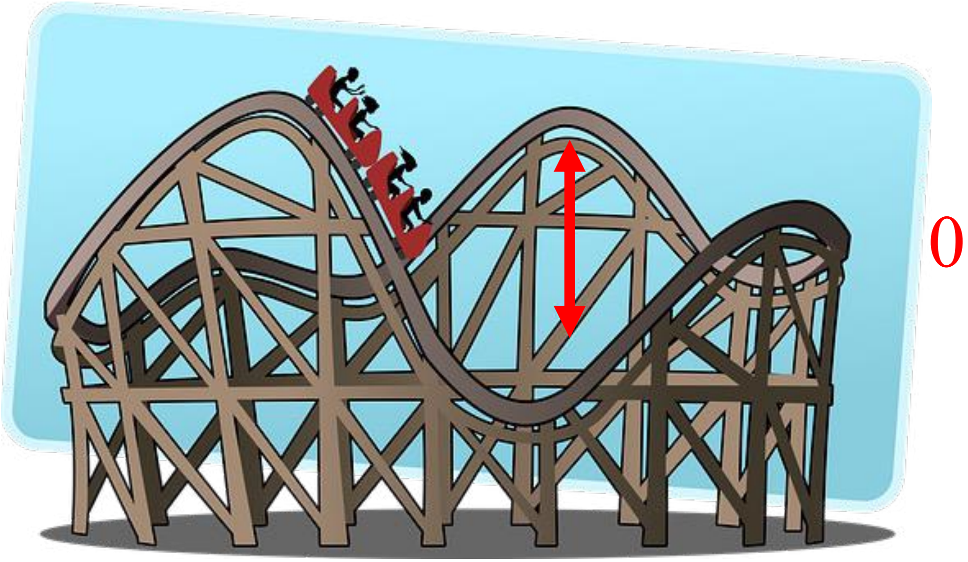

0.1 mm

Hybrid, symmetric lattice storage ring. Great for systematic error reduction.

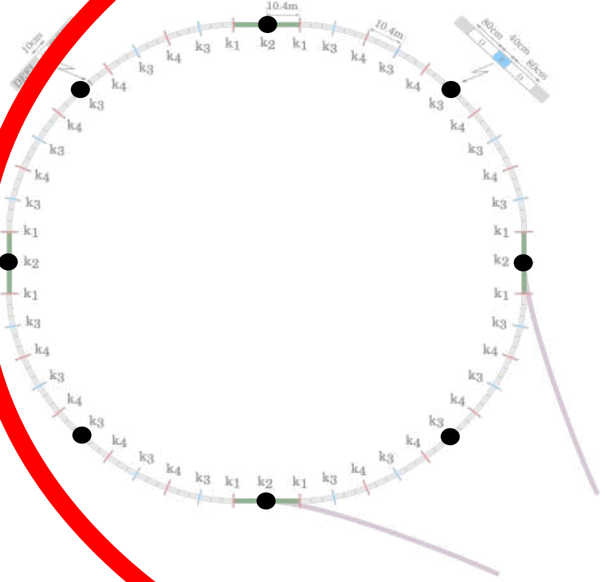

Z. Omarov *et al.*, PHYS. REV. D 105, 032001 (2022)

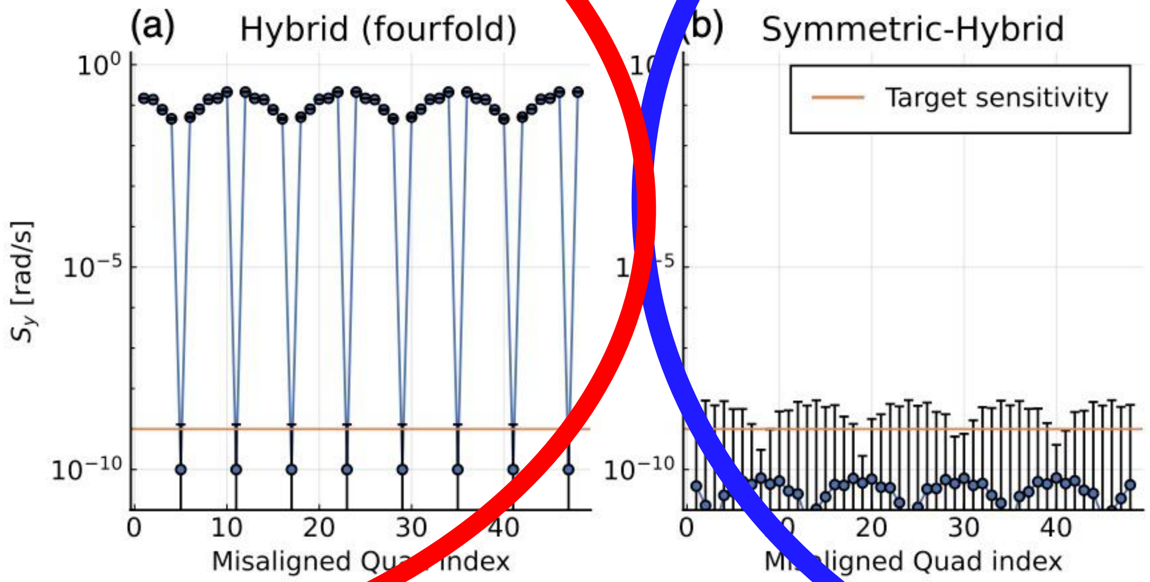

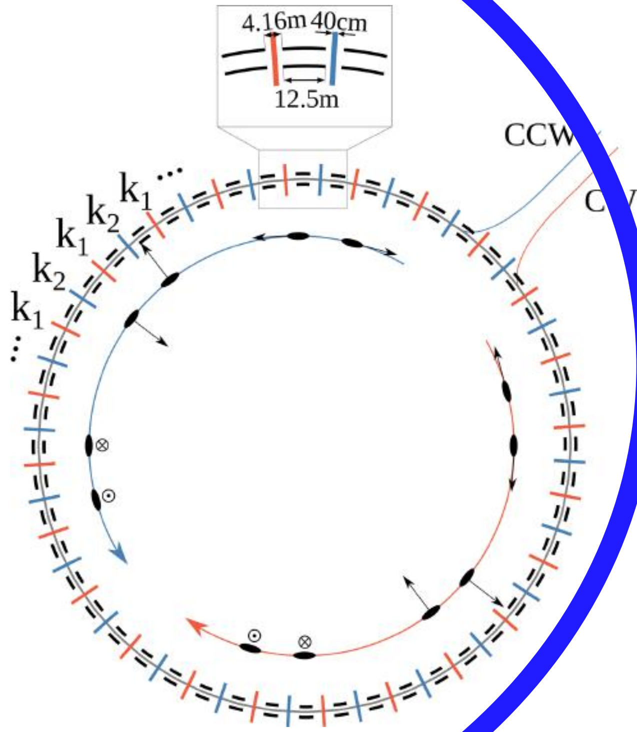

Sensitivity of radially polarized beam (sensitive to V. Dark Matter/Dark Energy, P. Graham *et al.*, PRD, 055 010, 2021), most sensitive to vertical velocity problem

Vertical velocity effect cancels

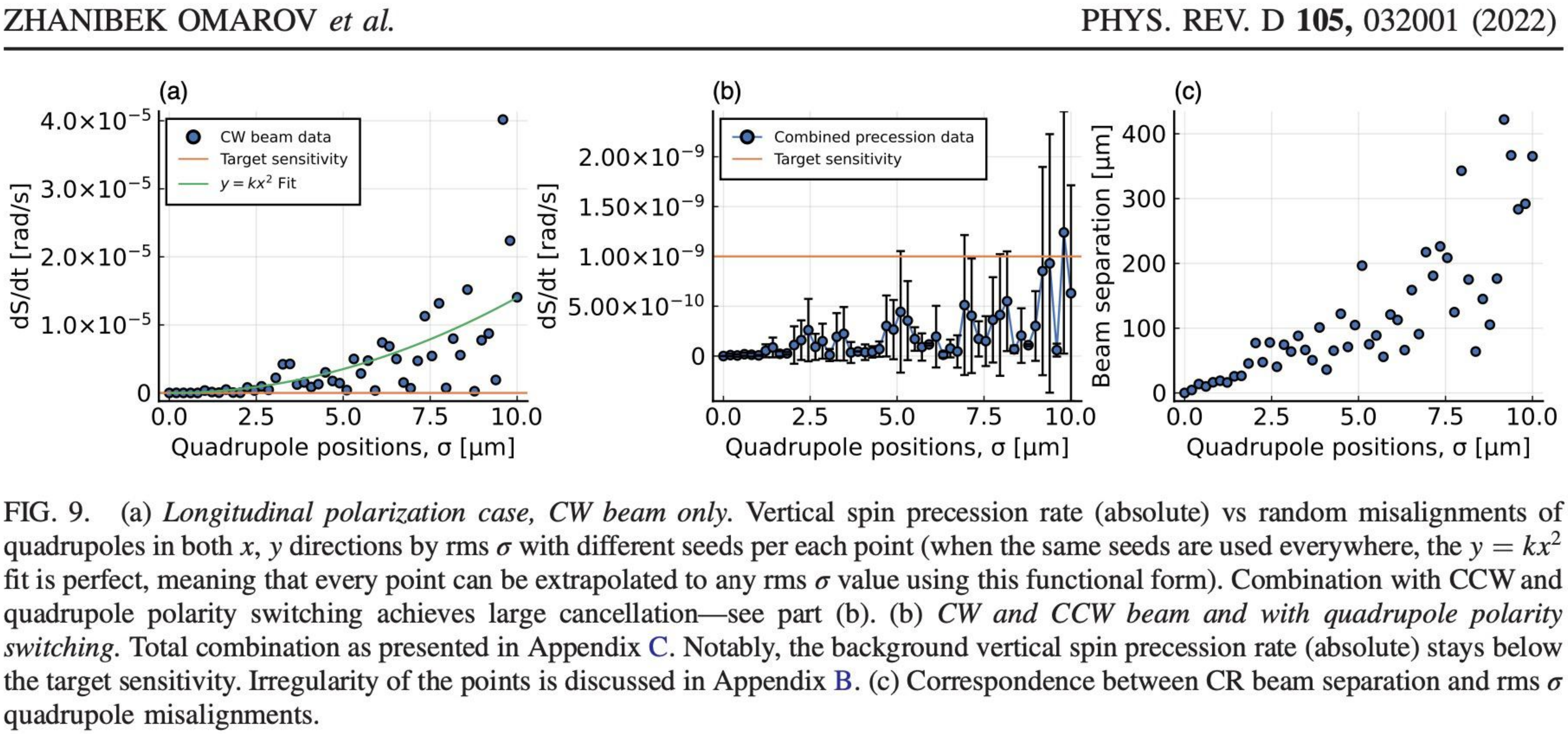
ZHANIBEK OMAROV *et al.* PHYS. REV. D **105,** 032001 (2022)

FIG. 9. (a) *Longitudinal polarization case, CW beam only*. Vertical spin precession rate (absolute) vs random misalignments of quadrupoles in both x, y directions by rms σ with different seeds per each point (when the same seeds are used everywhere, the $y = kx^2$ fit is perfect, meaning that every point can be extrapolated to any rms σ value using this functional form). Combination with CCW and quadrupole polarity switching achieves large cancellation—see part (b). (b) *CW and CCW beam and with quadrupole polarity switching*. Total combination as presented in Appendix C. Notably, the background vertical spin precession rate (absolute) stays below the target sensitivity. Irregularity of the points is discussed in Appendix B. (c) Correspondence between CR beam separation and rms σ quadrupole misalignments.

Classification of systematic errors at 10^{-29} *e*-cm for hybrid-symmetric lattice

- ✓Alternate magnetic focusing allows simultaneous CW & CCW storage and shields against external B-fields. Vertical dipole E-fields eliminated (its own "co-magnetometer"), unique feature of this lattice.

- ✓Symmetric lattice significantly reduces systematic errors associated with vertical velocity (major source). Using longitudinal, radial and vertical polarization directions, sensitive to different physics/systematic errors.

- ✓Required ring planarity <0.1mm; CW & CCW beam separation <0.01mm, resolves issues with geometrical phases

Symmetries against systematic errors

- Clock-wise (CW) vs. Counter-Clock-Wise (CCW)
  - Eliminates vertical Electric field background
- Hybrid lattice (electric bending, magnetic focusing)
  - Shields against background magnetic fields
- Highly symmetric lattice (24 FODO systems)
  - Eliminates vertical velocity background
- Positive and negative helicity
  - Reduce polarimeter systematic errors
- Flat ring to 0.1 mm, beams overlap within 0.01 mm, spin-based alignment
  - Geometrical phases; High-order vertical E-field

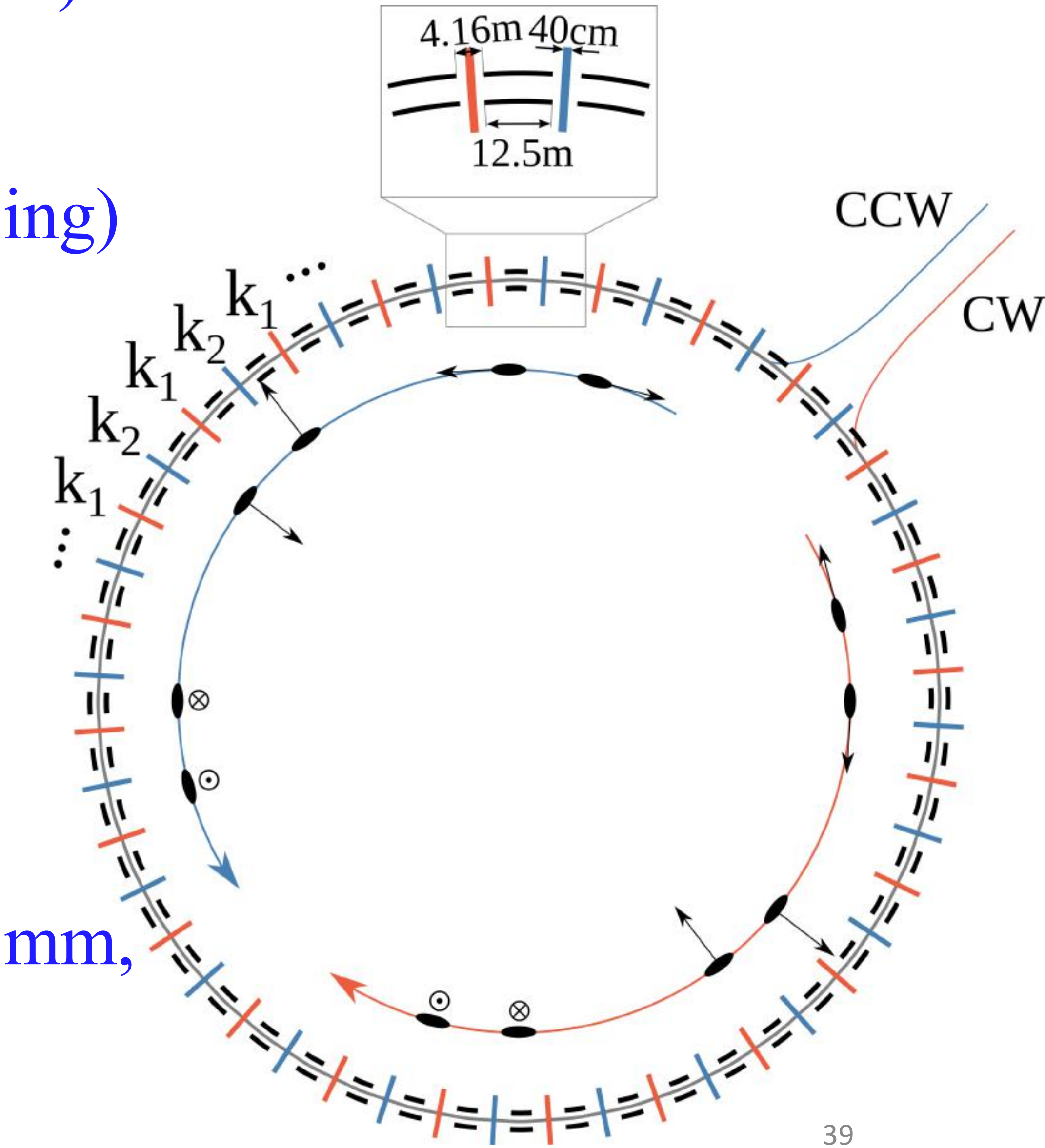

Spin-based alignment/background reduction

- Omarov’s method: a combination of background fields can create false EDM signals. Artificially inflate one component to reduce the other.

- Vary the radial B-field (B_x) and observe the ds_y/dt slope vs. B_x.
- The EDM signal does not depend on the value of B_x.
- Tune out the background field (here electric field focusing) until we get zero slope in ds_y/dt vs. B_x.

From Zhanibek Omarov’s presentation

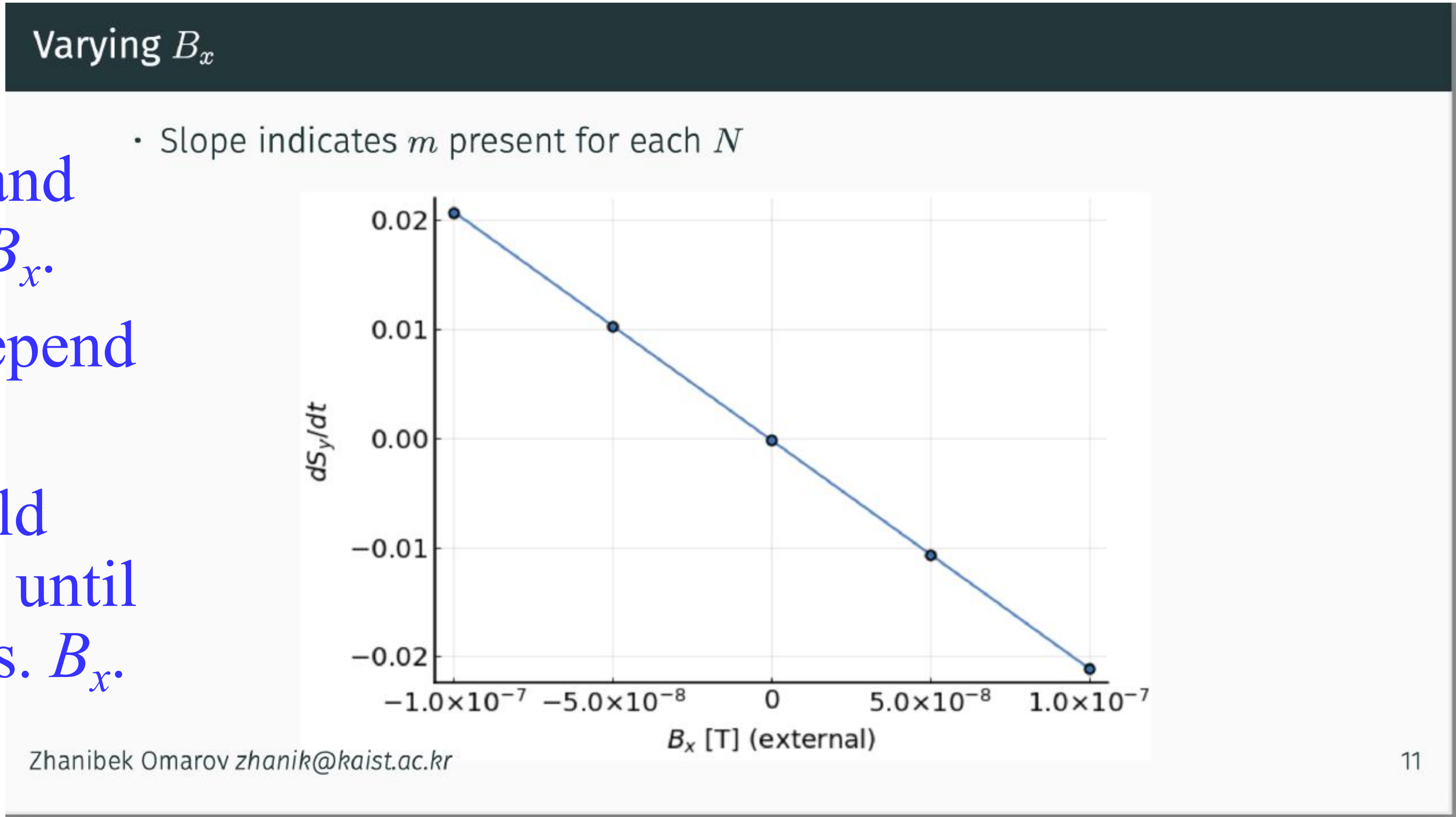

Varying B_x

- Slope indicates m present for each N

Zhanibek Omarov *zhanik@kaist.ac.kr* 11

Protons in a hybrid-symmetric ring: no new technology

- No need to develop/test new technology
  - Simultaneous CW/CCW beam storage is possible
  - Electric field ~4.5 MV/m with present technology
  - Magnetic fields from misplaced quads are self-shielded by the magnetic focusing
  - Hybrid/symmetric ring options are simple. Large tune in both planes, beam position monitor (BPM) tasks are achievable with present technology.
  - Estimated SCT are large, injection into ring works, while all primary systematic error sources are kept small.

- After protons, add dipole magnetic field in bending sections:
  - Can do proton, deuteron, ^{3}He, (and muons)

System	Risk factor, comments
Ring construction, beam storage, stability, IBS	Low. Strong (alternate) focusing, a ring prototype has been built (AGS analog at BNL) in 60's. Lattice elements placement specs are ordinary. Intra-beam-scattering (IBS) OK below transition.
E-field strength	Low. Plate-units are similar to those ran at Tevatron with higher specs.
E-field plates shape	Medium. Make as flat as conveniently possible. Probe and shim out high order fields by intentionally splitting the CR-beams
Spin coherence time	Low. Ordinary sextupoles will provide $>10^3$s.
Beam position monitors (BPM), SQUID-based BPMs.	Medium. Ordinary BPMs and hydrostatic level system (HLS) to level the ring to better than 0.1mm; SQUID-based or more conventional BPMs to check CR-beams split to 0.01mm.
High-precision, efficient software	Low. Cross-checking our results routinely
Polarimeter	Low. Mature technology available

The proton EDM in the AGS tunnel at BNL

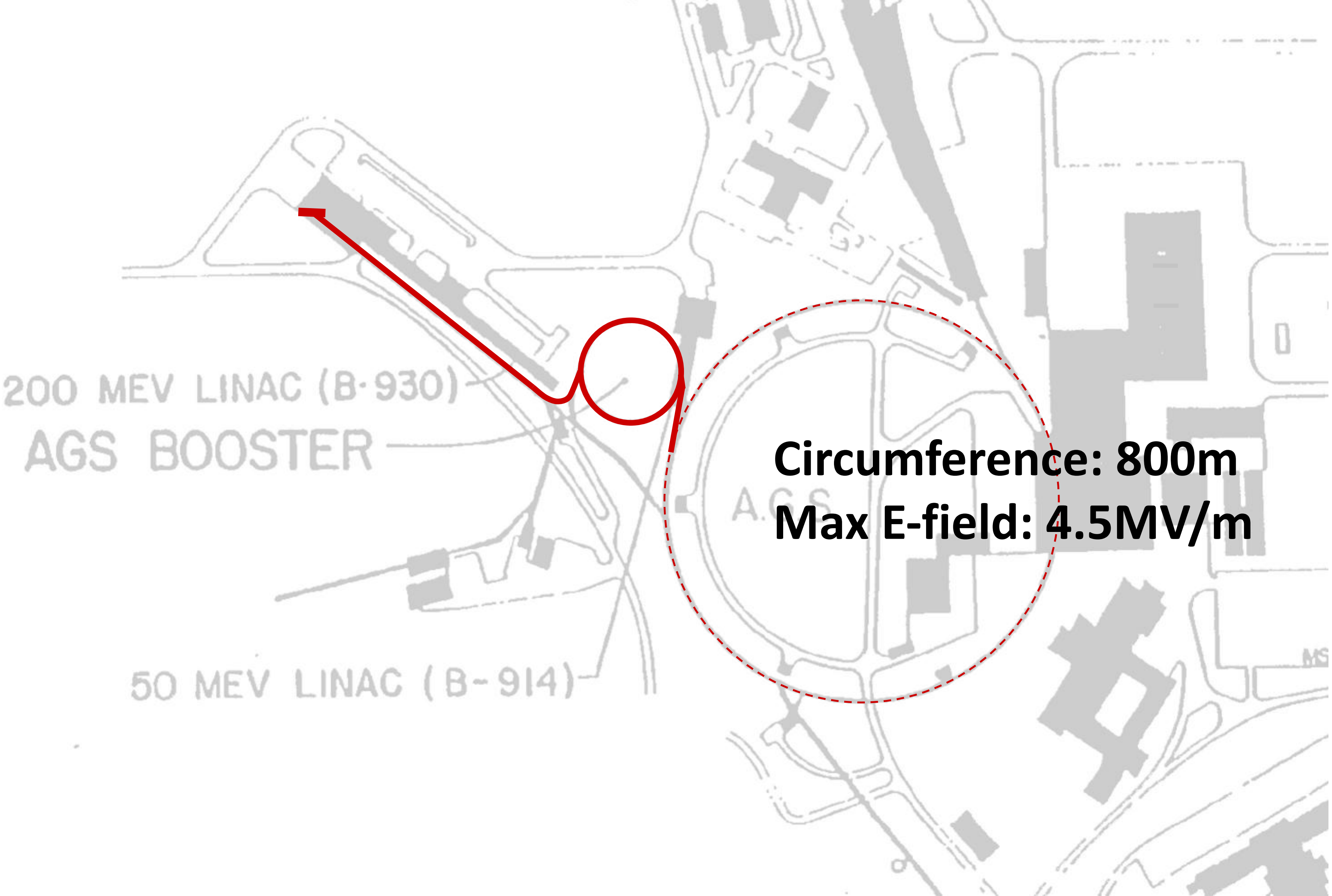

Circumference: 800m

Max E-field: 4.5MV/m

John Benante, Bill Morse in AGS tunnel, plenty of room for the EDM ring.

Hybrid, symmetric lattice storage ring, designed by Val. Lebedev (FNAL)

Z. Omarov *et al.*, PHYS. REV. D **105**, 032001 (2022)

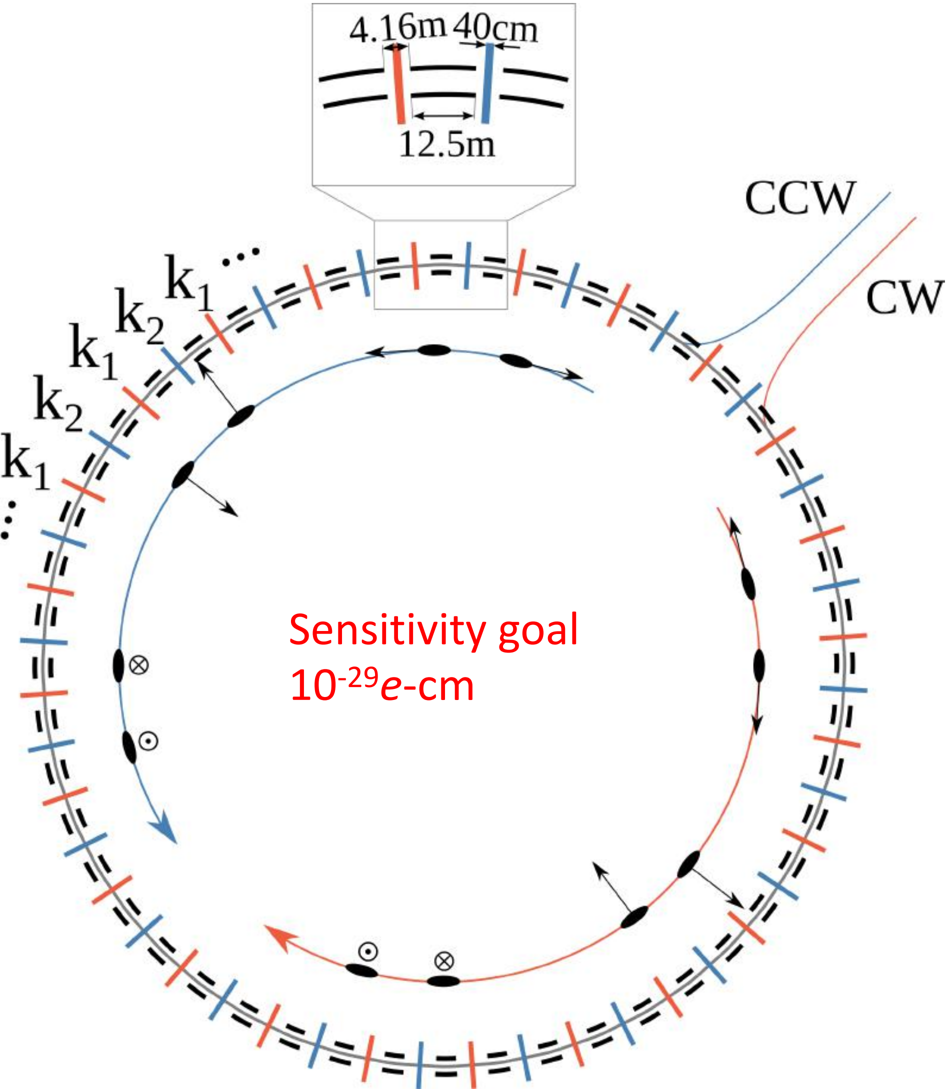

Sensitivity goal 10^{-29}*e*-cm

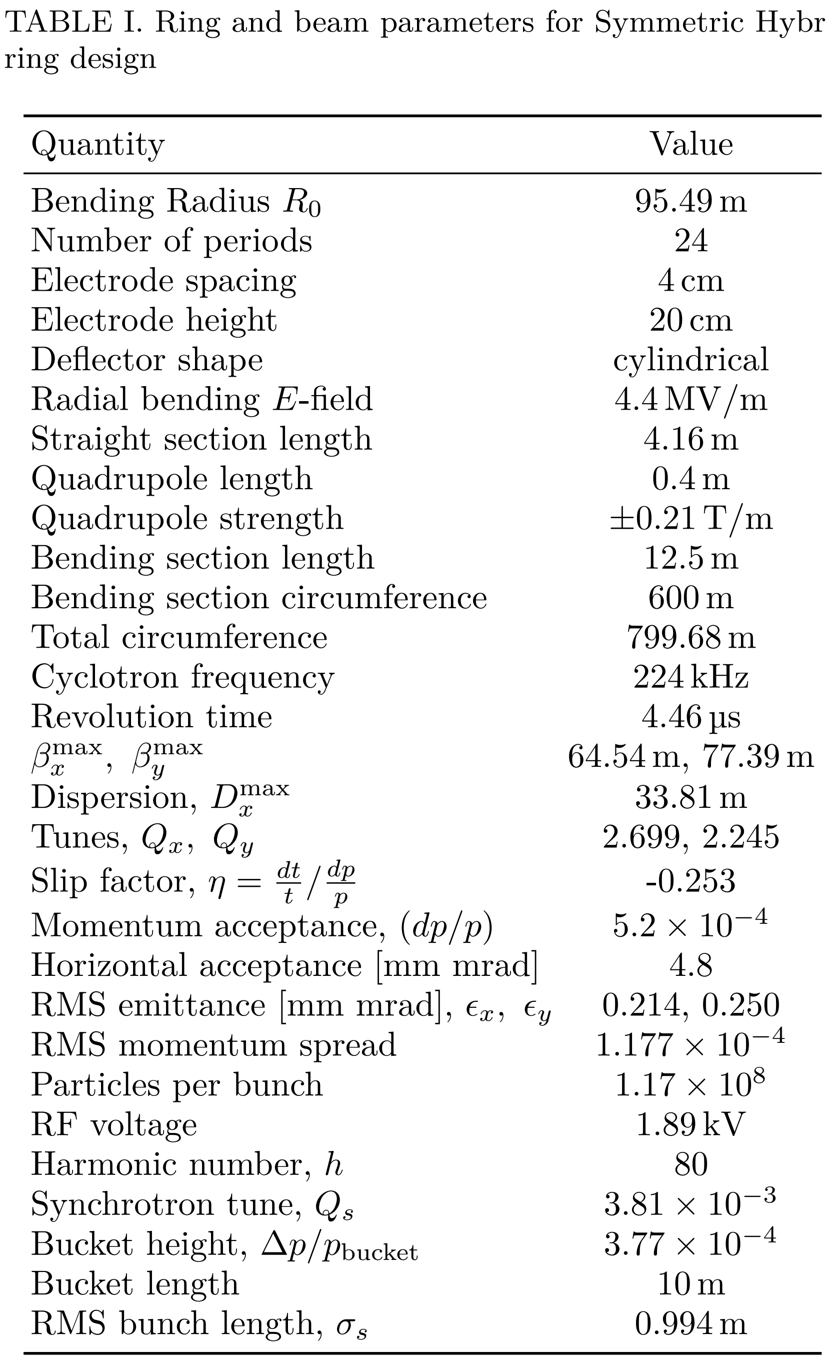

TABLE I. Ring and beam parameters for Symmetric Hybrid ring design

Quantity	Value
Bending Radius R_0	95.49 m
Number of periods	24
Electrode spacing	4 cm
Electrode height	20 cm
Deflector shape	cylindrical
Radial bending E-field	4.4 MV/m
Straight section length	4.16 m
Quadrupole length	0.4 m
Quadrupole strength	$\pm$0.21 T/m
Bending section length	12.5 m
Bending section circumference	600 m
Total circumference	799.68 m
Cyclotron frequency	224 kHz
Revolution time	4.46 µs
$\beta_x^{\max}$, $\beta_y^{\max}$	64.54 m, 77.39 m
Dispersion, $D_x^{\max}$	33.81 m
Tunes, Q_x, Q_y	2.699, 2.245
Slip factor, $\eta = \frac{dt}{t} / \frac{dp}{p}$	-0.253
Momentum acceptance, (dp/p)	5.2×10^{-4}
Horizontal acceptance [mm mrad]	4.8
RMS emittance [mm mrad], ϵ_x, ϵ_y	0.214, 0.250
RMS momentum spread	1.177×10^{-4}
Particles per bunch	1.17×10^8
RF voltage	1.89 kV
Harmonic number, h	80
Synchrotron tune, Q_s	3.81×10^{-3}
Bucket height, $\Delta p/p_{\text{bucket}}$	3.77×10^{-4}
Bucket length	10 m
RMS bunch length, σ_s	0.994 m

Low risk

Strong focusing

Timeline

- Snowmass/white paper, CDR, proposal/TDR, prototype/string-test, ring construction (3-5 years), storage (2-3 years) to first publication
- Effort similar to muon g-2 experiments (under evaluation at BNL)
- Possible interesting results within a decade.

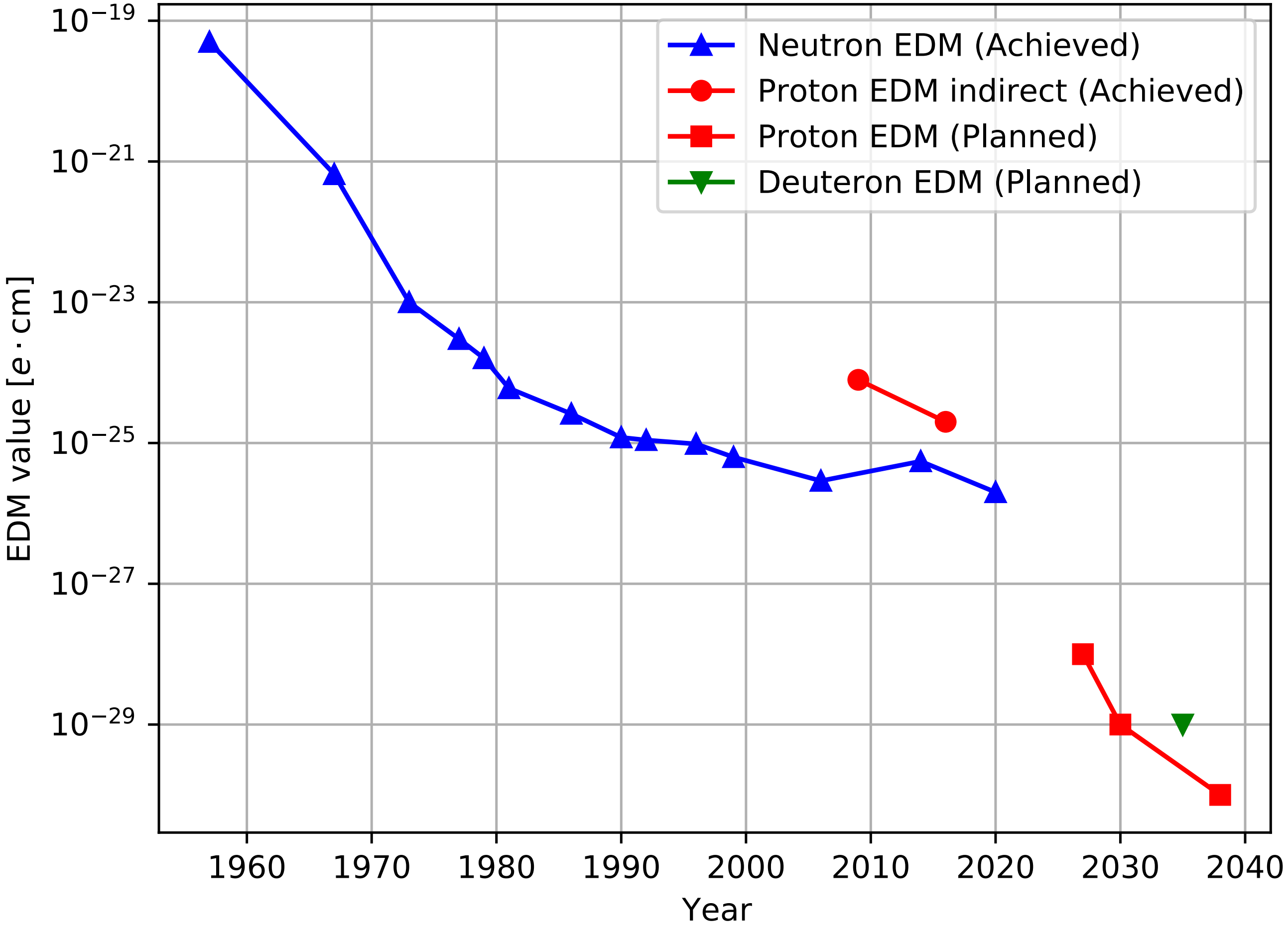

Summary

✓EDM physics is must do, exciting and timely, CP-violation, ~10^3 TeV New-Physics reach, axion physics, DM/DE.

✓Hybrid, symmetric ring lattice and spin-based alignment. Minimized systematic error sources. Statistics and systematics of pEDM to better than $10^{-29}e$-cm.

✓Snowmass encouraged BNL to come up with a technically strong proposal for a storage ring proton EDM. BNL is currently funding the cost estimate of the storage ring EDM experiment. Next critical, do well in P5 process.

✓Great progress in statistics and systematics promises two to three orders improvement in sensitivity of eEDM, nEDM, μEDM, and pEDM within the current and next decade.

References

1. Z. Omarov *et al.,* Comprehensive Symmetric-Hybrid ring design for pEDM experiment at below 10^{-29} e-cm, Phys. Rev. D 105, 032001 (2022)
2. On Kim *et al.,* New method of probing an oscillating EDM induced by axionlike dark matter…, Phys. Rev. D 104 (9), 096006 (2021)
3. P.W. Graham *et al.,* Storage ring Probes for Dark Matter and Dark Energy, Phys. Rev. D 103 (5), 055010 (2021)
4. S. Haciomeroglu and Y.K. Semertzidis, Hybrid ring design in the storage-ring proton EDM experiment, Phys. Rev. Accel. Beams 22 (3), 034001 (2019)
5. S.P. Chang *et al.,* Axionlike dark matter search using the storage ring EDM method, Phys. Rev. D 99 (8), 083002 (2019)
6. S. Haciomeroglu *et al.,* SQUID-based Beam Position Monitor, *PoS* ICHEP2018 (2019) 279
7. N. Hempelmann *et al.,* Phase locking the spin precession in a storage ring, Phys. Rev. Lett. 119 (1), 014801 (2017)
8. G. Guidoboni *et al.,* How to reach a Thousand-second in-plane Polarization Lifetime with 0.97 GeV/c Deuterons in a storage ring, Phys. Rev. Lett. 117 (5), 054801 (2016)
9. V. Anastassopoulos *et al.,* A storage ring experiment to detect a proton electric dipole moment, Rev. Sci. Instrum. 87 (11), 115116 (2016)
10. E.M. Metodiev *et al.,* Analytical benchmarks for precision particle tracking in electric and magnetic rings, NIM A797, 311 (2015)
11. E.M. Metodiev *et al.,* Fringe electric fields of flat and cylindrical deflectors in electrostatic charged particle storage rings, Phys. Rev. Accel. Beams 17 (7), 074002 (2014)
12. W.M. Morse *et al.,* rf Wien filter in an electric dipole moment storage ring: The “partially frozen spin” effect, Phys. Rev. Accel. Beams 16 (11), 114001 (2013)
13. N.P.M. Brantjes *et al.,* Correction systematic errors in high-sensitivity deuteron polarization measurements, Nucl. Instrum. Meth. A664, 49 (2012)
14. G.W. Bennett *et al.,* An improved limit on the muon electric dipole moment, Phys. Rev. D 80, 052008 (2009)
15. F.J.M. Farley *et al.,* A new method of measuring electric dipole moments in storage rings, Phys. Rev. Lett. 93, 052001 (2004)
16. …

Extra slides

Ring planarity critical to control geometrical phase errors

- Numerous studies on slow ground motion in accelerators, Hydrostatic Level System for slow ground motion studies at Fermilab. (Part of the linear collider studies!)

- Thorough review by Vladimir Shiltsev (FNAL):

https://arxiv.org/pdf/0905.4194.pdf

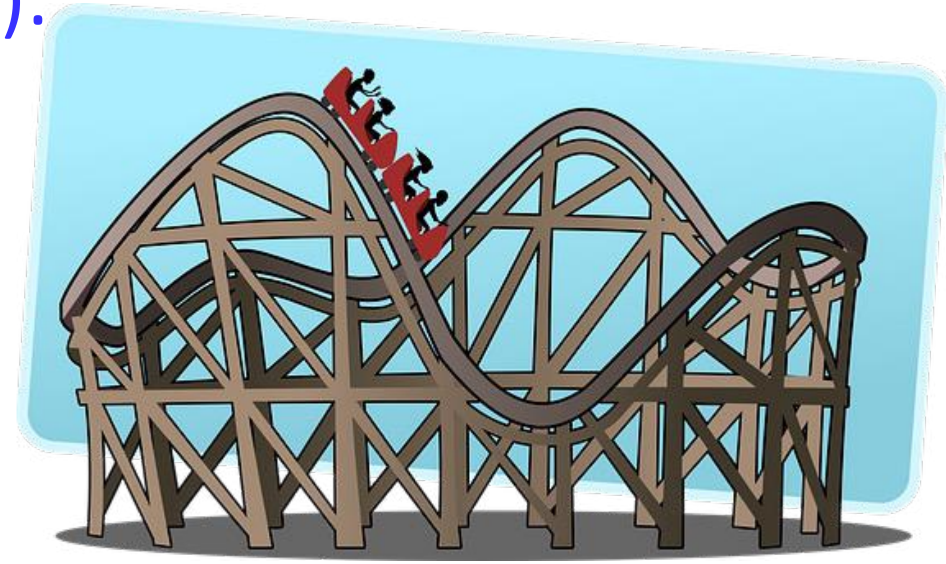

Tevatron Sensors on Quad

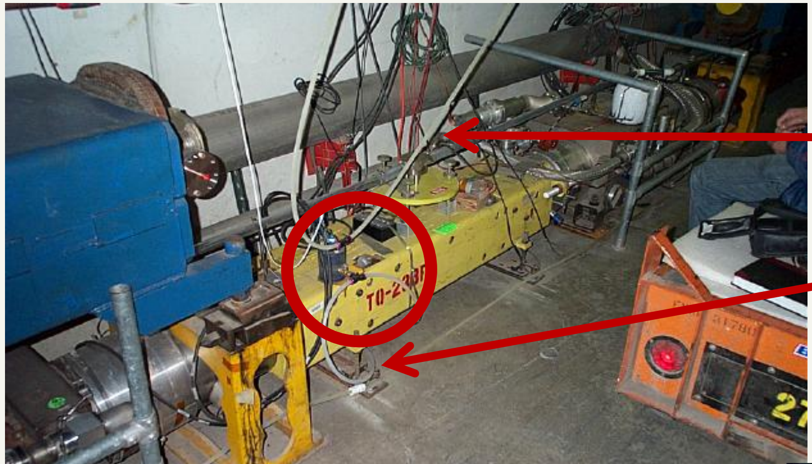

In the circle is a water level pot on a Tevatron quadrupole

HLS measurements at Fermilab

Fig.35. HLS probe on Tevatron accelerator focusing magnet.

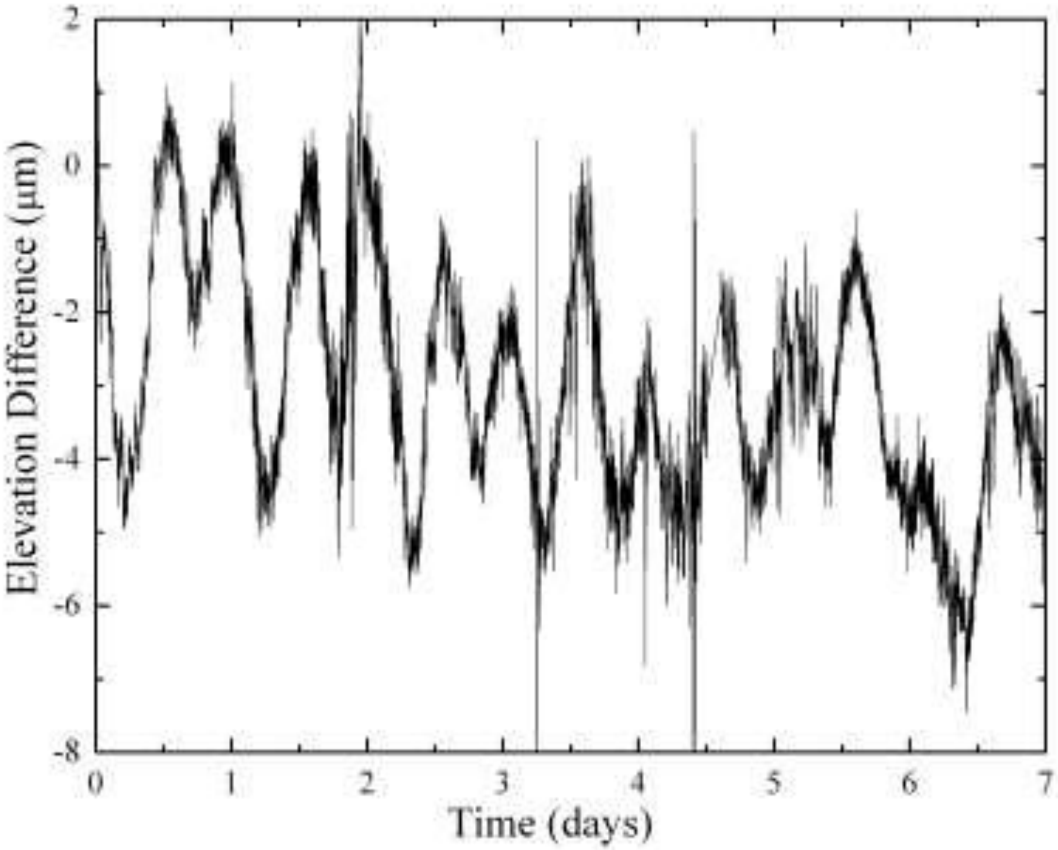

MINOS Tidal Data

Difference in two sensors 90 meters apart

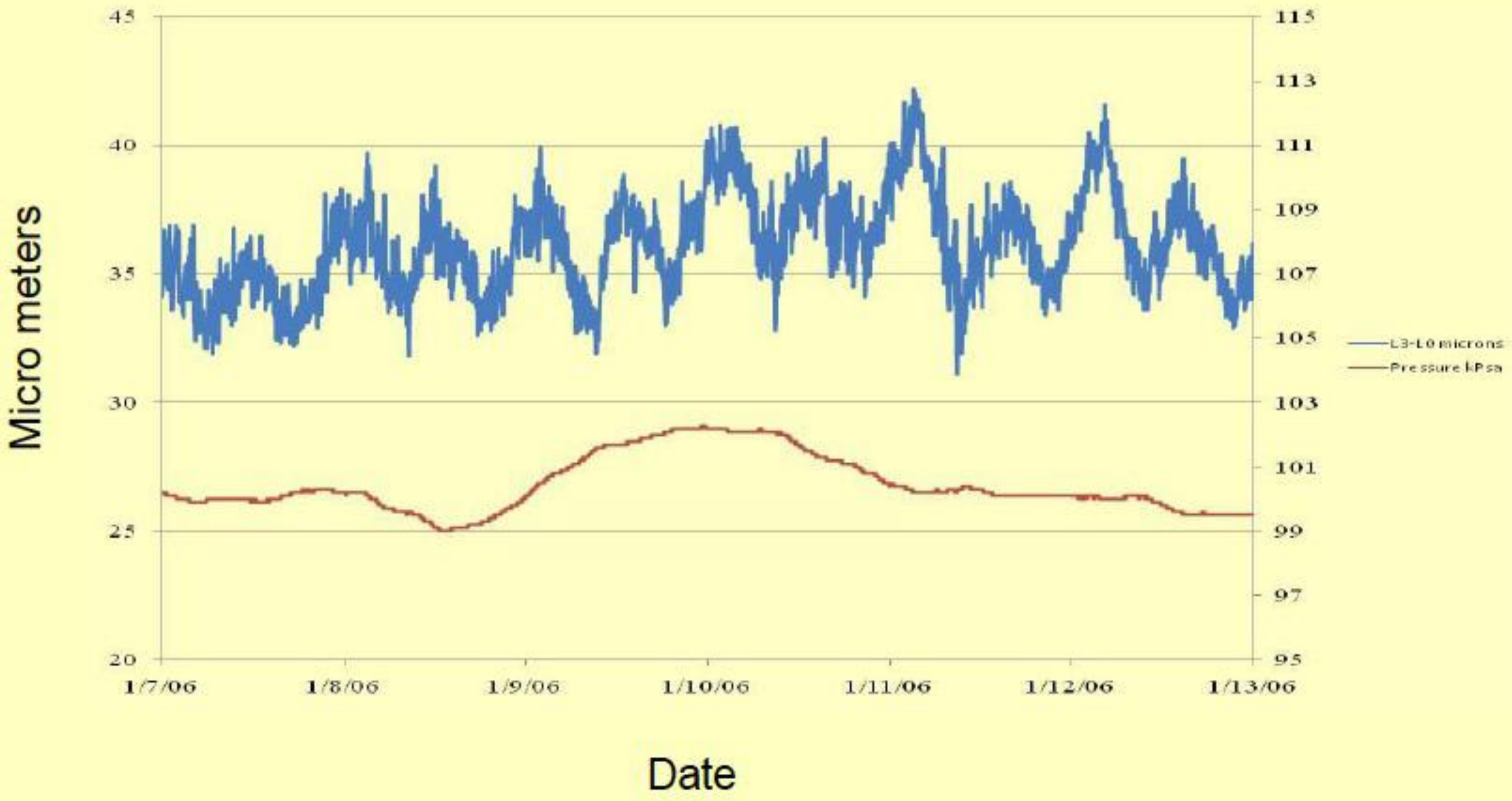

J T Volk Fermilab Dec 2008

Sketch of the AGS Accumulator Ring

- It was sketched for 1.5GeV ring. Space needed: 1mX1m.

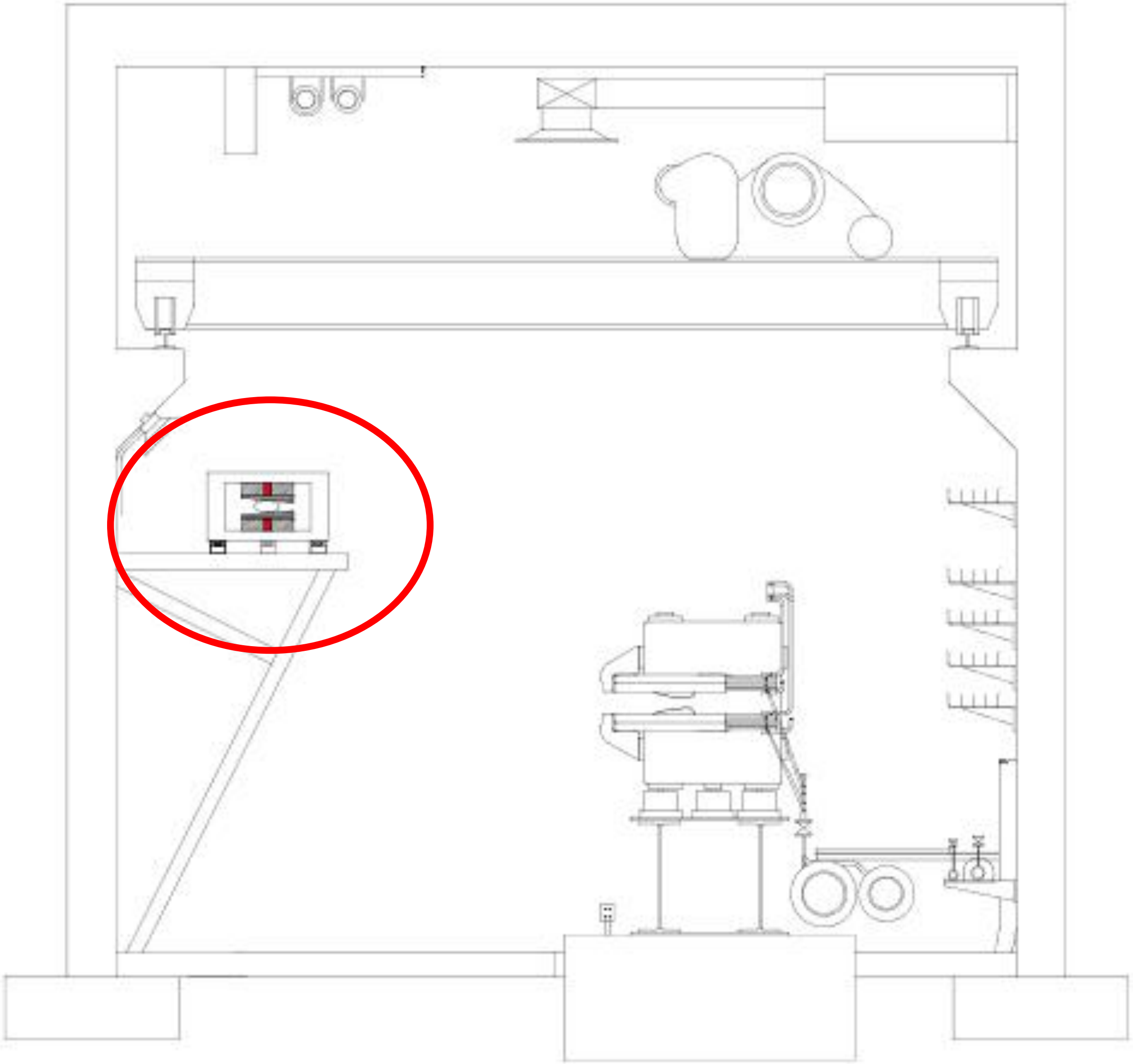

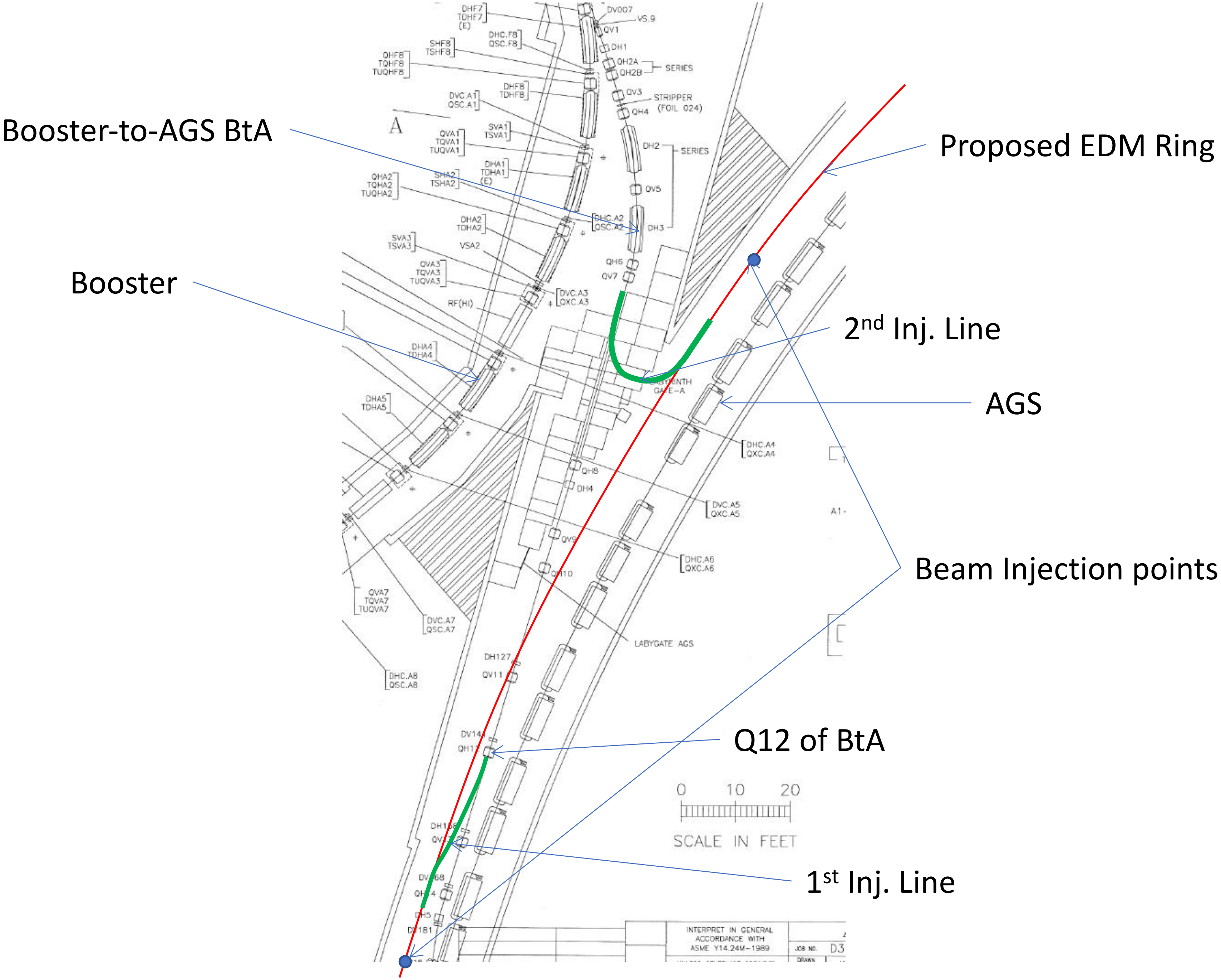

Booster-to-AGS BtA

Proposed EDM Ring

Booster

2nd Inj. Line

AGS

Beam Injection points

Q12 of BtA

1st Inj. Line

Emittance out of Booster

These intensity scan was done in 2009 with Booster input 3*10^{11}. Not much horizontal scan was done since then. The vertical scale is normalized 95% emittance.

The corresponding normalized rms emittance at 10^{11} is 0.7π horizontal, 1.0π vertical for horizontal scraping.

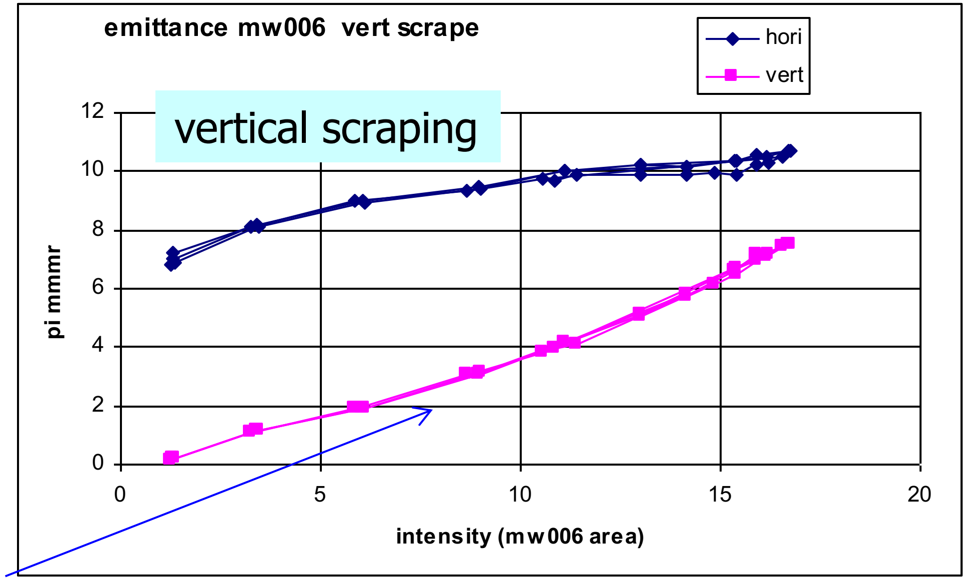

Intensity: 15~2e11 protons

@10^{11}

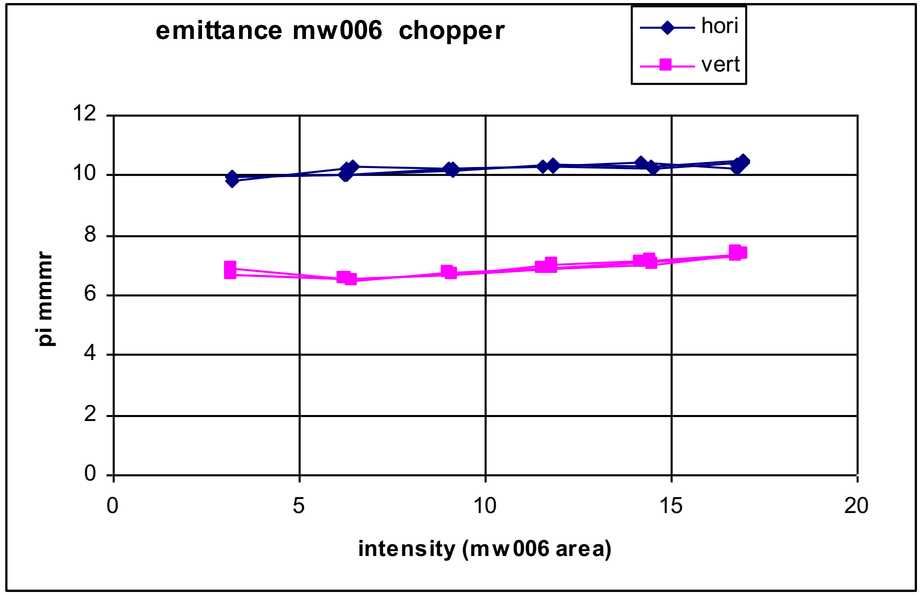

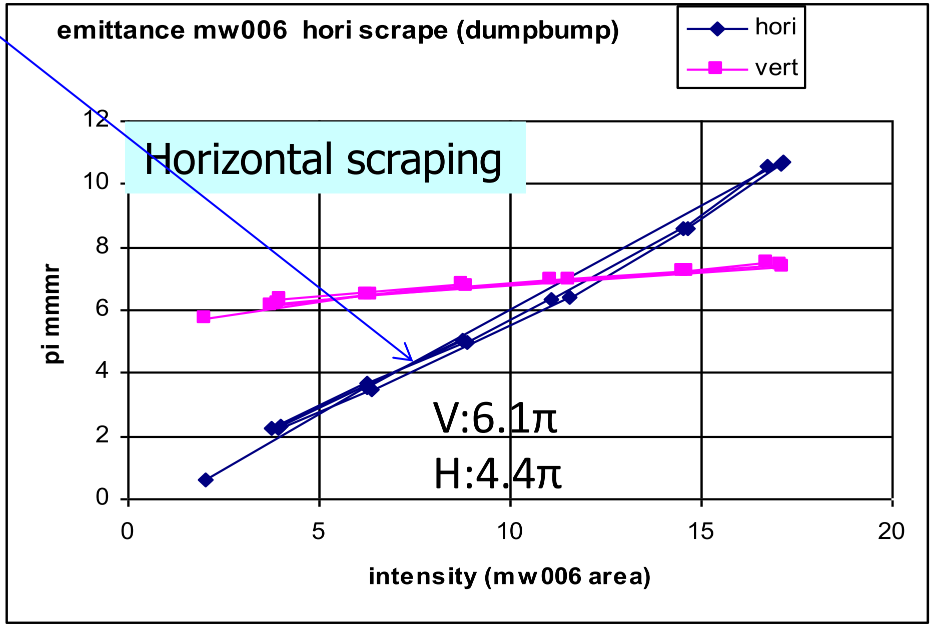

Lattice with 800 m circumference for a sensitive experiment on EDM, Dark Matter (DM) and Dark Energy (DE)

- Electric bending with cylindrically shaped E-field plates
  - Radial E-field: 4.4 MV/m, 4-cm plate separation
- Alternate-magnetic-focusing (k_1=-k_2)
  - Simultaneous counter-rotating beams
  - Strong focusing in both horizontal and vertical planes
- Store Longitudinal, Radial and Vertical polarizations
  - Sensitive to EDM (L), DM/DE (R), and both (V)

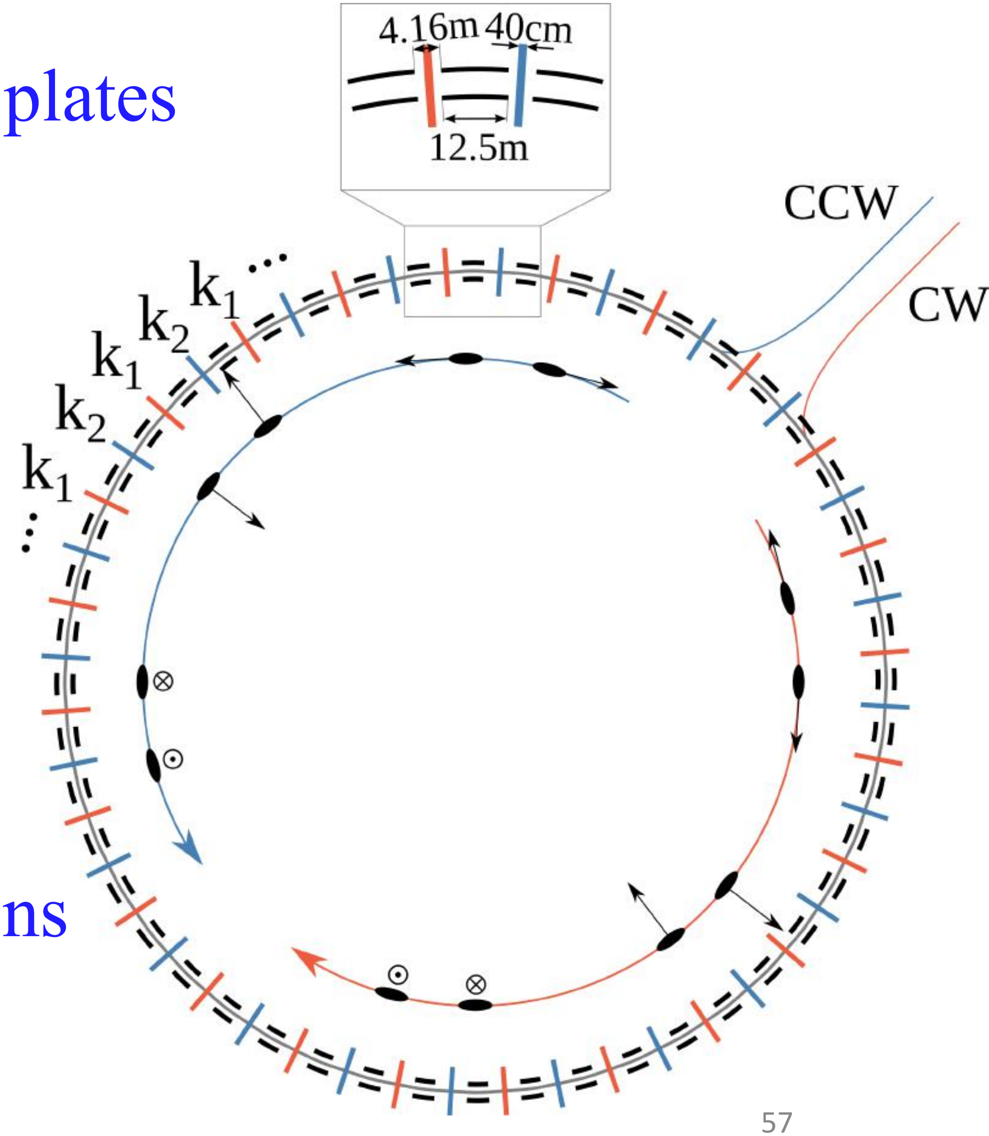

Sensitivity to Rule on Several New Models

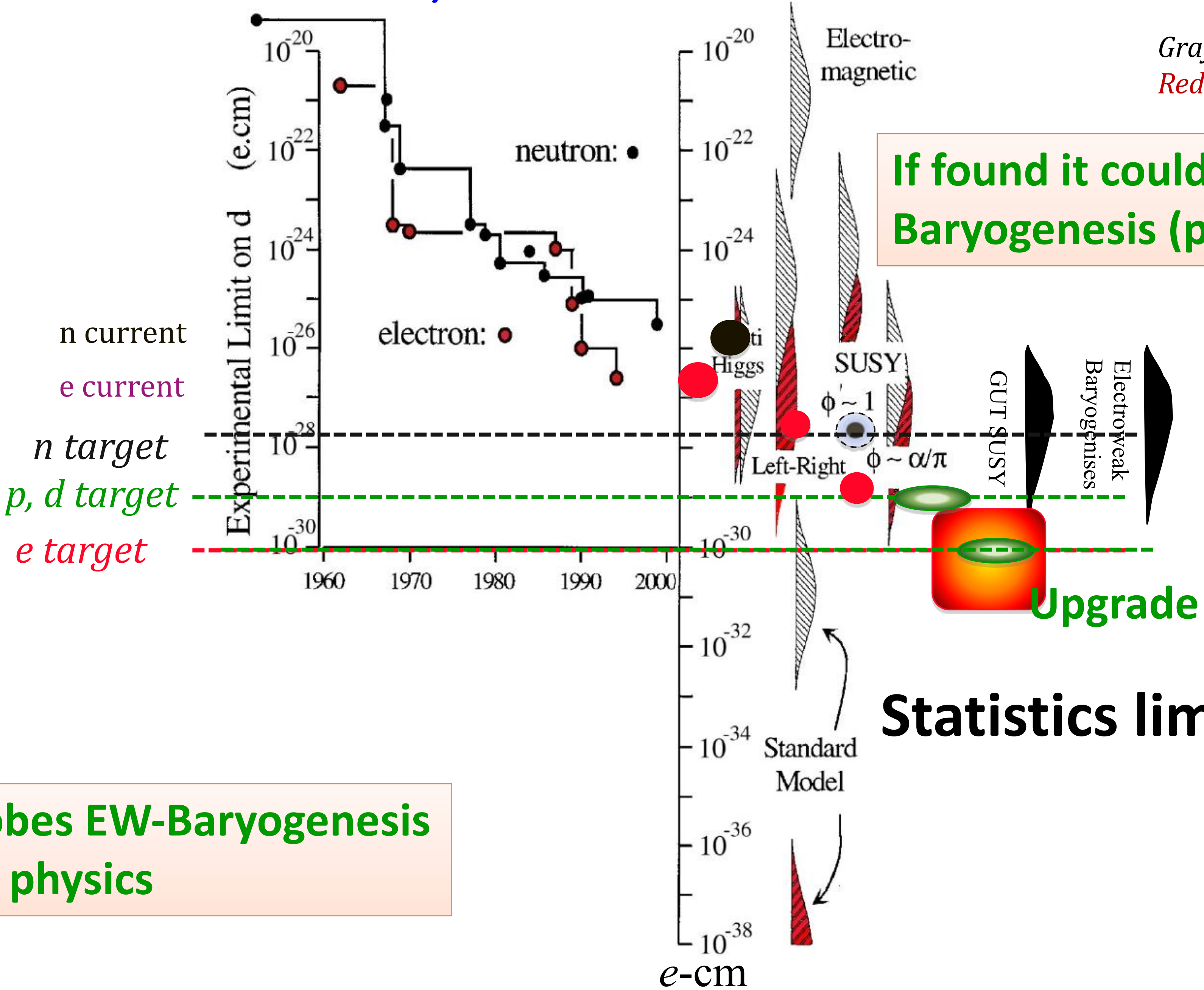

Gray: Neutron
Red: Electron

If found it could explain Baryogenesis (p, d, n (or ^{3}He))

Statistics limited

pEDM probes EW-Baryogenesis and axion physics

J.M.Pendlebury and E.A. Hinds, NIMA 440 (2000) 471

SQUID-based BPMs

Beam position monitor: SQUID array

Goal: sense counter-rotating beam separation to 10μm

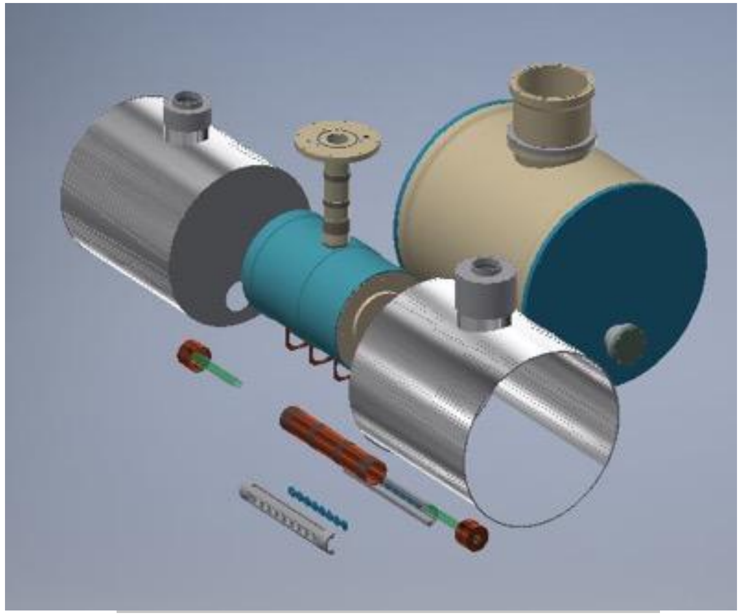

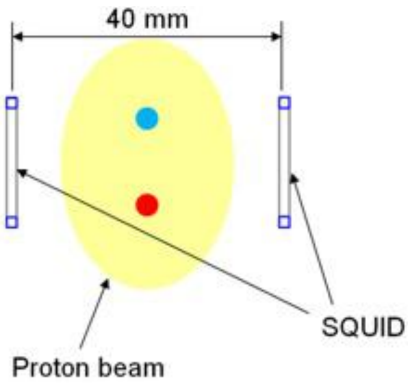

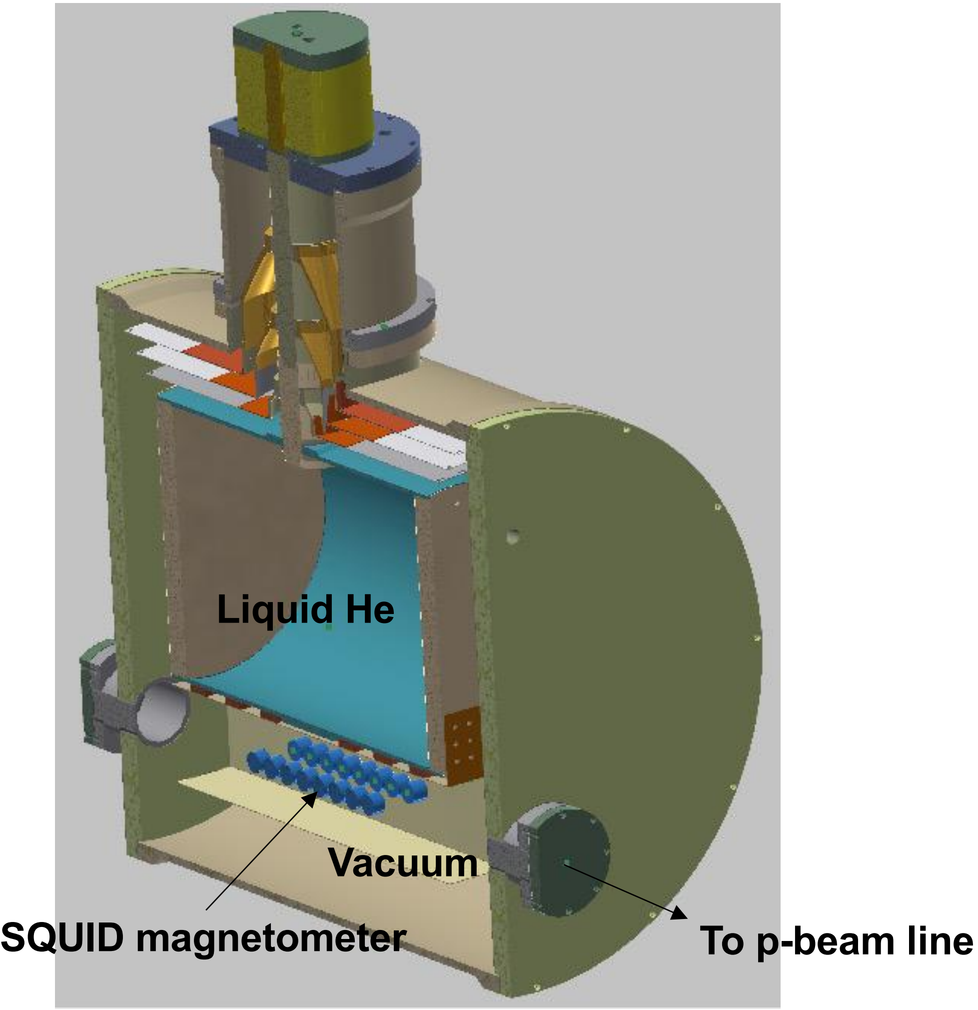

Cylindrical Dewar: original design (KRISS)

SQUID-based BPMs, Korea

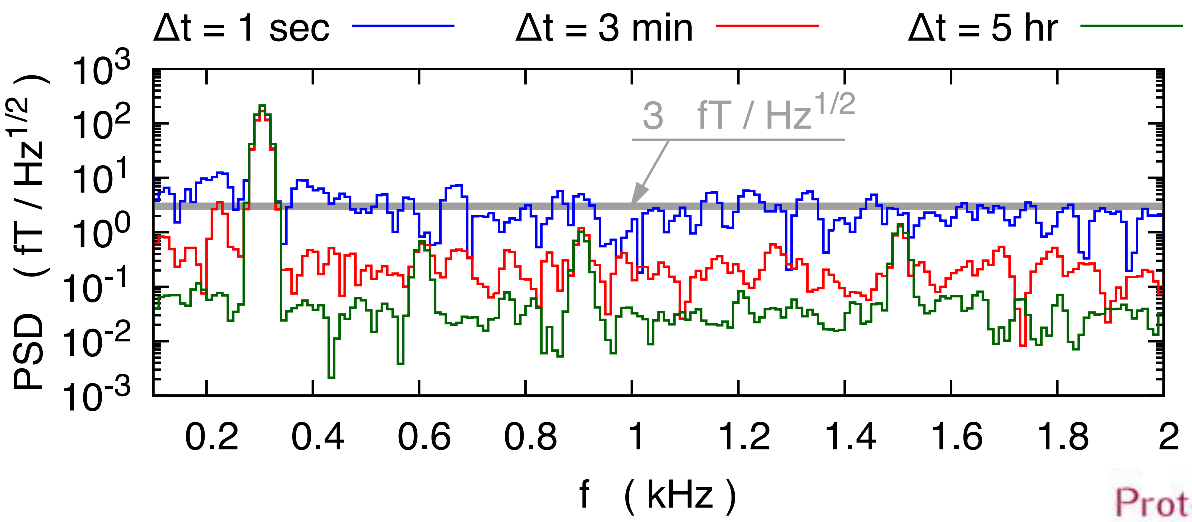

Next: Testing the concept at an accelerator.

Prototype

- The new design is to be delivered by summer
- Will be 2fT$\sqrt{Hz}$
- We will make wire tests in Korea
- Would be good to test here at COSY

Large Surface Area Electrodes

Parameter	Tevatron pbar-p Separators	BNL K-pi Separators	pEDM (low risk)
Length/unit	2.6m	4.5m	5×2.5m
Gap, E-field	5cm, 7.2 MV/m	10cm, 4 MV/m	4cm, 4.5 MV/m
Height	0.2m	0.4m	0.2m
Number	24	2	48
Max. HV	±(150-180)KV	±200KV	±90KV

E-field plate modules: The (24) FNAL Tevatron ES-separators ran for years with harder specs

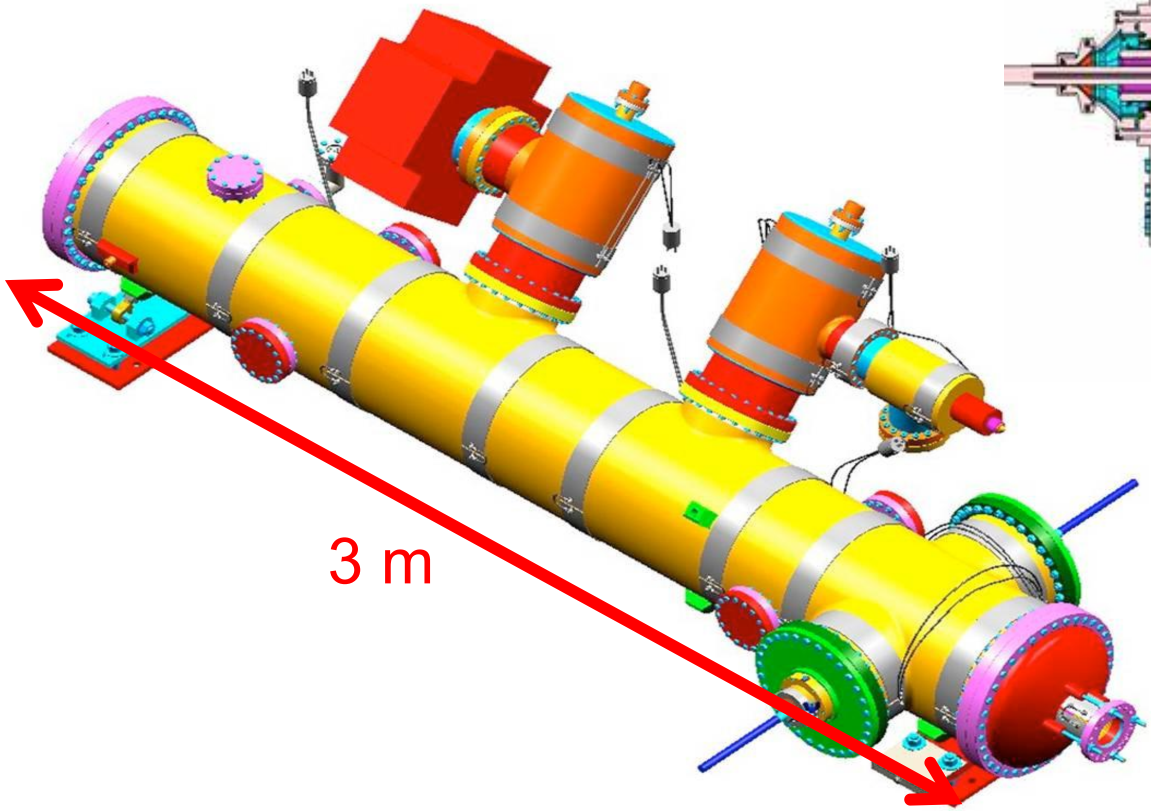

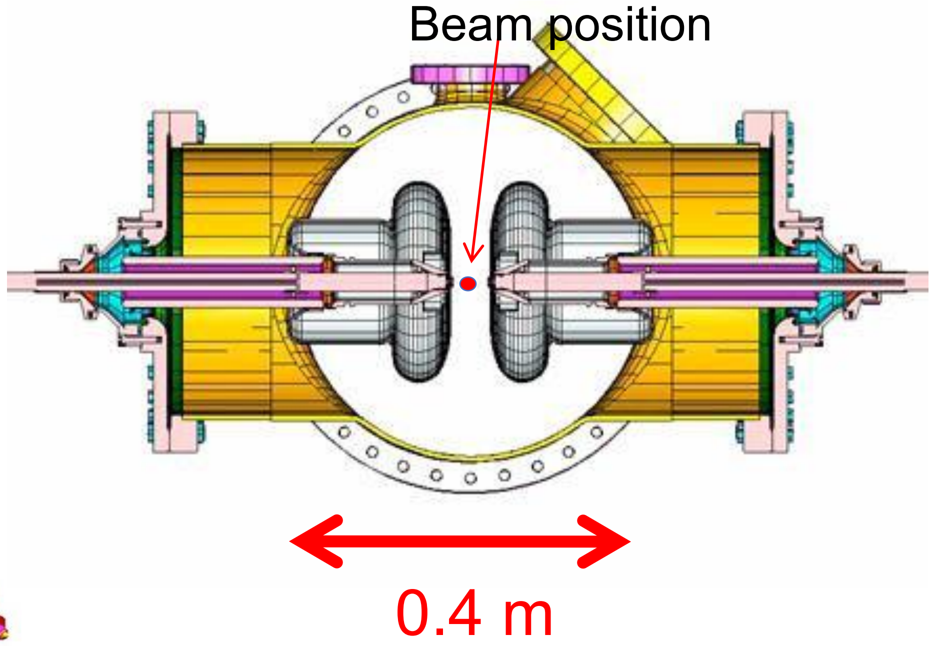

Polarimeter analyzing power at P_{magic} is great

Analyzing power can be further optimized

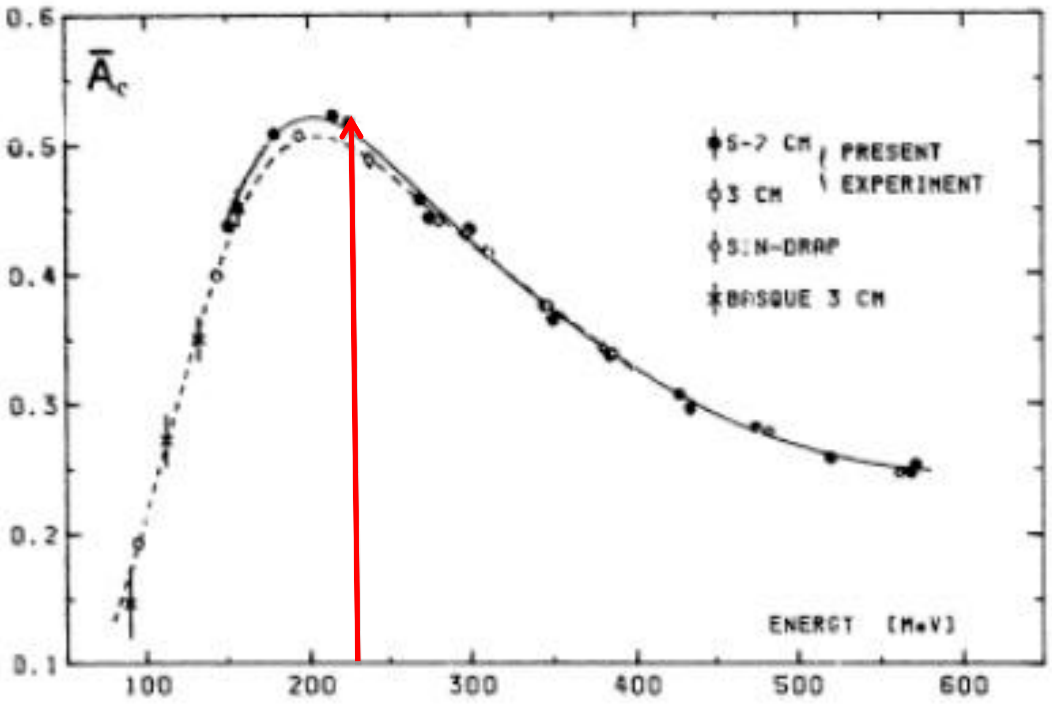

Fig. 4. Angle-averaged effective analyzing power. Curves show our fits. Points are the data included in the fits. Errors are statistical only

Fig.4. The angle averaged effective analyzing power as a function of the proton kinetic energy. The magic momentum of 0.7GeV/c corresponds to 232MeV.

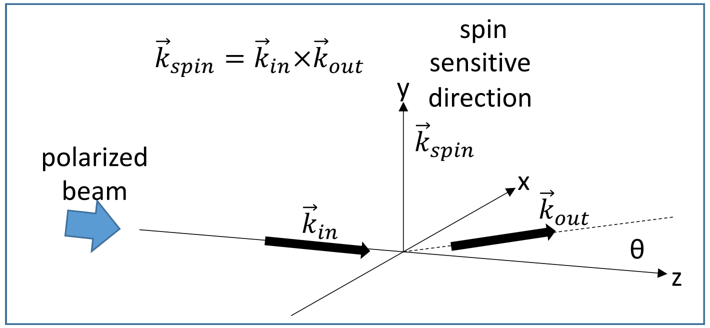

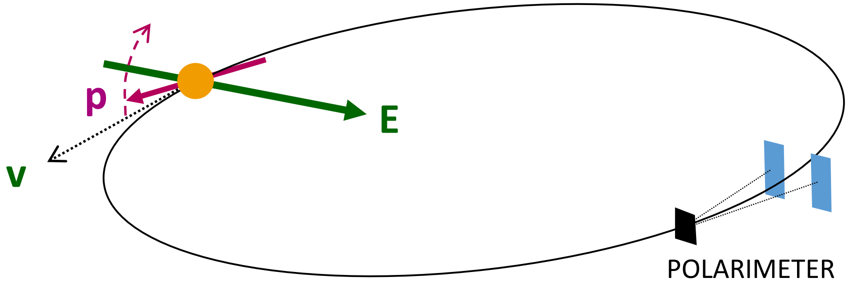

Spin Coherence Time

- Not all particles have same deviation from magic momentum, or same horizontal and vertical divergence (second order effects)

- They Cause a spread in the g-2 frequencies:

$$d\omega_a = a\vartheta_x^2 + b\vartheta_y^2 + c\left(\frac{dP}{P}\right)^2$$

- Correct by tuning plate shape/straight section length plus fine tuning with sextupoles (current plan) or cooling (mixing) during storage (under evaluation).

Hybrid, symmetric lattice storage ring. Spin Coherence Time with sextupoles

Z. Omarov *et al.*, PHYS. REV. D **105**, 032001 (2022)

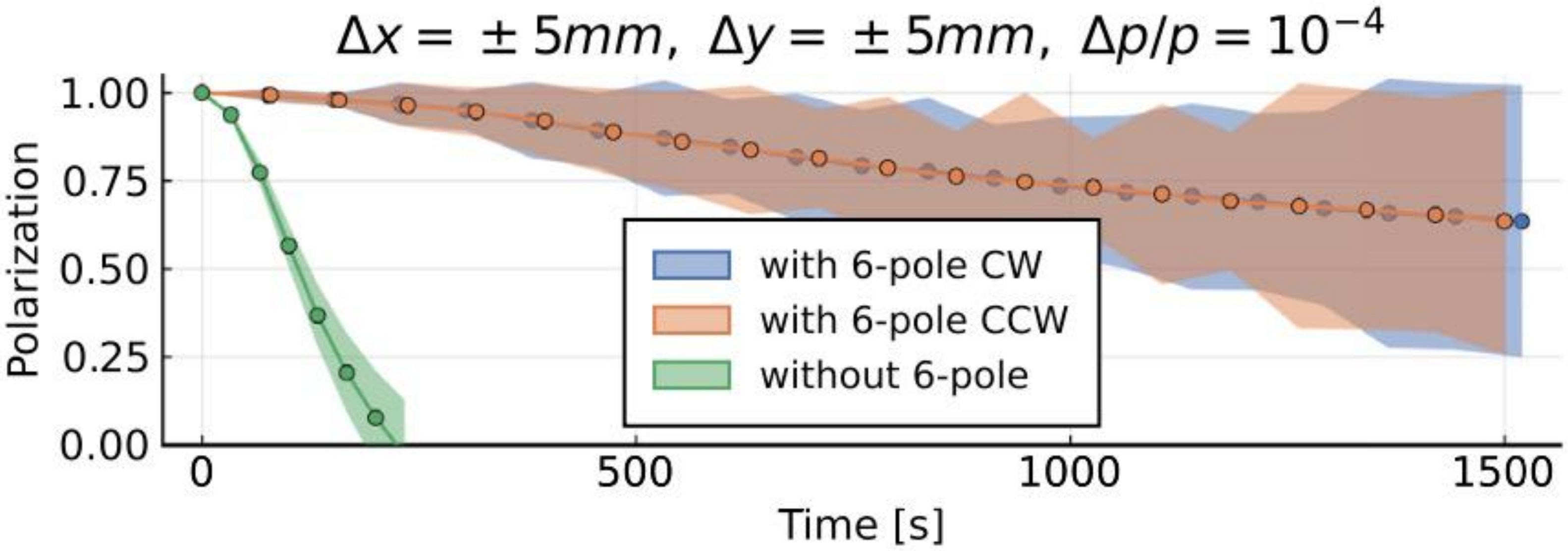

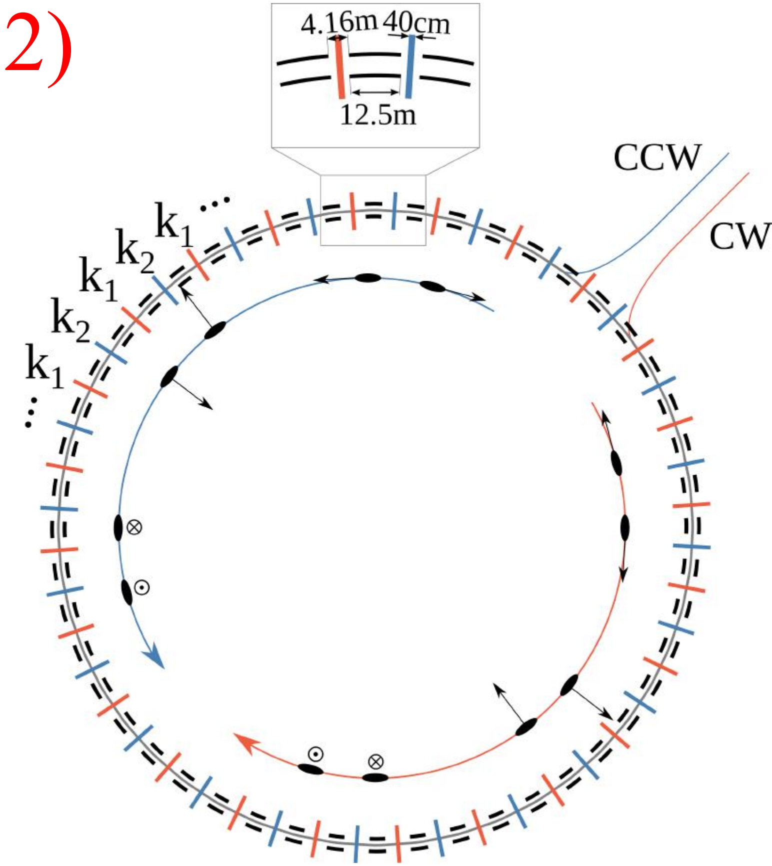

Hybrid (magnetic and elecric) sextupoles were used to achieve long SCT.

Physics strength comparison (Marciano)

System	Current limit [e·cm]	Future goal	Neutron equivalent
Neutron	$<1.6 \times 10^{-26}$	$\sim 10^{-28}$	10^{-28}
^{199}Hg atom	$<7 \times 10^{-30}$	$<10^{-30}$	10^{-26}
^{129}Xe atom	$<6 \times 10^{-27}$	$\sim 10^{-29}$-10^{-31}	10^{-25}-10^{-27}
Deuteron nucleus		$\sim 10^{-29}$	3×10^{-29}-5×10^{-31}
Proton nucleus	$<2 \times 10^{-25}$	$\sim 10^{-29}$	10^{-29}

From theta-QCD

From SUSY-like CPV

How the srEDM exp. at 10^{-29} *e*-cm works

✓Required radial E-field <5 MV/m, for 40mm plate separation

✓Beam and spin dynamics stable for required beam intensity

✓Spin coherence time estimated $>10^3$s using sextupoles (no stochastic cooling)

✓Alternate magnetic focusing greatly shielding external B-fields

✓Symmetric lattice significantly reducing systematic error sources

✓Required ring planarity <0.1mm; CW & CCW beam separation <0.01mm

The spin precession relative to momentum in the plane is kept near zero. A vert. spin precession vs. time is an indication of an EDM (*d*) signal.

$$p=\frac{mc}{\sqrt{G}} = 0.7\ \mathrm{GeV/c}$$

for protons

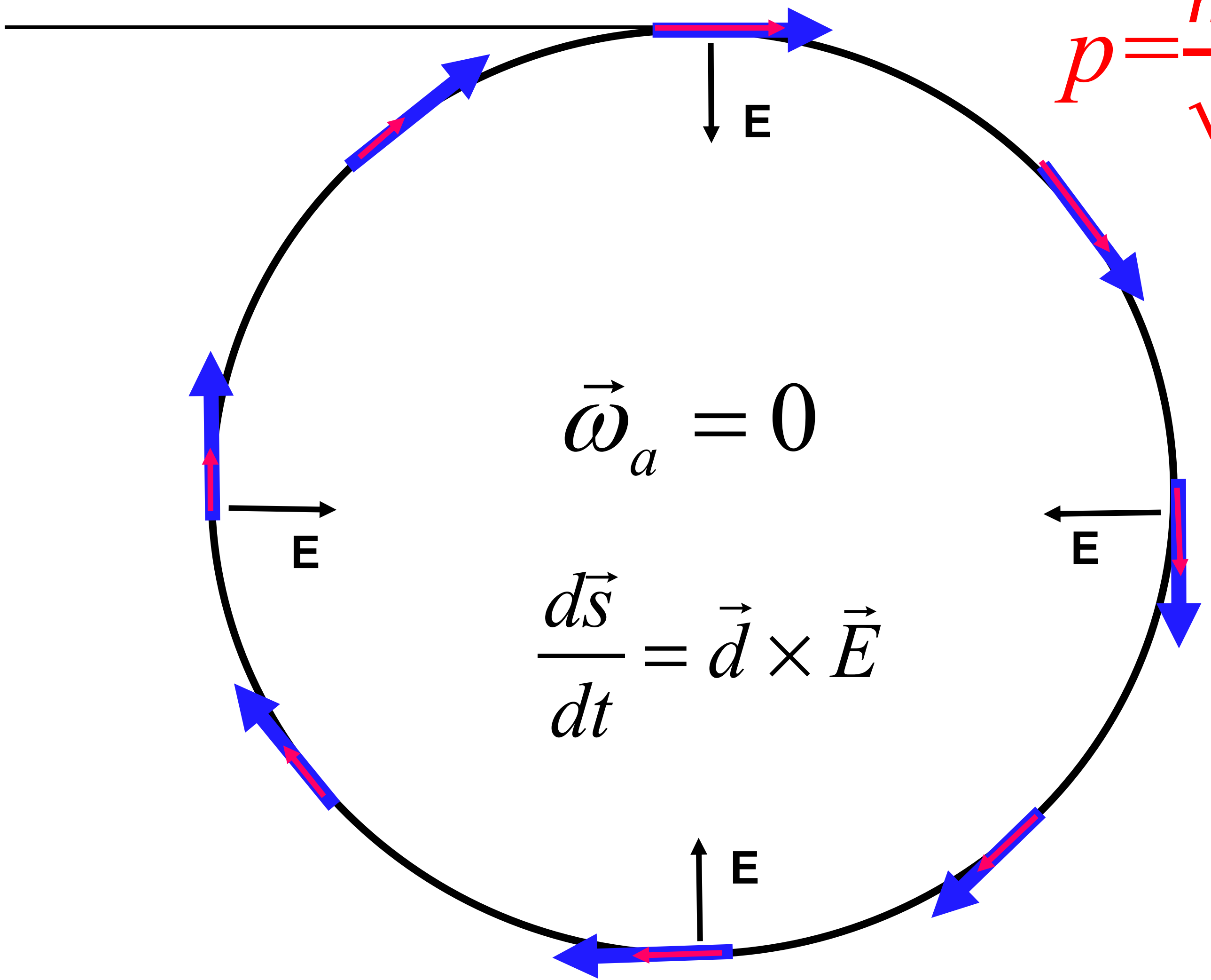

$$\vec{\omega}_a = 0$$

$$\frac{d\vec{s}}{dt} = \vec{d} \times \vec{E}$$

The spin precession relative to momentum in the plane is kept near zero. A vert. spin precession vs. time is an indication of an EDM (*d*) signal.

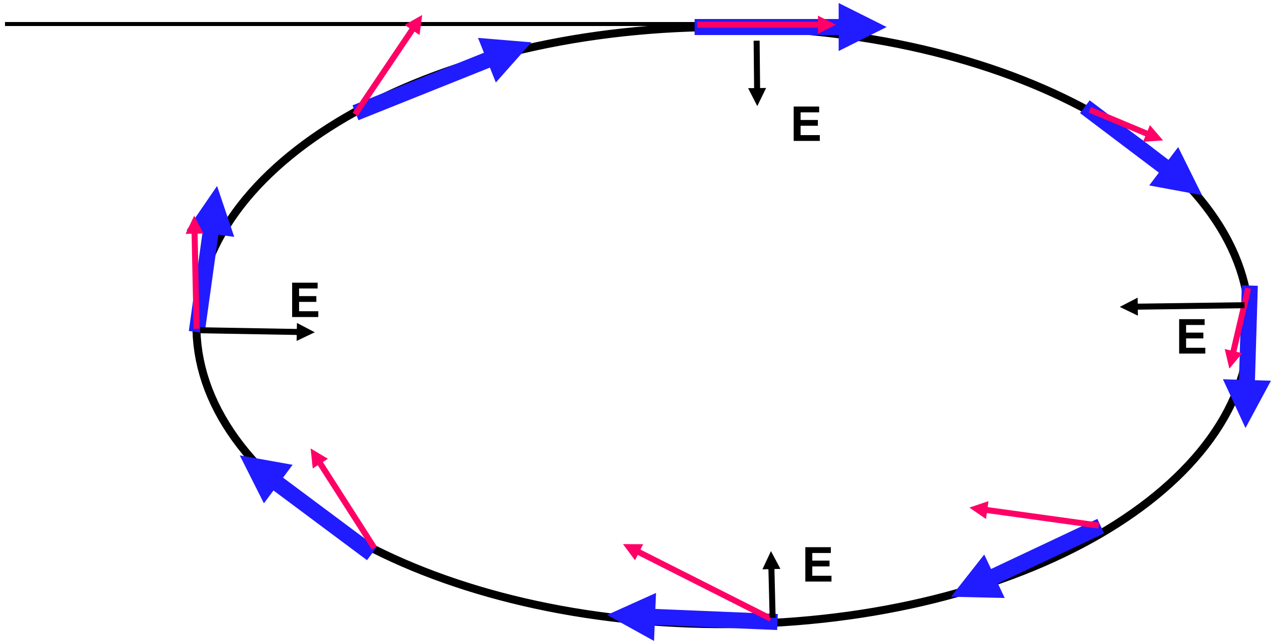

$$\vec{\omega}_a = 0$$

$$\frac{d\vec{s}}{dt} = \vec{d} \times \vec{E}$$

EDM theory, from Snowmass process.

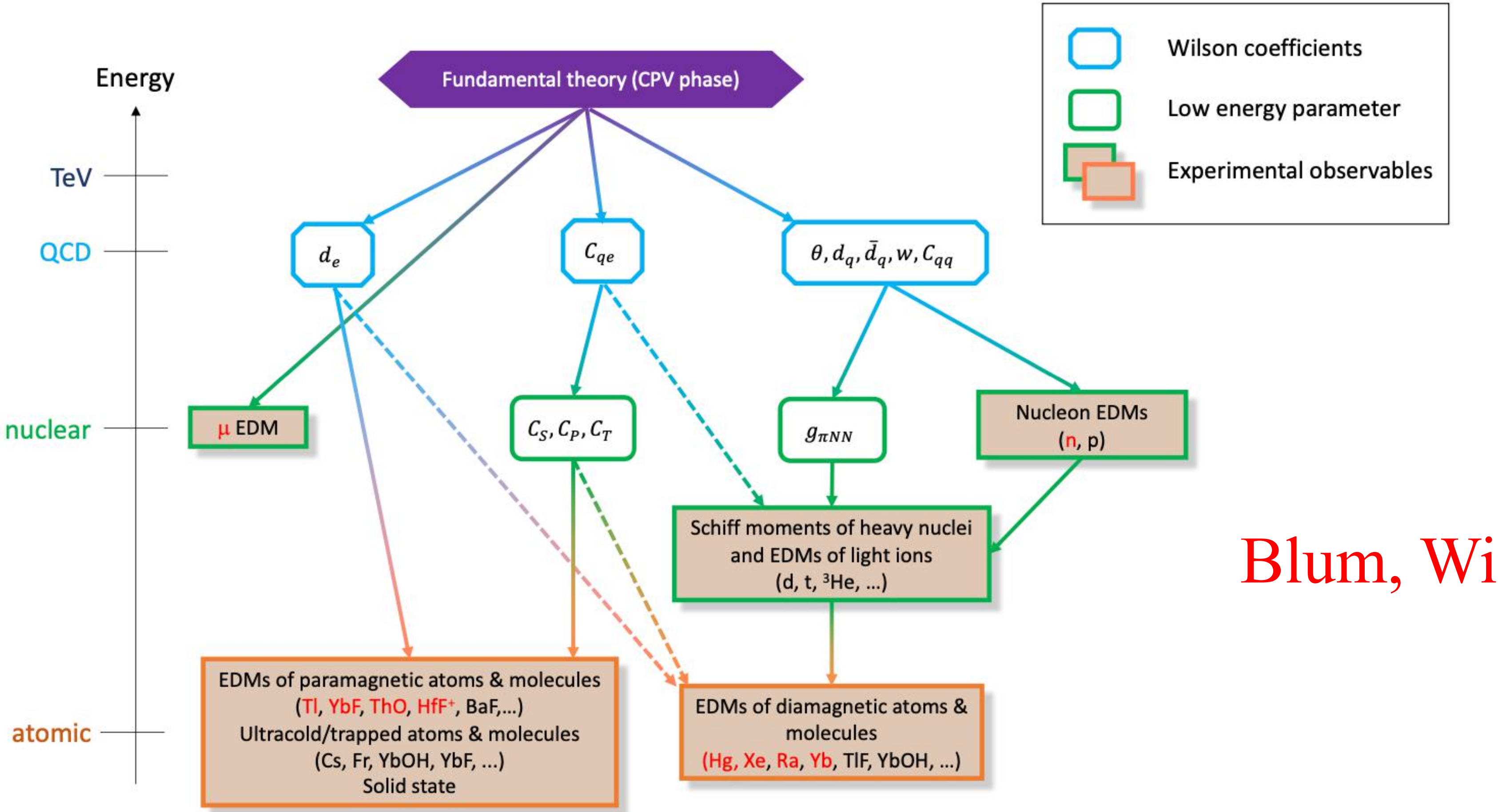

Blum, Winter *et al.*

Figure 3-2. *Flowdown diagram from the fundamental physics at high energy scales, to the Wilson coefficients of the effective field theory, low energy parameters, and the experimental CPV observables. Color outlines of the various boxes inidcate the different energy scales. Solid arrows between the boxes indicate strong connection, whereas dashed arrows indicate weaker influence onto the lower lying parameter. Experimental systems shown in red have already been used in EDM searches; those shown in black (as well as many of those in red) are being developed for future searches. This figure was adapted from [12].*